



**HAL**  
open science

## The yeast mitophagy receptor Atg32 is ubiquitinated and degraded by the proteasome, in press PlosOne

Nadine Camougrand, Pierre Vigié, Cécile Gonzalez, Stéphen Manon, Ingrid Bhatia Kissova

### ► To cite this version:

Nadine Camougrand, Pierre Vigié, Cécile Gonzalez, Stéphen Manon, Ingrid Bhatia Kissova. The yeast mitophagy receptor Atg32 is ubiquitinated and degraded by the proteasome, in press PlosOne. PLoS ONE, 2020. hal-03008951

**HAL Id: hal-03008951**

**<https://hal.science/hal-03008951>**

Submitted on 17 Nov 2020

**HAL** is a multi-disciplinary open access archive for the deposit and dissemination of scientific research documents, whether they are published or not. The documents may come from teaching and research institutions in France or abroad, or from public or private research centers.

L'archive ouverte pluridisciplinaire **HAL**, est destinée au dépôt et à la diffusion de documents scientifiques de niveau recherche, publiés ou non, émanant des établissements d'enseignement et de recherche français ou étrangers, des laboratoires publics ou privés.

# PLOS ONE

## The yeast mitophagy receptor Atg32 is ubiquitinated and degraded by the proteasome

--Manuscript Draft--

<b>Manuscript Number:</b>	PONE-D-20-11526R3
<b>Article Type:</b>	Research Article
<b>Full Title:</b>	The yeast mitophagy receptor Atg32 is ubiquitinated and degraded by the proteasome
<b>Short Title:</b>	Atg32 protein is regulated by ubiquitination
<b>Corresponding Author:</b>	Nadine Camougrand Centre National de la Recherche Scientifique BORDEAUX, FRANCE
<b>Keywords:</b>	Yeast <i>Saccharomyces cerevisiae</i> ; mitochondria; quality control, autophagy; mitophagy; Ubiquitination; mitophagy receptor
<b>Abstract:</b>	Mitophagy, the process that degrades mitochondria selectively through autophagy, is involved in the quality control of mitochondria in cells grown under respiratory conditions. In yeast, the presence of the Atg32 protein on the outer mitochondrial membrane allows for the recognition and targeting of superfluous or damaged mitochondria for degradation. Post-translational modifications such as phosphorylation are crucial for the execution of mitophagy. In our study we monitor the stability of Atg32 protein in the yeast <i>S. cerevisiae</i> and show that Atg32 is degraded under normal growth conditions, upon starvation or rapamycin treatment. The Atg32 turnover can be prevented by inhibition of the proteasome activity, suggesting that Atg32 is also ubiquitinated. Mass spectrometry analysis of purified Atg32 protein revealed that at least lysine residue in position 282 is ubiquitinated. Interestingly, the replacement of lysine 282 with alanine impaired Atg32 degradation only partially in the course of cell growth, suggesting that additional lysine residues on Atg32 might also be ubiquitinated. Our results provide the foundation to further elucidate the physiological significance of Atg32 turnover and the interplay between mitophagy and the proteasome.
<b>Order of Authors:</b>	Nadine Camougrand Pierre Vigié Cécile Gonzalez Stéphen Manon Ingrid Bhatia Kissova
<b>Opposed Reviewers:</b>	Koji Okamoto Osaka Ika Daigaku Kango Gakubu Daigakuin Kangogaku Kenkyuka conflict of interest hagai Abeliovich Hebrew University of Jerusalem - Edmond J Safra Campus conflict of interest
<b>Response to Reviewers:</b>	Answers to reviewer 1 Reviewer #1: In the revised manuscript by Camougrand et al, the authors made modest changes to address concerns raised in their original submission. While I have my doubts that their purification strategy is effectively working (ie, a concern is that the oligomerized band is non-specifically cross-reacting with the anti-his antibody), the authors have now provided the requested data.  However, it is somewhat glaring that the authors have now removed data from Figure 8 related to the ubiquitinated band they identified via proteomic analysis. They had previously generated two clonal lines of a K282A mutant, one of which showed no change in Atg32 turnover and the other which mildly stabilized Atg32 at the 8h

timepoint. In the revised manuscript, the “negative” data is removed while “significantly ( $P<0.05$ ) impaired” is added to the text. The authors should return “clone 1” to the manuscript for transparency purposes and graphically display the values that led to this conclusion.

We would like to thank you for all your effort and comments. We believe they helped us to make our manuscript better.

We apologize if the noninclusion in our revised manuscript of the immunoblot result with clone 1 in Figure 4A gave the impression that we are trying to intentionally select the results that fit into our story. By no means was this our intent. We only tried to simplify the presentation of the results and eliminate unnecessary duplication. Let us provide you with a more detailed explanation.

In the original version, we presented in Figure 8A an image of blots for two different clones (1 and 2). In Figure 8C, there is only one column for the mutant K282A (it does not specify if it is clone 1 or clone 2). We apologize for not explaining this better in the text—the column (48h) contains results from 6 independent experiments from 3 different clones that we tested (clone 1 and clone 2 from Figure 8A plus a third clone that was not mentioned in the manuscript). Also, it has to be noted that in the original version, the y-axis of the graph in Figure 8C shows the amount of Atg32-V5 normalized to T0 value of Atg32-V5, which, based on the reviewer’s request, was normalized in the revised version to the amount of Pgk1 at each time.

Again, Figure 8 in the revised version of our manuscript does include the results of 6 independent experiments from 3 individual clones. Because quantification normalized to Pgk1 did not show significant changes between individual clones (1-2-3), we decided to keep only one of the clones in part A. When compared to wild-type Atg32 protein, there is about 15% ( $P<0.05$ ) more mutant protein in the late stationary phase cells (Fig. 8A, C; 48 h).

For the reviewer, we attach here the immunoblot results obtained from 3 individual clones with individual quantification for each of them for comparison.

Figure for reviewer only

Figure 8 : first soumission

Figure 8 : second revision

My other primary concern regarding lengthy treatment with MG-132 was not addressed. In their response, the authors write that “we did not present results from shorter than 24 hours in the presence of inhibitors, so we are not sure what led the reviewer to raise a concern that stabilization of Atg32 occurs only after long incubation times and may be an indirect effect.” This is exactly the point – because the authors do not examine other time points (for example, 1h, 2h, 4h) after MG-132 addition at 8h, they can only state that 16h of treatment leads to stabilization of Atg32 during stationary growth. While the authors now demonstrate that such treatment does not inhibit cell growth, they also cannot state whether the protein is acutely stabilized or stabilized as part of an adaptive cellular response to prolonged proteasomal inhibition.

In our previous answer we tried to explain to the reviewer that we did not examine the shorter times (fewer than 16 hours; T24) of treatment with MG-132 because our aim was to study levels of Atg32 protein at the beginning of and during the stationary phase—the time of cell growth when mitophagy is induced. We believe that our results provide clear evidence that inhibition of proteasome activity with MG-132 leads to

stabilization of Atg32 during the stationary phase and that this correlates with an increase in mitophagy activity.

However, to address the reviewer's comment, we performed an experiment in which MG-132 was added to the culture at T0 (instead of at T8 as we used during our study) and examined the levels of Atg32 after 8 hours (exponential phase, no appreciable mitophagy), 24 hours (early stationary phase, beginning of mitophagy induction), and 48 hours (late stationary phase). The obtained results were included in the manuscript as supplementary Fig. 4D (for your convenience the results are attached to this letter as well). As you can see, the level of Atg32p at T8 is about half compared to the level at T0, and it further decreases to where there is almost no detectable Atg32 when measured at T48. On the contrary, the presence of MG-132 drastically recovers Atg32 levels in both short (8h) and long (24h and 48h) incubation times. We provide the quantification of the immunoblot results here as well. We strongly believe these results support the view that the Atg32 protein is acutely stabilized instead of being stabilized as a part of an adaptive cellular response to prolonged proteasomal inhibition.

New supplementary Figure S4 (with new results in part D - included into manuscript):

Quantification figure S4D- an average from 2 independent experiment (for reviewer only):

In exponentially growing cells, where there is no appreciable mitophagy, the authors use short-term MG132 treatment in combination with cycloheximide and observe a very modest inhibition of proteasomal turnover. So while the authors can conclude that Atg32 can be targeted to the proteasome during exponential growth, it is not clear that this is an acute cellular response to regulate mitophagy when cells reach stationary phase. If the authors are unwilling to perform new experiments, they must substantially improve the clarity of the manuscript and acknowledge the potential caveats and alternative explanations of their results.

Beside our aforementioned explanation, our experiments with cycloheximide (Figs. 4B and 4C) showed that the turnover of the Atg32 protein is extremely rapid compared to other proteins (porin, Pgk1) and that this turnover involves the activity of the proteasome. This also explains why the activity of the promoter increases during growth (Fig. 4A). After one hour with the cycloheximide, the effect of MG-132 is striking and significant ( $P=0.0146$ ; we included data for "1h+cycloheximide+MG-132" in Fig. 4C that were missing in the previous version). Respectfully, we cannot agree with the reviewer's statement that this change is "very modest."

Our results support the conclusion that Atg32 can be targeted to the proteasome during exponential growth as well as favoring an acute cellular response to regulate levels of Atg32 protein (as an essential mitophagy regulator) when cells reach the stationary phase.

We slightly modified some parts of the Results and Discussion sections to make the text clearer.

The manuscript was proofread by a native English-speaking person.

**Additional Information:**

Question	Response
<p><b>Financial Disclosure</b></p> <p>Enter a financial disclosure statement that describes the sources of funding for the work included in this submission. Review the <a href="#">submission guidelines</a> for detailed requirements. View published research articles from <a href="#">PLOS ONE</a> for specific examples.</p> <p>This statement is required for submission and <b>will appear in the published article</b> if the submission is accepted. Please make sure it is accurate.</p> <p><b>Unfunded studies</b> Enter: <i>The author(s) received no specific funding for this work.</i></p> <p><b>Funded studies</b> Enter a statement with the following details:</p> <ul style="list-style-type: none"> <li>• Initials of the authors who received each award</li> <li>• Grant numbers awarded to each author</li> <li>• The full name of each funder</li> <li>• URL of each funder website</li> <li>• Did the sponsors or funders play any role in the study design, data collection and analysis, decision to publish, or preparation of the manuscript?</li> <li>• <b>NO</b> - Include this sentence at the end of your statement: <i>The funders had no role in study design, data collection and analysis, decision to publish, or preparation of the manuscript.</i></li> <li>• <b>YES</b> - Specify the role(s) played.</li> </ul> <p>* typeset</p>	<p>IBK: Slovak APVV agency (SK-FR-2015-0005) NC and PV: CNRS, the University of Bordeaux and the Doctoral International Program from IDEX of Bordeaux supported by Agence Nationale pour la Recherche (ANR-10-IDEX-03-02) NC and IBK: France/Slovakia collaboration was supported by Campus France (Stefanik n° 35809VC) The funders had no role in study design, data collection and analysis, decision to publish, or preparation of the manuscript.</p>
<p><b>Competing Interests</b></p> <p>Use the instructions below to enter a competing interest statement for this submission. On behalf of all authors, disclose any <a href="#">competing interests</a> that could be perceived to bias this work—acknowledging all financial support and any other relevant financial or non-financial competing interests.</p> <p>This statement <b>will appear in the published article</b> if the submission is</p>	<p>The authors have declared that no competing interests exist.</p>

accepted. Please make sure it is accurate. View published research articles from [PLOS ONE](#) for specific examples.

**NO authors have competing interests**

Enter: *The authors have declared that no competing interests exist.*

**Authors with competing interests**

Enter competing interest details beginning with this statement:

*I have read the journal's policy and the authors of this manuscript have the following competing interests: [insert competing interests here]*

\* typeset

**Ethics Statement**

N/A

Enter an ethics statement for this submission. This statement is required if the study involved:

- Human participants
- Human specimens or tissue
- Vertebrate animals or cephalopods
- Vertebrate embryos or tissues
- Field research

Write "N/A" if the submission does not require an ethics statement.

General guidance is provided below. Consult the [submission guidelines](#) for detailed instructions. **Make sure that all information entered here is included in the Methods section of the manuscript.**

**Format for specific study types**

**Human Subject Research (involving human participants and/or tissue)**

- Give the name of the institutional review board or ethics committee that approved the study
- Include the approval number and/or a statement indicating approval of this research
- Indicate the form of consent obtained (written/oral) or the reason that consent was not obtained (e.g. the data were analyzed anonymously)

**Animal Research (involving vertebrate animals, embryos or tissues)**

- Provide the name of the Institutional Animal Care and Use Committee (IACUC) or other relevant ethics board that reviewed the study protocol, and indicate whether they approved this research or granted a formal waiver of ethical approval
- Include an approval number if one was obtained
- If the study involved *non-human primates*, add *additional details* about animal welfare and steps taken to ameliorate suffering
- If anesthesia, euthanasia, or any kind of animal sacrifice is part of the study, include briefly which substances and/or methods were applied

**Field Research**

Include the following details if this study involves the collection of plant, animal, or other materials from a natural setting:

- Field permit number
- Name of the institution or relevant body that granted permission

**Data Availability**

Authors are required to make all data underlying the findings described fully available, without restriction, and from the time of publication. PLOS allows rare exceptions to address legal and ethical concerns. See the [PLOS Data Policy](#) and [FAQ](#) for detailed information.

Yes - all data are fully available without restriction

A Data Availability Statement describing where the data can be found is required at submission. Your answers to this question constitute the Data Availability Statement and **will be published in the article**, if accepted.

**Important:** Stating 'data available on request from the author' is not sufficient. If your data are only available upon request, select 'No' for the first question and explain your exceptional situation in the text box.

Do the authors confirm that all data underlying the findings described in their manuscript are fully available without restriction?

**Describe where the data may be found in full sentences. If you are copying our sample text, replace any instances of XXX with the appropriate details.**

- If the data are **held or will be held in a public repository**, include URLs, accession numbers or DOIs. If this information will only be available after acceptance, indicate this by ticking the box below. For example: *All XXX files are available from the XXX database (accession number(s) XXX, XXX).*
- If the data are all contained **within the manuscript and/or Supporting Information files**, enter the following: *All relevant data are within the manuscript and its Supporting Information files.*
- If neither of these applies but you are able to provide **details of access elsewhere**, with or without limitations, please do so. For example:

*Data cannot be shared publicly because of [XXX]. Data are available from the XXX Institutional Data Access / Ethics Committee (contact via XXX) for researchers who meet the criteria for access to confidential data.*

*The data underlying the results presented in the study are available from (include the name of the third party*

\*\*Note to PA at accept: authors will make data available at accept, please follow up for accession/ DOI\*\*\*\*  
Same data, but not all, presented in this article, have been loaded on BioRxiv 652933; doi:https://doi.org/10.1101/652933

<p><i>and contact information or URL).</i></p> <ul style="list-style-type: none"><li>• This text is appropriate if the data are owned by a third party and authors do not have permission to share the data.</li></ul> <p>* typeset</p>	
Additional data availability information:	Tick here if the URLs/accession numbers/DOIs will be available only after acceptance of the manuscript for publication so that we can ensure their inclusion before publication.; Tick here if your circumstances are not covered by the questions above and you need the journal's help to make your data available.

PONE-D-20-11526

*The yeast mitophagy receptor Atg32 is ubiquitinated and degraded by the proteasome*

PLOS ONE

Dear Editor

Following the first round of reviewing, we have tried to give explanations and perform modifications to address the reviewer's comments. It seems that the first reviewer did not make any further requests and was satisfied with the modifications made and the explanations provided. With respect to his comment, the manuscript was proofread by a native-English-speaking person.

In this second round, we also tried to provide the best possible explanations to the second reviewer's requests, modified the text in the Results and Discussion section, and performed the required experiment, the results of which are presented in Figure S4D.

As we described in detail in Answers to the reviewer, we apologize if the noninclusion in our revised manuscript of the immunoblot result with clone 1 in Figure 4A gave the impression that we are trying to intentionally select the results that fit into our story. By no means was this our intent. We only tried to simplify the presentation of the results and eliminate unnecessary duplication. In the original version, we presented in Figure 8A an image of blots for two different clones (1 and 2). In Figure 8C, there is only one column for the mutant K282A (it does not specify whether it is clone 1 or clone 2). We apologize for not explaining this better in the text—the column (48h) contains results from six independent experiments using three different clones that we tested (clone 1 and clone 2 from Figure 8A plus a third clone that was not mentioned in the manuscript). Also, it must be noted that in the original version, the y-axis of the graph in Figure 8C shows the amount of Atg32-V5 normalized to T0 value of Atg32-V5, which, based on the reviewer's request, was normalized in the revised version to the amount of Pgk1 at each time.

Again, Figure 8 in the revised version of our manuscript does include the results of six independent experiments from three individual clones. Because quantification normalized to Pgk1 did not show significant changes between individual clones (1–2–3), we decided to keep only one of the clones in part A. When compared with wild-type Atg32 protein, there is about 15% ( $P < 0.05$ ) more mutant protein in the late stationary-phase cells (Fig. 8A, C; 48h).

To respond to the second comment, which concerns the duration of treatment with MG-132 (beginning and late stationary phase, T24 or T48, respectively; mitophagy induced), we performed a new experiment in which we examined a shorter treatment time (8h, exponential phase; no mitophagy).

We included the results in Figure S4D. They showed that a short-term inhibition of proteasome also stabilized Atg32-V5 protein. This suggests that upon MG-132 treatment, the Atg32 protein is acutely stabilized instead of being stabilized as a part of an adaptive cellular response to prolonged proteasomal inhibition.

In addition, our experiments with cycloheximide (Figs. 4B and 4C) showed that the turnover of the Atg32 protein is extremely rapid compared with other proteins (porin, Pgk1) and that this turnover involves the activity of the proteasome. This also explains why the activity of the promoter increases during growth (Fig. 4A). After one hour with the cycloheximide, the effect of MG-132 is marked and significant ( $P=0.0146$ ; we included data for “1h+cycloheximide+MG-132” in Fig. 4C that were missing in the previous version). Respectfully, we cannot agree with the reviewer’s statement that this change is “very modest.”

We believe that the data presented in this manuscript are now robust and unequivocally show regulation of the Atg32 protein by ubiquitination.

We hope that this revised version of the manuscript will be acceptable for publication in PLOS One. We strongly believe that the data we present in this work are important for the scientific community interested in mitophagy and in the interactions between this mechanism involved in mitochondrial quality control and the ubiquitin proteasome system.

Dr. Nadine Camougrand

## The yeast mitophagy receptor Atg32 is ubiquitinated and degraded by the proteasome

Nadine Camougrand<sup>(a,b)</sup>, Pierre Vigie<sup>(a,b)</sup>, Cécile Gonzalez<sup>(a,b,d)</sup>, Stephen Manon<sup>(a,b)</sup> and Ingrid Bhatia-Kiššová<sup>(c)</sup>

<sup>a</sup> CNRS, UMR5095, 1 rue Camille Saint-Saëns, 33077 Bordeaux, France

<sup>b</sup> Université de Bordeaux, UMR5095, 1 rue Camille Saint-Saëns, 33077 Bordeaux, France

<sup>c</sup> Comenius University, Faculty of Natural Sciences, Department of Biochemistry, Ilkovicova 6, 84215 Bratislava, Slovak Republic

<sup>d</sup> Present address: IBCP, UMR5086, Université de Lyon, 7 passage du Vercors, 69367 Lyon cedex 07, France

Correspondence: [n.camougrand@ibgc.cnrs.fr](mailto:n.camougrand@ibgc.cnrs.fr)

**Abstract:** Mitophagy, the process that degrades mitochondria selectively through autophagy, is involved in the quality control of mitochondria in cells grown under respiratory conditions. In yeast, the presence of the Atg32 protein on the outer mitochondrial membrane allows for the recognition and targeting of superfluous or damaged mitochondria for degradation. Post-translational modifications such as phosphorylation are crucial for the execution of mitophagy. In our study we monitor the stability of Atg32 protein in the yeast *S. cerevisiae* and show that Atg32 is degraded under normal growth conditions, upon starvation or rapamycin treatment. The Atg32 turnover can be prevented by inhibition of the proteasome activity, suggesting that Atg32 is also ubiquitinated. Mass spectrometry analysis of purified Atg32 protein revealed that at least lysine residue in position 282 is ubiquitinated. Interestingly, the replacement of lysine 282 with alanine impaired Atg32 degradation only partially in the course of cell growth, suggesting that additional lysine residues on Atg32 might also be ubiquitinated. Our results provide the

foundation to further elucidate the physiological significance of Atg32 turnover and the interplay between mitophagy and the proteasome.

## **Introduction**

Mitochondria are organelles in charge of many crucial functions in cells. In eukaryotes, they are known to be the powerhouse of cells by producing ATP via oxidative phosphorylation; they are also involved in different synthesis pathways such as the synthesis of certain amino acids and lipids and in signaling pathways, such as apoptosis and calcium. Mitochondrial dysfunctions have been associated with aging and with an increasing number of pathologies, including neurodegenerative diseases, cancer, and metabolic perturbation. To maintain cell survival and homeostasis, cells have developed ways to remove superfluous or damaged cell components and organelles such as mitochondria. Mitophagy is one of the processes involved in mitochondrial quality control. Mitophagy is a selective form of autophagy [1,2]. Macroautophagy (hereafter called autophagy) is conserved among eukaryotic species and involves specific lytic compartments: the vacuole in yeast and lysosomes in mammals. It also involves specific autophagy-related (Atg) proteins. To date, more than 40 Atg proteins have been identified, about half are involved in the core autophagy machinery, and the rest are implicated in specific autophagy processes and regulations.

In mammalian cells, mitophagy and recognition of the mitochondria that need to be removed are complex processes. Two main mechanisms of mitophagy signaling have been identified: ubiquitin-mediated mitophagy and receptor-mediated mitophagy. To be degraded by mitophagy, mitochondria must be labeled with a flag that is recognized by autophagic machinery. For these mitophagy-signaling pathways, ubiquitin/proteins, receptors/adaptors containing the

LIR (LC3-interacting region) domain act to recruit LC3 family members for mitochondria and thus induce mitophagy.

In yeast, Atg32 is the only characterized mitophagy receptor, which suggests mitophagy could be a simpler mechanism in yeast than in mammals [3,4]. The Atg32 protein is an outer mitochondrial membrane protein with its C-terminus in the intermembrane space and its N-terminus in the cytosol [3,4]. As mammalian protein receptors, Atg32 possesses the Atg8-interacting motif (AIM, LIR domain). When mitophagy is induced, Atg32 interacts with Atg11, a cytosolic adaptor protein required for selective autophagy. Atg11 is believed to target mitochondria to the pre-autophagosomal structure (PAS), where an autophagosome is generated to enclose the mitochondria. At the PAS, Atg32 interacts with Atg8, a protein anchored in autophagosome membranes, and the Atg32-Atg8 interaction facilitates the formation of autophagosomes surrounding mitochondria [3,4,5,6]. Both interactions are required for the recruitment of mitochondria to the phagophore followed by their sequestration within autophagosomes and their degradation in the vacuole.

The Atg32 expression is regulated by multiple factors. It has been shown that N-acetylcysteine (NAC), which increases the cellular level of reduced glutathione (GSH), inhibits mitophagy [7] through suppression of Atg32 expression [4]. Indeed, the absence of an Opi3 protein, an enzyme required in the conversion of phosphatidylethanolamine to phosphatidylcholine, causes an increase in intracellular reduced glutathione, leading to a decrease in Atg32 protein expression [8]. Moreover, the absence of some components of the NatA N-acetyltransferase complex also results in a decrease in Atg32 protein expression [9]. However, the precise role of NatA concerning Atg32 protein remains unclear. In addition, it has

been shown that Atg32 phosphorylation on serines 114 and 119, is required for mitophagy activation [10,11]. More recently, Levchenko et al. detected another post-translational modification of Atg32 when mitophagy was induced by rapamycin treatment in a *pep4Δ* background, where vacuolar proteolysis is impaired. However, its precise nature remains to be characterized [12].

Because mitophagy induction is highly regulated, we reasoned, as a key mitophagy factor, Atg32 protein may be subject to degradation control. In this study, we monitored the expression and the stability of the Atg32 protein during mitophagy in the yeast *S. cerevisiae*. We showed the existence of an interplay between mitophagy and the proteasome. We demonstrated that a novel post-translational modification of Atg32, ubiquitination at least on lysine 282 residue, modulated Atg32 protein level during the cell growth. Because uncontrolled mitophagy activation can lead to dire consequences, understanding Atg32 regulation would help us understand the control of mitophagy activity and also the cooperation between the proteasome and mitophagy.

## **Material and methods**

### **Yeast strains, plasmids and growth conditions**

All yeast strains used in this study are listed in the supplementary Table I and derived from BY4742 (Euroscarf bank). Yeast cells were grown aerobically at 28°C in complete minimal synthetic medium (CMS; 0.175% yeast nitrogen base without amino acids and ammonium sulfate, 0.5% ammonium sulfate, 0.1% potassium phosphate, 0.2% Drop-Mix, 0.01% of auxotrophic amino acids and nucleotide, pH 5.5), supplemented with 2% lactate as a carbon source (CMS-L). Cell growth was followed by optical density at 600 nm. Atg32 expression was examined in cells harvested in the mid-exponential phase of growth (1.5–2 OD<sub>600</sub>; T0), after 8 h

(8 h; late exponential phase), after 1 day (24 h; early stationary phase), and after 2 days (48 h; late stationary phase) of culture. To inhibit the proteasome, 75  $\mu$ M MG-132 + 0.003% SDS were added to the cell culture at 8 h time point. To inhibit vacuolar proteolysis, 2 mM PMSF was added to the cell culture at 8 h time point; this step was repeated twice during the course of cell growth. For starvation experiments, cells were harvested at the mid-exponential phase of growth (1.5–2 OD<sub>600</sub>; T0), washed three times with water and incubated in a nitrogen starvation medium (-N; 0.175% yeast nitrogen base without amino acids and ammonium sulfate, and 2% lactate, pH 5.5) for 3-, 6- or 24 h (-N3h, -N6h, -N24h). The *pre2-2* mutant strain was unable to grow in the lactate-containing medium; for this reason, the experiments including *pre2-2* mutant strain were performed in a CMS medium supplemented with 2% galactose as a carbon source (CMS-G). The *pre2-2* mutant strain was a gift of Dr. Sagot (UMR5095 CNRS, France).

Mitophagy was studied in cells expressing the mitochondrial matrix Idp1-GFP protein, and subjected to nitrogen starvation or during different phases of growth. The plasmid *pIDP1-GFP* was a gift from Dr. Abeliovich (Hebrew University of Jerusalem, Israel). To study autophagy, cells were transformed with plasmid *pGFP-ATG8* kindly provided by Dr. Dan Klionsky (Michigan University, USA). The plasmid expressing HA-Atg32 from copper promoter was a gift from Dr. Dan Klionsky. The plasmid expressing Atg32-V5-6HIS from *ATG32* promoter was a gift from Axel Athané (UMR5095 CNRS, France). To prepare the *pPROM-ATG32- $\beta$ -galactosidase* plasmid, the promoter of *ATG32* gene was amplified by PCR using forward primer (5'-GTGATGTATCCACAGGGAATTCCGCTC-3') and reverse primer (5'-CTTTTAGATGAGGATCCTTTACCT-3'), and cloned into *Bam*H1-digested YEp357 plasmid kindly provided by Dr. Pinson (UMR5095 CNRS, France). The plasmid *pYES2-ATG32-V5*

expressing mutated Atg32<sup>K282A</sup>-V5 or Atg32-AAAA-V5 proteins were generated using the QuikChange Site-Directed Mutagenesis approach with the following primers: K282A forward (5'-CAATATTCTCAAGGCGCGCCTGTAATA-3'), K282A reverse (5'-GATCGGTATTACAGGCGCGCCTTGAGA-3'); Rsp5-binding motif forward (5'-AAAGAATACCAATCTCTTTTTGAAGCAQGCGGCAGCTCACGATTCCGCAACATTC-3'); Rsp5-binding motif reverse (5'-TTGCGGGAATGTTGCGGAATCGTGAGCTGCCGCTGCTTCAAAAAGAGATTGGTA-3').

### **Preparation of protein extracts and western blots**

For preparation of total protein extracts,  $2 \times 10^7$  cells were harvested by centrifugation, washed with water, and resuspended in 450  $\mu$ l of water and 50  $\mu$ l of lysis buffer (1.85 M NaOH, 3.5%  $\beta$ -mercaptoethanol). After 10 min on ice, 50  $\mu$ l of trichloroacetic acid 3 M was added followed by another incubation of 10 min on ice. Proteins were pelleted by centrifugation, 8 min at 13 000 g, washed with acetone and resuspended in 20  $\mu$ l of 5% SDS and 20  $\mu$ l of loading buffer (2%  $\beta$ -mercaptoethanol, 2% SDS, 0.1 M Tris-HCl, pH 8.8, 20% glycerol, 0.02% bromophenol blue). Samples were boiled for 5 min and 50  $\mu$ g of proteins/total protein extracts corresponding to  $5 \times 10^6$  cells per line were separated by electrophoresis by 12.5% SDS-PAGE and subjected to immunoanalysis with either anti-GFP (Roche), anti-Pgk1 (Invitrogen), anti-porin (Invitrogen), anti-Dpms1 (Invitrogen), anti-HA (Roche), anti-V5 (Invitrogen), anti-HIS (Euromedex) and anti-ubiquitin (Calbiochem) antibodies. Detection was performed with ECL<sup>+</sup> reagent (Luminata Forte, Perkin Elmer). Pgk1, the cytosolic phosphoglycerate kinase, was used as a loading control. The Atg32-V5/Pgk1, HA-Atg32/Pgk1 or GFP/GFP + Idp-GFP ratios were quantified by using ImageJ software (NIH). Results of calculations were expressed as the mean  $\pm$

SEM. To study Atg32-V5 turnover, between 5 and 8 independent experiments were carried out for each tested condition; one representative western blot result is presented for each experimental condition. *P*-values were assessed using paired Student's *t*-tests; \* *P* < 0.05 or \*\* *P* < 0.01 were considered statistically significant.

For preparation of cell lysates,  $5 \times 10^7$  cells were broken with glass beads in a buffer containing 0.6 M sorbitol, 20 mM MES pH 6 plus protease inhibitor cocktail (Roche); lysates were centrifuged 10 min at 800 g. The supernatants, an equivalent of 400  $\mu$ g of proteins, were loaded on 20–55% OptiPrep density gradients in a buffer with 0.6 M sorbitol 20 mM MES pH6, 5 mM EDTA, pH6 plus protease inhibitor cocktail (Roche). Fractions were collected, precipitated with TCA and pellets were resuspended in 20  $\mu$ l of 5% SDS and 20  $\mu$ l of loading buffer (2%  $\beta$ -mercaptoethanol, 2% SDS, 0.1 M Tris-HCl, pH 8.8, 20% glycerol, 0.02% bromophenol blue). Samples were boiled for 5 min and 4  $\mu$ l of samples were separated by 12.5% SDS-PAGE and subjected to immunoanalysis.

### **Monitoring mitophagy by western blot**

BY4742, *atg32 $\Delta$*  mutant cells and *atg32 $\Delta$*  cells expressing Atg32-V5 and the mitochondrial matrix Idp1-GFP were grown in a CMS-L medium in presence or absence of MG-132 or exposed to nitrogen starvation, respectively. At different times (as indicated in each figure), total protein extracts were prepared from  $2 \times 10^7$  cells as described above. Extracts were immunoblotted, 12.5 % SDS-PAGE gels were used. Under basal condition (T0), only the Idp1-GFP form (75 kDa) was detected with a monoclonal mouse anti-GFP antibody. Upon mitophagy induction, Idp1-GFP (75 kDa) and free GFP (27 kDa) were detected with anti-GFP antibodies.

Pgk1 was used as a loading control. Quantification of GFP signals was done using ImageJ software by calculating the ratio of free GFP to total GFP (GFP/GFP + Idp1-GFP). Between 4 and 5 independent experiments were carried out for each experimental condition; one representative western blot result is presented.

### **Monitoring autophagy by western blot**

BY4742 and *atg32*Δ cells expressing Atg32-V5 and GFP-Atg8 were grown in a CMS-L medium in presence or absence of MG-132. At different times (as indicated in each figure), total protein extracts were prepared from  $2 \times 10^7$  cells as described above. Extracts were immunoblotted. Under basal condition (T0), only the GFP-Atg8 form (40.6 kDa) was detected with anti-GFP antibody. Upon autophagy induction, GFP-Atg8 localized in autophagosome membranes is delivered into vacuoles, here the proteolysis of GFP-Atg8 releases an intact GFP moiety (27 kDa) that can be detected with anti-GFP antibodies. Pgk1, was used as a loading control. Three independent experiments were carried out for each examined condition; one representative result is shown.

### **ALP activity**

Alkaline phosphatase activity was measured on *pho8*Δ strain, expressing the mitochondria-targeted truncated version of Pho8, mtPho8Δ60 [13], during the mid-exponential (T0) and the stationary phase (48 h) in absence or presence of MG-132. For each point,  $5 \times 10^7$  cells expressing mitochondria-targeted Pho8Δ60 (mtPho8Δ60) were harvested and lysed with glass beads in lysis buffer

(20 mM PIPES, 0.5% Triton X-100 0.5%, 50 mM KCl, 100 mM potassium acetate, 10 mM MgCl<sub>2</sub>, 10 μM ZnSO<sub>4</sub>, 2 mM PMSF). After centrifugation, 20 μl of supernatant were put with 80 μl of water and 400 μl of activity buffer (250 mM Tris HCl pH 8, 0.4% Triton X-100, 10 mM MgCl<sub>2</sub>, 10 μM ZnSO<sub>4</sub>, 125 mM p-nitrophenyl-phosphate) during 20 minutes at 30°C. The reaction was stopped by the addition of 500 μl of 1 M glycine pH 11. Activity was then measured by optical density at 400 nm. Protein concentration was measured with the Lowry method. ALP activities were expressed as arbitrary fluorescence units/minute/mg proteins (AU/min/mg). 4 independent experiments were carried out for each condition. Results of quantification were expressed as the mean ± SEM. *P*-values were assessed using paired Student's t-tests; \*\* *P* < 0.01 were considered statistically significant.

### **β-galactosidase activity**

BY4742 cells, expressing β-galactosidase protein under control of *ATG32* promoter were grown in a lactate-containing medium and harvested at different time points: mid-exponential phase of growth (T0), late exponential phase of growth (8 h), early stationary phase of growth (24 h) and late stationary phase of growth (48 h). For proteasome inhibition, 75 μM MG-132 + 0.003% SDS were added at 8 h time point. To measure β-galactosidase activity, five OD<sub>600</sub> (corresponding to 5.0 × 10<sup>7</sup> cells) were harvested and broken with glass beads in lysis buffer (100 mM Tris-HCL pH 8, 1 mM DTT, 20% glycerol, 2 mM PMSF) during 4 min at 20 hertz using Mixer Mill MM400 (Retsch). Then, 20 μl of cell lysate were used to measure β-galactosidase activity by absorbance at 420 nm in 60 mM Na<sub>2</sub>HPO<sub>4</sub>, 40 mM NaH<sub>2</sub>PO<sub>4</sub>, 10 mM KCl, 1 mM MgSO<sub>4</sub>, 50 mM β-mercaptoethanol, pH 7 and with 0.8 mg/ml of ortho-Nitrophenyl-β-galactoside (ONPG). Protein concentrations were measured using Lowry's method and

activities were normalized to T0. Between 5 and 8 independent experiments were carried out for each experimental condition. Results of quantification were expressed as the mean  $\pm$  SEM. *P*-values were assessed using paired Student's *t*-tests; \*\* *P* < 0.01 were considered statistically significant.

### **Atg32 purification**

To purify Atg32 protein,  $20 \times 10^7$  cells expressing Atg32-V5-6xHIS and grown until late stationary phase (48 h) in the presence of 75  $\mu$ M MG-132 were collected, and lysates were prepared as described in Becuwe et al. [14]. Cells were precipitated with TCA to a final concentration of 10% overnight at 4°C, and lysed with glass beads for 20 min at 4°C. After centrifugation, the lysate was collected and centrifuged at 16,000 *g* for 10 min. The pellet was resuspended with 30  $\mu$ l of 1 M non buffered Tris and 200  $\mu$ l of guanidinium buffer (6 M GuHCl, 20 mM Tris-HCl, pH 8, 100 mM K<sub>2</sub>HPO<sub>4</sub>, 10 mM imidazole, 100 mM NaCl, and 0.1% Triton X-100) and incubated for 1 h at room temperature on a rotating platform. After centrifugation (16,000 *g* for 10 min at room temperature), the lysate was loaded on a HisTrap FF Crude column (GE Healthcare Life Sciences). The column was then washed with a speed of 1 ml/min with guanidinium buffer, then with wash buffer 1 (20 mM Tris-HCl, pH 8.0, 100 mM K<sub>2</sub>HPO<sub>4</sub>, 20 mM imidazole, 100 mM NaCl, and 0.1% Triton X-100) and then with wash buffer 2 (20 mM Tris-HCl, pH 8.0, 100 mM K<sub>2</sub>HPO<sub>4</sub>, 10 mM imidazole, 1 M NaCl, and 0.1% Triton X-100). His6-tagged proteins were finally eluted with an elution buffer (50 mM Tris-HCl, pH 8.0, and 250 mM imidazole). Fractions absorbing at 254 nm were pooled, analyzed by 11% SDS-PAGE and submitted to blue colloidal staining and immuno-analysis.

### **Sample preparation and protein digestion for MS analysis**

After colloidal blue staining, both obtained bands (B1, B2) were cut out from the SDS-PAGE gel and subsequently cut in 1 mm x 1 mm gel pieces. Gel pieces were destained in 25 mM ammonium bicarbonate, 50% acetonitrile (ACN), rinsed twice in ultrapure water and shrunk in ACN for 10 min. After ACN removal, gel pieces were dried at room temperature, covered with the trypsin solution (10 ng/ $\mu$ l in 50 mM  $\text{NH}_4\text{HCO}_3$ ), rehydrated at 4 °C for 10 min, and finally incubated overnight at 37 °C. Spots were then incubated for 15 min in 50 mM  $\text{NH}_4\text{HCO}_3$  at room temperature with rotary shaking. The supernatant was collected, and an  $\text{H}_2\text{O}/\text{ACN}/\text{HCOOH}$  (47.5:47.5:5) extraction solution was added onto gel slices for 15 min. The extraction step was repeated twice. Supernatants were pooled and concentrated in a vacuum centrifuge to a final volume of 100  $\mu$ l. Digests were finally acidified by the addition of 2.4  $\mu$ l formic acid (5%, v/v) and stored at -20 °C.

### **nLC-MS/MS analysis**

Peptide mixture was analyzed on the Ultimate 3000 nanoLC system (Dionex, Amsterdam, The Netherlands) coupled to the Electrospray Orbitrap Fusion™ Lumos™ Tribrid™ Mass Spectrometer (Thermo Fisher Scientific, San Jose, CA). Ten microliters of peptide digests were loaded onto a 300- $\mu$ m-inner diameter x 5-mm  $\text{C}_{18}$  PepMap™ trap column (LC Packings) at a flow rate of 10  $\mu$ L/min. The peptides were eluted from the trap column onto an analytical 75-mm id x 50-cm  $\text{C}_{18}$  Pep-Map column (LC Packings) with a 4–40% linear gradient of solvent B in 45 min (solvent A was 0.1% formic acid and solvent B was 0.1% formic acid in 80% ACN). The separation flow rate was set at 300 nL/min. The mass spectrometer operated in positive ion mode at a 1.8-kV needle voltage. Data were acquired using Xcalibur 4.1 software in a data dependent

mode. MS scans ( $m/z$  375-1500) were recorded at a resolution of  $R = 120\,000$  (at  $m/z$  200) and an AGC target of  $4 \times 10^5$  ions collected within 50 ms. Dynamic exclusion was set to 60 s and top speed fragmentation in HCD mode was performed over a 3 s cycle. MS/MS scans with a target value of  $3 \times 10^3$  ions were collected in the ion trap with a maximum fill time of 300 ms. Additionally, only +2 to +7 charged ions were selected for fragmentation. Other settings were as follows: no sheath nor auxiliary gas flow, heated capillary temperature, 275 °C; normalized HCD collision energy of 30% and an isolation width of 1.6  $m/z$ . Monoisotopic precursor selection (MIPS) was set to Peptide and an intensity threshold was set to  $5 \times 10^3$ .

## Results

### Amount of the mitophagy receptor Atg32 decreases during the stationary phase

Mitophagy in yeast is induced during nitrogen starvation, during the stationary phase of growth, or through rapamycin treatment, where cells are grown in a strictly respiratory carbon source medium. To study Atg32 expression in cells grown in a lactate-containing medium (CMS-L), we C-terminally tagged the Atg32 protein with a V5-6HIS epitope (hereafter referred to as Atg32-V5), and the tagged protein was expressed under the control of its promoter. First, we ensured the fusion protein Atg32-V5 was localized to mitochondria by analyzing total cellular extracts from cells harvested in the mid-exponential growth phase on a 20–55% OptiPrep gradient (Fig. 1A) or isolated mitochondria on a 20–60% sucrose gradient (Fig. S1A). In both cases, Atg32-V5 is colocalized with porin, an outer mitochondrial membrane protein. Moreover, by using mitophagy-dependent processing of the Idp1-GFP technique [15] we showed that Atg32-V5 protein was able to reverse the mitophagy defect of the *atg32Δ* mutant strain in

both the stationary phase of cell growth (Fig. 1B) as well as during starvation (Fig. S1B). These observations align with the data of Levchenko *et al.* (2016), who showed that the C-terminal tagging of Atg32 by a ZZ tag did not interfere with mitophagy induced by nitrogen starvation or rapamycin treatment [12].

We then determined Atg32 expression from cells harvested in the mid-exponential phase of growth (1.5-2 OD<sub>600</sub>; T0), after 8 hours (late exponential phase; 8 h), after 1 day (early stationary phase; 24 h), and after 2 days (late stationary phase; 48 h) of culture. We found that under respiratory conditions, the Atg32-V5 protein level decreased during cell growth and almost completely disappeared in the stationary phase (Fig. 2A, B). Similarly, we observed that when the Atg32 protein was N-terminally tagged with an HA epitope, its amount also decreased gradually during cell growth into the stationary phase (Fig. 2C, D). It is evident that mitophagy alone cannot be responsible for the decreasing amount of Atg32 protein, as cells in the stationary phase still contain mitochondria, and mitochondrial functions are essential for their viability.

At the same time, during the first 3 hours of nitrogen starvation, Atg32-V5 levels dropped by 40% on average, changing only minimally and steadying at about 50% of the original amount after 24 hours (Fig. S2A,B). Moreover, Atg32-V5 degradation was not compromised under normal growth conditions in cells lacking Atg5 or Atg8, two essential autophagy effectors, or Atg11, a protein required for selective autophagy degradation (Fig. S3A, B). Okamoto *et al.* (2009) described a similar disappearance of the Atg32 protein in *atg7Δ* mutant strains [4]. Assuming Atg32 is essential for only mitophagy, this finding was surprising. The reason for this finding is uncertain; however, a small quantity of Atg32 might be sufficient to mediate the selective elimination of mitochondria. Alternatively, a yet to be identified posttranslational

modification of Atg32 might function in mitophagy. Also, we cannot exclude the possibility that during respiratory growth, Atg32 might be involved in unknown pathways related to mitochondrial function.

### **Atg32 turnover can be prevented by inhibition of the proteasome**

To understand why the Atg32 protein level decreases when mitophagy is induced, we examined both possibilities that could lead to its reduction: increased degradation and a reduced synthesis of the Atg32 protein. As first, we evaluated the effect of inhibitors of the two main cellular proteolytic pathways (vacuolar-autophagy systems and the ubiquitin-proteasome) on the Atg32 protein level. We observed that the addition of PMSF, an inhibitor of serine proteases that blocks several yeast vacuolar proteases (e.g., proteinase B and carboxypeptidase Y) but does not affect proteasome function, only slightly affected Atg32 protein levels, in an increment probably corresponding to the part of a protein that is degraded by mitophagy (Fig. 3A, B; 24 h and 48 h). Accordingly, the degradation of Atg32-V5 was not compromised in cells lacking Pep4, a vacuolar protease (Fig. 3C, D), confirming that degradation of Atg32 in the vacuole does not play a significant role in degradation control of the Atg32 protein.

Meanwhile, the addition of MG-132, a proteasome inhibitor that reduces the degradation of ubiquitin-conjugated proteins in mammalian cells and effectively blocks the proteolytic activity of the 26S proteasome in yeast, counteracted the Atg32 protein loss observed during the stationary growth phase (Fig. 3A, upper panel) and rapamycin treatment (Fig. S4A). We observed the same Atg32 protein level dynamic in the BY4742 strain expressing Atg32-V5 (Fig. S4B, C). Further, inhibition of proteasomal activity stabilized the Atg32 protein in exponentially growing cells, in which there is no detectable mitophagy yet (T8; Fig. S4D). However, MG-132

had only a limited effect on Atg32-V5 levels during nitrogen starvation (Fig. S2A,B). In Figures 3A and S2A (lower panels), the accumulation of ubiquitin-conjugated complexes (Ub) becomes easily detectable because these complexes are not degraded in the presence of MG-132; this serves as evidence that MG-132 is a potent proteasome inhibitor in yeast. Also, the Atg32-V5 level was restored with MG-132 treatment in *atg5Δ* mutant cells in the stationary phase (Fig. S3C).

The addition of MG-132 or PMSF did not significantly affect cell growth or growth yield (Fig. S5A). Furthermore, the simultaneous addition of MG-132 and PMSF had no significant cumulative effect on the reduction of Atg32 protein levels (Fig. S5B). Consistent with these observations, Atg32 may be degraded in both an autophagy-dependent and autophagy-independent manner.

To answer the question of whether the reduction of the Atg32 protein level during the stationary phase in respiratory conditions is due to a decrease in Atg32 synthesis or an increase in Atg32 degradation, we examined *ATG32* promoter activity. We used a construct pPROM-*ATG32-lac Z* in which the reporter gene *lacZ* was expressed from the *ATG32* promoter. Interestingly, we found that *ATG32* promoter activity increased through the course of cell growth (Fig. 4A). In the late stationary phase, *ATG32* promoter activity increased threefold to fourfold compared to *ATG32* promoter activity in cells in the early exponential phase of growth (T0). MG-132 treatment prevented this rise in *ATG32* promoter activity (Fig. 4A).

To evaluate further whether the Atg32 protein is subject to degradation control, we monitored the Atg32 protein turnover. To assess the alteration of Atg32 protein levels, *atg32Δ* mutant cells expressing ATG32-V5 were grown in a minimal lactate medium, and in the mid-

exponential growth treated with cycloheximide (250  $\mu$ g/ml CHX) to turn off protein expression. After the first 20 minutes of CHX treatment, the Atg32-V5 protein level had already decreased dramatically compared to the levels of the cytosolic protein Pgk1 or of mitochondrial protein porin, indicating that Atg32 turnover is rapid (Fig 4B, C). Additionally, Atg32-V5 was significantly stabilized upon treatment by the proteasome inhibitor MG-132; hourly inhibition of the proteasomal turnover in combination with the cycloheximide resulted in a more-than-fourfold increase in the amount of the Atg32 protein (from 15 percent to approximately 68 percent;  $P = 0.015$ ) (Fig. 4B, C). These results suggest that the half-life of the Atg32 protein is very short and is degraded by the proteasome.

Consistent with the requirement of the chymotryptic activity of the proteasome in proteasome-mediated proteolysis, Atg32-V5 turnover was impaired in yeast mutant cells that contain a mutation in the protein Pre2 (Fig. 5). Pre2 is the  $\beta$ 5 subunit of the 20S proteasome, which is required for efficient assembly of the 20S proteasome catabolic core particle essential for degrading the protein into fragments [16]. The expression of the fusion protein Atg32-V5 decreased significantly in the stationary phase in the medium with galactose in the control strain (*atg32 $\Delta$*  + Atg32-V5), just as it would in a lactate-containing medium, whereas we observe a less pronounced change for the *pre2-2* mutant strain (Fig. 5). This supports the hypothesis of the involvement of the proteasome in the disappearance of the Atg32-V5 protein in the stationary phase of cell growth.

Our data showed that under respiratory conditions, the Atg32 protein had a high turnover rate. Its level decreased during mitophagy, whereas *ATG32* promoter activity increased suggesting the decrease of the Atg32 protein level during the stationary phase is due to an

increase of Atg32 degradation. Our observations support the hypothesis that Atg32 might regulate its own protein level and activity.

The fact that treatment with MG-132 prevented the disappearance of Atg32 indicates that Atg32 protein degradation seems to be directly or indirectly dependent on proteasome activity. These results imply that Atg32 is ubiquitinated and targeted for proteasomal degradation. Accordingly, several bands exhibiting a molecular weight shift of Atg32-V5 (Figs. 3A upper panel, asterisk mark; 5A; S3C; S4A, B; S5B) ranging between 70 and 190 kDa were identified in protein extracts prepared from cells following MG-132 treatment or in *pre2-2* mutant cells. They may correspond to ubiquitinated Atg32 protein forms that were stabilized within cells due to dysfunctional proteasome.

### **Inhibition of the proteasome with MG-132 stimulates mitophagy**

It has been shown that cells lacking the Atg32 protein are deficient in mitophagy induction and that Atg32 overexpression is responsible for an increase in mitophagy [3, 4]. We showed Atg32-V5 is degraded under normal cell growth conditions (Figs. 2, 3, 5, S4B), but the protein did not disappear in the stationary phase when cells were treated with MG-132 (Figs. 2, 3, S4B) or in the *pre2-2* mutant (Fig. 5). To check whether the higher Atg32 protein level in the stationary phase after MG-132 treatment correlated with an increase of mitophagy, we assessed mitophagy induction in cells treated or untreated with MG-132. We first studied mitophagy in BY4742 + Atg32-V5 or *atg32Δ* + Atg32-V5 cells growing in respiratory conditions and expressing the mitochondrial Idp1-GFP fusion protein. Under basal conditions, Idp1-GFP is exclusively located in the mitochondrial matrix, and only the Idp1-GFP band (Fig. 6A, B; T0, 75 kDa) can be visualized by immunoanalysis. When mitophagy is induced, mitochondria are

trapped within autophagosomes and delivered into the vacuole to be degraded. GFP moiety is much more resistant to hydrolase degradation than Idp1 moiety, and thus residual GFP (27 kDa) will remain in the vacuolar lumen and serves as evidence of mitophagy induction. In untreated control cells, the GFP band first appeared in the mid-exponential phase (8 h), indicating mitophagy was activated (Fig. 6A, B). MG-132 stimulated both Idp1-GFP cleavage (Fig. 6A–C) and ATG32-V5 level (Fig. 3), consistent with the published data [3, 4] demonstrating a direct correlation between Atg32 content and mitophagy activity. To confirm these results, we measured alkaline phosphatase (ALP) activity in BY4742 cells expressing the mitochondria-targeted Pho8 $\Delta$ 60 (mtPho8 $\Delta$ 60) protein [15]. In control cells, we observed a twofold increase in ALP activity in the late stationary phase (48 h) compared to the mid-exponential phase (T0; Fig. 6D). Furthermore, at the 48 h point, MG-132 treatment induced a fourfold increase in ALP activity compared with that of T0, confirming proteasome inhibition by MG-132 causes an increase in mitophagy in the stationary phase compared to mitophagy of untreated cells. Notably, MG-132 had no stimulating effect on macroautophagy (Fig. S6).

### **Identification of ubiquitination site in Atg32 protein by LC-MS/MS analysis**

To confirm our hypothesis that the level and the activity of the Atg32 protein is regulated by ubiquitination, we purified Atg32 protein from *atg32 $\Delta$*  mutant cells expressing Atg32-V5-6xHIS harvested in the late stationary growth phase (48 h) in the presence of MG-132. The cell lysate was loaded on an affinity Ni-NTA column, as described in the Material and Methods section. After elution, individual fractions were examined by western blot (Fig. S7) first. The presence of Atg32-V5 was confirmed by immunodetection with antibodies directed against histidine and ubiquitin (Fig. S7C,D). Subsequently, fractions absorbing at 254 nm (Fig. S7A)

were pooled together, separated on 11% SDS-PAGE, and submitted to blue colloidal staining (Fig. 7A) or immunoanalysis using antibodies directed against histidine and ubiquitin (Fig. 7B), respectively.

Two bands (B1 and B2) were detected by colloidal blue staining (Fig. 7A). Nevertheless, Atg32-V5 did not migrate at its expected mass of 58.9 kD. Although we detected a small amount of protein of theoretical size in eluted fractions (Fig. S7C), most of the signal was discovered in oligomer form with a high mass (larger than 170 kD) despite the presence of SDS. The shift in mobility of Atg32 after purification is a surprising finding but not impossible to understand. Atg32 is a protein inserted into the outer membrane of the mitochondria. It has already been observed that a mitochondrial membrane protein such as the ATP synthase subunit 9 is mainly found in the form oligomers in SDS-PAGE gel despite the presence of detergents in the gel [17, 18].

To ascertain Atg32 ubiquitination, the B1 and B2 bands were submitted to a standard proteomics workflow as described in the Material and Methods section, including an on-gel proteolysis step and an analysis by LC-MS/MS of peptides. Specifically, trypsin digestion of ubiquitinated proteins cleaves off all but the two C-terminal glycine residues of ubiquitin from the modified protein. These two C-terminal glycine (GG) residues remain linked to the epsilon amino group of the modified lysine residue in the tryptic peptide derived from the digestion of the substrate protein. The presence of the GG on the side chain of that Lys prevents cleavage by trypsin at that site, resulting in an internal modified Lys residue in a formerly ubiquitinated peptide.

Atg32 was unambiguously identified in a sample obtained from the B1 band based on 21

unique peptides leading to 55.6% sequence coverage (Table 1 and Fig. S8). One of these peptides was unambiguously shown to bear the typical GG tag (+144 Da) remaining after tryptic proteolysis of ubiquitination of Lysines using two distinct search engines (SEQUEST and MASCOT) and manual validation (visual inspection of the related MS/MS spectrum). The simultaneous detection into the MS/MS spectrum of 20 b fragments and 22 y fragments (over 22 possible fragments of each) ascertains the presence of a typical GG tag on the lysine 282 and confirms at least one ubiquitination site into Atg32 (Table 1 and Fig. S8). However, the Atg32 protein contains 43 lysines, and only 17 were covered by MS analysis. Thus, 26 lysines remain to be tested. In a sample obtained from the band B2, MS analysis identified a histidine-rich protein which was also found ubiquitinated.

### **Investigation of Atg32 expression in ubiquitination-deficient Atg32 mutants**

To understand the specific role of proteasome-mediated Atg32 turnover, the identification of the specific pathway that selects Atg32 for degradation is required.

Because our principal aim was to determine the involvement of lysine 282 residue in Atg32 turnover, we replaced lysine 282 with alanine (mutant K282A). We found that the Atg32<sup>K282A</sup>-V5 mutant form is also degraded during growth. When compared to wild-type Atg32 protein, there is about 10–15% ( $P < 0.05$ ) more mutant protein in the late stationary phase cells (Fig. 8A, C; 48 h). The fact that Atg32 expression was not fully restored in the K282A mutant could indicate that additional lysine residues on Atg32 might also be ubiquitinated and thus involved in degradation control and regulation of mitophagy activity of Atg32.

When the Atg32 protein sequence was analyzed, we noticed the presence of an Rsp5-

binding motif (Leu-Pro-Lys-Tyr, LPKY) at the position 243-246. The *RSP5* gene encodes an essential ubiquitin ligase. Proteasomal substrates are usually first recognized by a ubiquitin ligase (E3), which works with a ubiquitin-activating enzyme (E1) and a ubiquitin-conjugating enzyme (E2) to decorate the substrates with the ubiquitin molecule. Ubiquitin-modified substrates are then delivered to the proteasome for degradation [19]. Because the ubiquitin ligase E3 is the rate-limiting and substrate-recognition component of the proteasome system, we examined the involvement of Rsp5 in Atg32 turnover. We replaced the LPKY motif in the *ATG32* sequence with AAAA (Ala-Ala-Ala-Ala), and we evaluated the expression of this mutant protein during cell growth. The turnover rate of the Atg32-AAAA-V5 protein was significantly ( $P<0.05$ ) impaired compared to the wild-type protein (Fig. 8B, C). This result thus indicates that the ubiquitination of Atg32 is not a straightforward process and could be (i) executed at various other lysine residues besides lysine 282 and (ii) governed by several E3 ligases (from more than 60 identified) involved in ubiquitin-mediated degradation in the yeast *S. cerevisiae*.

Next, we assessed mitophagy induction in the stationary phase in the different mutant cells potentially involved in Atg32 ubiquitination, such as Atg32<sup>K282A</sup> and Atg32-AAAA. We observed that the mitophagy activity in these two mutants is very similar to that of the control strain, with only a slight but significant increase in strains expressing K282A ( $P<0.05$ ) or Atg32-AAAA ( $P<0.01$ ) (Fig. 9 A, B).

These data suggest the link between Atg32 expression, its turnover, and that mitophagy may be more complex than we expected.

## **Discussion**

### **Regulation of mitophagy by ubiquitination**

Atg32 executes a key role as a receptor for multiple mitophagy inducing pathways and governs the final turnover of mitochondria. Therefore, a thorough regulation of its activity is expected. Besides regulation of its gene expression, post-translational modifications seem to control Atg32-mediated mitophagy. However, the pathways perceiving mitochondrial damage/impairment and Atg32 activation are not fully understood.

In this work, we were interested in (i) the expression and the stability of the Atg32 protein during mitophagy and (ii) the relationship between mitophagy, Atg32, and the proteasome. We observed that the Atg32-V5 protein was expressed in the mid-exponential phase of growth, disappeared progressively with growth, and was almost entirely missing in the stationary phase of growth as well as during longer durations of nitrogen starvation or upon rapamycin treatment. Several groups have already shown that Atg32 protein was expressed during growth in respiratory conditions and disappeared in the stationary phase of growth [4,20]. Wang *et al.* (2013) demonstrated that Atg32 is processed by Yme1 protease, resulting in Atg32 C-terminus cleavage, and this processed form is required for mitophagy [20]. We tagged Atg32 protein with a V5 tag in the C-terminus, and this recombinant protein may be subjected to Yme1 dependent processing, resulting in the loss of the V5 tag upon mitophagy induction. However, in Wang *et al.*'s study, Atg32 processing by Yme1 was weak and slow in cells grown in the presence of lactate as a carbon source, only about 5% of Atg32 was cleaved by Yme1 in both nitrogen starvation and in the stationary phase of growth [20]. Moreover, in the same article, the authors showed the disappearance of Atg32 tagged in N-terminus with a TAP tag in the

stationary phase of growth, and we also observed Atg32 turnover with the use of HA-Atg32 fusion protein. Therefore, our results concerning the disappearance of Atg32-V5 in the stationary phase of growth are in line with the published data, and Yme1 probably only plays a minor role in the disappearance of Atg32-V5 recombinant protein in this phase.

Considering the important role of the proteasome in the regulation of numerous proteins of the outer mitochondrial membrane [21,22], we assessed whether the proteasome is also involved in Atg32 degradation. Indeed, blocking the proteolytic activity of proteasome by MG-132 allowed us to prevent a decline in the Atg32 levels through the course of growth and in the stationary phase and to stabilize the modified form of Atg32. Moreover, in the proteasome *pre2-2* mutant strain, the Atg32 levels decreased to a much lesser extent than did control cells. Furthermore, the limited effect of treatment with PMSF, an inhibitor of vacuolar serine proteases, or of the deletion of the vacuolar protease Pep4 indicated that only a small part of Atg32 is degraded by mitophagy. We showed that the half-life of the Atg32 protein is short and that Atg32 protein levels are regulated by proteasome activity. Moreover, our results suggest that this regulatory mechanism is already active in exponentially growing cells, hence, before mitophagy induction. To some extent, our results differ from the observations that Levchenko et al. (2016) published. Besides differences in strains, the only explanation we can offer is that a difference in growing conditions and/or mitophagy induction leads to the involvement of various pathways regulating expression/stability of Atg32; one pathway can be more dependent on vacuolar degradation while another can undergo proteasomal degradation control.

Previous studies have shown that overexpression of Atg32 stimulates mitophagy, while it has long been known that the absence of Atg32 protein causes mitophagy impairment in yeast

[3,4]. These published data suggest that mitophagy is dependent on the amount of Atg32 protein present. Our results are in line with this observation. We showed that upon proteasome inhibition with MG-132, there is an increase in the amount of Atg32 protein, which correlates with the stimulation of mitophagy in the stationary phase of growth when compared to control (untreated) cells. It is expected that during this stimulation/induction of mitophagy, the amount of Atg32 protein is crucial, and our findings suggest that the proteasome may regulate the Atg32 protein amount so that yeast cells can control mitophagy activity.

Recently, it was found that two other Atg proteins are regulated by ubiquitination: Atg14 is degraded by the ubiquitin-proteasome system as a means to modulate autophagy activity [23], and Atg9 is degraded by the proteasome under normal conditions but stabilized upon starvation and rapamycin treatment [24].

Altogether, our data indicate that, as in mammalian cells, an interplay exists between mitochondria degradation by autophagy and the proteasome. It has been shown that outer mitochondrial membrane ubiquitin ligases, such as mammalian MULAN, MARCHV/MITOL, and yeast Mdm30, can ubiquitinate proteins involved in mitochondrial fusion and fission, targeting them for proteasome degradation and thus affecting mitochondrial dynamics [25,26,27]. These ligases ensure outer mitochondrial membrane quality control. Moreover, the Rsp5 E3 ligase has been shown to ubiquitinate Mdm34 and Mdm12, two components of ERMES, and this event is required for efficient mitophagy in yeast [28].

In mammals, mitophagy is governed by two different pathways. Numerous data show that the UPS plays a major role in Parkin-dependent mitophagy. Chan et al. (2011) observed robust recruitment of the 26S proteasome onto mitochondria, leading to widespread degradation

of mitochondrial outer membrane proteins via the UPS [29]. Strikingly, activation of the UPS not only precedes mitophagy but is also required for mitophagy. Inhibition of the UPS causes complete abrogation of mitophagy [27]. Tanaka *et al.* showed that ubiquitination of the mitofusins Mfn1 and Mfn2, two large GTPases that mediate mitochondrial fusion, is induced by Parkin upon membrane depolarization and leads to their degradation in a proteasome- and p97-dependent manner [30]. More recently, Wei *et al.* showed that proteasome-dependent mitochondrial membrane rupture is necessary for Parkin-mediated mitophagy in mammalian cells, in part via the cytoplasmic exposure to an IMM mitophagy receptor [31]. Concerning the pathway involving receptors, ubiquitination could play a different role. In mammalian cells, such a situation was observed in the case of the FUNDC1 receptor, which is primarily involved in mitophagy during hypoxia. This receptor is regulated by both phosphorylation and ubiquitination [32,33,34,35]. The mitochondrial PGAM5 phosphatase interacts with and dephosphorylates FUNDC1 serine 13 (Ser-13) residue upon hypoxia or carbonyl cyanide p-trifluoromethoxyphenylhydrazone treatment. Dephosphorylation of FUNDC1 catalyzed by PGAM5 enhances its interaction with LC3. CK2 phosphorylates FUNDC1 to reverse the effect of PGAM5 in mitophagy activation. Indeed, the mitochondrial E3 ligase MARCH5 plays a role in regulating hypoxia-induced mitophagy by ubiquitinating and degrading FUNDC1 to limit excessive mitochondria degradation [34]. Our study shows that, in yeast, in addition to phosphorylation regulation, Atg32-V5 turnover seems to be dependent on proteasome activity, and lysine 282 and Rsp5-binding motif are identified as one of the targets of ubiquitination. The fact that the mutation of the Rsp5-binding motif, Rsp5 being an E3 ligase, slightly but significantly perturbs Atg32 expression and mitophagy could indicate that this E3 ligase is

involved in the regulation of Atg32. However, we can not exclude the participation of other E3 ligases. Indeed, the effect of these mutations on mitophagy is rather subtle compared to the data obtained with inhibition of the proteasome by MG-132. This could be due to the presence of various different ubiquitination sites present in *ATG32* sequence.

Further study aimed at revealing other potential ubiquitination sites in Atg32 protein as well as examining strains with mutated both ubiquitination and phosphorylation sites could shed more light on this process.

Ubiquitination of mitochondrial proteins can play two different roles: (i) ubiquitination of proteins allows their turnover by proteasomal degradation and, consequently, their abundance and quality control; and (ii) ubiquitination of proteins localized on the outer mitochondrial membrane is a signal to trigger mitophagy. In the case of Atg32 or FUNDC1 mitophagy receptors, different post-translational modifications take place to modulate its activity and regulate mitophagy level. We can hypothesize that ubiquitination will be useful for regulating Atg32's own expression and controlling the mitophagy level. This would prevent excessive mitochondria degradation and ensure a fine-tuned mitochondria turnover.

### **Why is Atg32 regulated by multiple posttranslational modifications?**

During mitophagy induction, Atg32 is activated by a post-translational modification. This, however, does not answer the question of why the Atg32 protein is subjected to several different post-translational modifications, such as phosphorylations, ubiquitination, or other unknown modifications, and what the roles of these modifications are. Are these modifications dependent on mitophagy induction conditions (e.g., nutrient starvation, stationary phase of growth, or rapamycin treatment)? Previously, we showed that depending on the condition of induction,

mitophagy may exploit various signaling pathways [36]. The need of cells to employ various pathways could reflect different purposes of self-eating mitochondria in cell physiology at certain moments, the bioenergetic state/deficit of cells, a cell's capacity to carry a burden of damaged components, and so on. Upon starvation and in the stationary phase, mitophagy requires the same key proteins, Atg32, Atg11, and Atg8; however, in this study we demonstrated that Atg32 turnover rates differ under both conditions, which supports the idea that Atg32 can be regulated through more than one mechanism. In mammalian cells, mitophagy also has several distinct variants based on the biological distinctions of cells: Type 1 mitophagy, which occurs during nutrient deprivation; Type 2 mitophagy, which is stimulated by mitochondrial damage; and micromitophagy [37].

From the published data, phosphorylation of Atg32 at serine 114 and serine 119 by a serine/threonine protein kinase Ck2 seems to be required for the interaction with the adaptor protein Atg11 and targeting mitochondria for a degradation into the vacuole [38]. Thus, vacuolar degradation is responsible for Atg32 stability bearing this kind of modification. What is the fate of Atg32 on mitochondria that have not been selected for mitophagy? We assumed that Atg32 could be eliminated by a separate pathway of degradation in its unmodified form or after acquiring another type of modification. In fact, our results suggest that Atg32 could also be ubiquitylated, and mitophagy can be regulated by ubiquitination/deubiquitination events.

Additional experiments are needed to further investigate how cells control the level and activity of Atg32 to be able to understand the mechanisms by which cells control selective degradation of mitochondria, and the physiological significance of mitophagy. In addition, an interesting question is whether Atg32 is also involved in other cellular processes. Future studies

of yeast will address these important questions.

### **Acknowledgments and fundings**

The work in the laboratories of the authors was supported by grants from the Slovak APVV agency (SK-FR-2015-0005) (to IBK), the CNRS, the University of Bordeaux and the Doctoral International Program from IDEX of Bordeaux supported by Agence Nationale pour la Recherche (ANR-10-IDEX-03-02) (to NC and PV). France/Slovakia collaboration was supported by Campus France (Stefanik n° 35809VC) (to NC and IBK). We thank Drs Sagot, Klionsky, Pinson and Abeliovich, and Mr Athané for the gift of strains and material and Drs Chaignepain and Claverol (CGFB, Bordeaux) for helpful discussions.

### **Bibliography**

- [1] Lemasters JJ; Selective mitochondrial autophagy, or mitophagy, as a targeted defense against oxidative stress, mitochondrial dysfunction, and aging. *Rejuvenation Res.* 2005; 8: 3-5
- [2] Kissová I, Salin B, Schaeffer J, Bhatia S, Manon S, Camougrand N. Selective and non-selective autophagic degradation of mitochondria in yeast. *Autophagy.* 2007; 3: 329-336.
- [3] Kanki T, Wang K, Cao Y, Baba M, Klionsky DJ. Atg32 is a mitochondrial protein that confers selectivity during mitophagy. *Dev Cell.* 2009; 17: 98-109
- [4] Okamoto K, Kondo-Okamoto N, Ohsumi Y. Mitochondria-anchored receptor Atg32 mediates degradation of mitochondria via selective autophagy. *Dev Cell.* 2009; 17: 87-97.
- [5] Kondo-Okamoto N, Noda NN, Suzuki SW, Nakatogawa H, Takahashi I, Matsunami

- M, Hashimoto A, Inagaki F, Ohsumi Y, Okamoto K. Autophagy-related protein 32 acts as autophagic degron and directly initiates mitophagy. *J Biol Chem.* 2012; 287: 10631-10638.
- [6] Mao K, Wang K, Liu X, Klionsky DJ. The scaffold protein Atg11 recruits fission machinery to drive selective mitochondria degradation by autophagy. *Dev Cell.* 2013; 26: 9-18.
- [7] Deffieu M, Bhatia-Kissová I, Salin B, *et al.* Glutathione participates in the regulation of mitophagy in yeast. *Journal of Biological Chemistry.* 2009; 284:14828-14837.
- [8] Sakakibara K, Eiyama A, Suzuki SW, Sakoh-Nakatogawa M, Okumura N, Tani M, Hashimoto A, Nagumo S, Kondo-Okamoto N, Kondo-Kakuta C, Asai E, Kirisako H, Nakatogawa H, Kuge O, Takao T, Ohsumi Y, Okamoto K. Phospholipid methylation controls Atg32-mediated mitophagy and Atg8 recycling. *EMBO J.* 2015, 34:2703- 2719.
- [9] Eiyama A, Okamoto K. Protein N-terminal Acetylation by the NatA Complex Is Critical for Selective Mitochondrial Degradation. *J Biol Chem.* 2015; 290: 25034-25044.
- [10] Mao K, Wang K, Zhao M, Xu T, Klionsky DJ. Two MAPK-signaling pathways are required for mitophagy in *Saccharomyces cerevisiae*. *J Cell Biol.* 2011;193: 755-767.
- [11] Aoki Y, Kanki T, Hirota Y, Kurihara Y, Saigusa T, Uchiumi T, Kang D. Phosphorylation of Serine 114 on Atg32 mediates mitophagy. *Mol Biol Cell.* 2011; 22: 3206-3217.
- [12] Levchenko M, Lorenzi I, Dudek J. The Degradation Pathway of the Mitophagy Receptor Atg32 Is Re-Routed by a Posttranslational Modification. *Plos One.* 2016;11: e0168518.

- [13] Kanki T, Wang K, Baba M, Bartholomew CR, Lynch-Day MA, Du Z, Geng J, Mao K, Yang Z, Yen WL, Klionsky DJ. A Genomic Screen for Yeast Mutants Defective in Selective Mitochondria Autophagy. *Mol Biol Cell* 2009,20:4730-4738.
- [14] Becuwe M, Vieira N, Lara D, Gomes-Rezende J, Soares-Cunha C, Casal M, Haguenaer-Tsapis R, Vincent O, Paiva S, Léon S. A molecular switch on an arrestin-like protein relays glucose signaling to transporter endocytosis. *J Cell Biol.* 2012,196:247-259.
- [15] Klionsky D et al. Guidelines for the Use and Interpretation of Assays for Monitoring Autophagy. 2012, *Autophagy*, 8: 445-454.
- [16] Arendt CS and Hochstrasser M. Eukaryotic 20S proteasome catalytic subunit propeptides prevent active site inactivation by N-terminal acetylation and promote particle assembly. *EMBO J.* 1999; 18:3575-3585
- [17] Arselin G, Vaillier J, Graves PV, Velours J. ATP Synthase of Yeast Mitochondria. Isolation of the Subunit H and Disruption of the ATP14 Gene. *J Biol Chem.* 1996, 271: 20284-20290.
- [18] Velours J, Paumard P, Soubannier V, Spannagel C, Vaillier J, Arselin G, Graves PV. Organization of the yeast ATP synthase FO: a study based on cysteine mutants, thiol modification and cross-linking reagents *Biochimica and Biophysica Acta* 2000, 1458: 443-456.
- [19] Finley D, Ulrich HD, Sommer T, Kaiser P. The ubiquitin-proteasome system of *Saccharomyces cerevisiae*. *Genetics.* 2012; 192:319-360.
- [20] Wang K, Jin M, Liu X, Klionsky DJ. Proteolytic processing of Atg32 by the mitochondrial i-AAA protease Yme1 regulates mitophagy. *Autophagy.* 2013; 9: 1828-1836.
- [21] Karbowski M, Youle RJ. Regulating mitochondrial outer membrane proteins by ubiquitination and proteasomal degradation. *Curr Opin Cell Biol.* 2011; 23: 476-482.
- [22] Braun RJ and Westermann B. With the Help of MOM: Mitochondrial Contributions to Cellular Quality Control. *Trends Cell Biol.* 2017; 27: 441-452.
- [23] Liu CC, Lin YC, Chen YH, Chen CM, Pang LY, Chen HA, Wu PR, Lin MY., Jiang ST,

- Tsai TF, Chen RH. Cul3-KLHL20 ubiquitin ligase governs the turnover of ULK1 and VPS34 complexes to control autophagy termination *Mol. Cell*, 61 (2016), pp. 84-97
- [24] Hu G, Rios L, Yan Z, Jasper AM, Luera D, Luo S, Rao H. Autophagy regulator Atg9 is degraded by the proteasome. *Biochem Biophys Res Commun*. 2020; 522:254-258.
- [25] Yonashiro R, Ishido S, Kyo S et al. A novel mitochondrial ubiquitin ligase plays a critical role in mitochondrial dynamics. *EMBO Journal* 2006; 25: 3618-3626.
- [26] Zhang B, Huang J, Li HL, Liu T, Wang YY, Waterman P, Mao AP, L.G. Xu LG, Zhai Z, Liu D, Murrack P, Shu HB. GIDE is a mitochondrial E3 ubiquitin ligase that induces apoptosis and slows growth. *Cell Res*. 2008; 18: 900-910.
- [27] Cohen MM, Leboucher GP, Livnat-Levanon N, Glickman MH, Weissman AM. Ubiquitin-proteasome-dependent degradation of a mitofusin, a critical regulator of mitochondrial fusion *Mol Biol Cell*. 2008; 19: 2457-2464.
- [28] Belgareh-Touzé N, Cavellini L, Cohen MM. Ubiquitination of ERMES components by the E3 ligase Rsp5 is involved in mitophagy. *Autophagy* 2017; 13: 114-132.
- [29] Chan NC, Salazar AM, Pham AH, Sweredoski MJ, Kolawa NJ, Graham RL, et al. Broad activation of the ubiquitin-proteasome system by Parkin is critical for mitophagy. *Hum Mol Genet*. 2011;20:1726–1737.
- [30] Tanaka A, Cleland MM, Xu S, Narendra DP, Suen DF, Karbowski M, Youle RJ. Proteasome and p97 mediate mitophagy and degradation of mitofusins induced by Parkin. *J Cell Biol*. 2010;191:1367–1380.
- [31] Wei Y, Chiang WC, Sumpter Jr. R, Prashant Mishra P and Beth Levine B. Prohibitin 2 Is an Inner Mitochondrial Membrane Mitophagy Receptor. *Cell*. 2017; 168: 224–238.
- [32] Liu L, Feng D, Chen G, Chen M, Zheng Q, Song P, Ma Q, Zhu C, Wang R, Qi W, Huang L, Xue P, Li B, Wang X, Jin H, Wang J, Yang F, Liu P, Zhu Y, Sui S, Chen Q. Mitochondrial outer-membrane protein FUNDC1 mediates hypoxia-induced mitophagy in mammalian cells. *Nat Cell Biol*. 2012; 14: 177-185.

- [33] Wu W, Tian W, Hu Z, Chen G, Huang L, Li W, Zhang X, Xue P, Zhou C, Liu L, Zhu Y, Zhang X, Li L, Zhang L, Sui S, Zhao B, Feng D. ULK1 translocates to mitochondria and phosphorylates FUNDC1 to regulate mitophagy. *EMBO Rep.* 2014; 15: 566-575.
- [34] Chen Z, Liu L, Cheng Q, Li Y, Wu H, Zhang W, Wang Y, Sehgal SA, Siraj S, Wang X, Wang J, Zhu Y, Chen Q. Mitochondrial E3 ligase MARCH5 regulates FUNDC1 to fine-tune hypoxic mitophagy. *EMBO Rep.* 2017;18: 495-509.
- [35] Chen G, Han Z, Feng D, Chen Y, Chen L, Wu H, Huang L, Zhou C, Cai X, Fu C, Duan L, Wang X, Liu L, Liu X, Shen Y, Zhu Y, Chen Q. A regulatory signaling loop comprising the PGAM5 phosphatase and CK2 controls receptor-mediated mitophagy. *Mol Cell.* 2014; 54: 362-377.
- [36] Vigié P, Cougouilles E, Bhatia-Kiššová I, Salin B, Blancard C, Camougrand N. The mitochondrial phosphatidylserine decarboxylase Psd1 is involved in nitrogen starvation-induced mitophagy in yeast. *J Cell Sci.* 2019 Jan 2;132(1). pii: jcs221655. doi: 10.1242/jcs.221655.
- [37] Lemasters JJ. Variants of mitochondrial autophagy: Types 1 and 2 mitophagy and micromitophagy (Type 3). *Redox Biol.* 2014;2:749-754.
- [38] Kanki T, Kurihara Y, Jin X; Goda T, Ono Y, Aihara M, Hirota Y, Saigusa T, Aoki Y, Uchiumi T, Kang D. Casein kinase 2 is essential for mitophagy. *EMBO Rep.* 2013;14: 788-794.

## Legends to figures

**Figure 1: Atg32-V5 protein localizes to mitochondria and restores mitophagy in *atg32Δ* mutant strain.** (A) *atg32Δ* mutant cells grown in a CMS-L medium and expressing Atg32-V5 fusion protein were harvested in a mid-exponential phase of growth (T<sub>0</sub>). Then cells were lysed and lysates were separated in a 20–55% OptiPrep density gradient. Fractions were collected after centrifugation and analyzed by western blots. Anti-V5 antibody was used to visualize Atg32-V5, and anti-Porin antibody was used to detect mitochondria-containing fractions. P<sub>gk1</sub>, the cytosolic phosphoglycerate kinase, was used as a cytosolic marker; and D<sub>pms</sub>, dolichyl phosphate mannose synthase, was used as an endoplasmic reticulum marker. (B) Mitophagy was

assessed using mitophagy-dependent processing of the Idp1-GFP tool in wild-type (BY4742), *atg32Δ* mutant, or *atg32Δ*-expressing Atg32-V5. Cells were harvested in a mid-exponential phase of growth (T0), an early stationary phase (24 h), or a late stationary phase (48 h). The total protein extracts corresponding to  $5 \times 10^6$  cells/50 ug proteins per line were separated by 12.5% SDS-PAGE and analyzed by immunodetection using anti-GFP antibody.

**Figure 2: The Atg32 protein is degraded during cell growth.** *atg32Δ* mutant cells grown in a CMS-L medium and expressing recombinant proteins were harvested in a mid-exponential phase of growth (T0) and after 8-, 24-, and 48 h from T0. (A,C) Total protein extracts were prepared at indicated times, and samples were analyzed as described in Fig. 1B. Anti-V5 and anti-HA antibodies were used to visualize Atg32-V5 or HA-Atg32 recombinant proteins. (B,D) The Atg32-V5/Pgk1 or HA-Atg32/Pgk1 ratios were quantified by using ImageJ software; \* $P < 0.05$ , \*\* $P < 0.01$ .

**Figure 3: Degradation of the Atg32 protein is prevented by inhibition of the proteasome.** (A) *atg32Δ* mutant cells grown in a CMS-L medium and expressing Atg32-V5 recombinant protein were harvested at indicated time points. To inhibit the proteasome, 75  $\mu$ M MG-132 was added to the cell culture at the 8 h time point. To inhibit vacuolar proteolysis, 2 mM PMSF was added to the cell culture at the 8 h time point; this step was repeated several times during the whole course of cell growth. Total protein extracts were prepared, and protein samples were analyzed as described in Fig. 1B. Anti-V5 antibody was used to visualize Atg32-V5 protein. Anti-ubiquitin (Ub) was used to detect the level of ubiquitinated proteins. (B) Atg32-V5 expression was quantified as the Atg32-V5/Pgk1 ratio; \*\*  $P < 0.01$ . (C) BY4742 and *pep4Δ* mutant cells expressing Atg32-V5 were grown in a CMS-L medium. Cells were harvested in a mid-exponential (T0) and a late stationary phase (48 h) of growth. Total protein extracts were prepared and analyzed by western blots. Anti-V5 antibody was used to visualize Atg32-V5 protein. (D) The Atg32-V5/Pgk1 ratio was quantified at T0 and 48 h time points for all tested strains— \* $P < 0.05$  and \*\* $P < 0.01$ .

**Figure 4: Evaluation of *ATG32* promoter activity and Atg32 protein stability.** (A) BY4742 cells grown in a CMS-L medium and expressing  $\beta$ -galactosidase under the *ATG32* promoter were harvested in a mid-exponential phase of growth (T0) and after 24 h and 48 h from T0 in the absence or presence of MG-132. After cell lysis, the  $\beta$ -galactosidase activity was measured. Results were obtained from 6 independent experiments and are expressed as the % of T0. The symbol \*\* indicates significant difference between 48 h in the absence of and 48 h in the presence of MG-132 ( $P < 0.01$ ). (B) *atg32Δ* mutant cells grown in a CMS-L medium and expressing Atg32-V5 protein were harvested in a mid-exponential phase (T0) and then treated with 250  $\mu$ g/ml of cycloheximide (CHX) in the presence or absence of 75  $\mu$ M MG-132 for 20 min, 40 min, and 1 h. Total protein extracts were analyzed by western blots. Anti-V5 antibody was used to visualize Atg32-V5 protein. Pgk1 was used as a loading control; Porin was used as a mitochondrial protein marker. At least 3 independent experiments were carried out for each condition. (C) Atg32-V5 expression was quantified as the Atg32-V5/Pgk1 ratio; \*  $P < 0.05$  and \*\* $P < 0.01$ .

**Figure 5: Degradation of Atg32 protein is impaired in *pre2-2* mutant cells.** (A) *atg32Δ* and *pre2-2* mutant cells transformed with a plasmid expressing Atg32-V5 were grown in a CMS-G medium. Cells were harvested in a mid-exponential phase of growth (T0) and after 8, 24, and 48 h of cell growth. (B) The Atg32-V5/Pgk1 ratio was quantified at T0 and 48 h time points for all tested strains— \*\*  $P < 0.01$ .

**Figure 6: Stabilization of Atg32 protein by proteasome inhibition stimulates mitophagy.** (A,B) *atg32Δ* mutant (A) and BY4742 (B) cells expressing Atg32-V5 and Idp1-GFP proteins grown in a CMS-L medium were harvested at indicated times of growth. To inhibit the proteasome, 75  $\mu$ M MG-132 was added to the cell culture at the 8 h time point. Total protein extracts were prepared and analyzed as described in Fig. 1B. Proteins were detected using antibodies against GFP or Pgk1. (C) GFP/GFP+Idp1-GFP ratios were quantified at the 24 h and

48 h time points for all tested conditions. Error bars represent standard error of the mean. **(D)** BY4742 cells expressing mtPHO8 $\Delta$ 60 protein grown in a CMS-L medium were harvested at the mid-exponential (T0) and late stationary (48 h) phases. MG-132 was added as described in (A). ALP activity was measured as described in the Material and Methods section. The symbol \*\* indicates significant difference between the 48-h time point with and without MG-132 ( $P < 0.01$ ).

**Figure 7: Atg32 purification and mass spectrometry analysis.** **(A)** *atg32 $\Delta$*  mutant cells expressing Atg32-V5-6HIS were grown in a CMS-L medium until a late stationary phase (48 h) in presence of MG-132. Cells were lysed and loaded on a Ni-NTA column as described in the Material and Methods section. After the last elution, collected fractions absorbing at 254 nm (from 14 to 17) were pooled together, precipitated with TCA. Pellet was resuspended in 60  $\mu$ l of the loading buffer, 50  $\mu$ l (eluted fraction) were loaded on a 11% SDS-PAGE. After migration, the gel was colored with colloidal blue. The bands B1 and B2 were excised and analyzed by mass spectrometry. **(B)** 5  $\mu$ L of pooled fraction from A (Eluted fraction) were separated in a 11% SDS-PAGE gel. Proteins were analyzed by western blots using antibodies against histidine (anti HIS) or ubiquitin (anti Ub), respectively. Input: 50  $\mu$ L of cell lysate prepared in (A) was precipitated with TCA, pellet was resuspended in 50  $\mu$ L of the loading buffer, and 4  $\mu$ L were loaded on the gel.

**Figure 8: Evaluation of Atg32 degradation in ubiquitination-deficient Atg32 mutants.** *atg32 $\Delta$*  cells grown in a CMS-L medium and expressing wild-type Atg32-V5 or Atg32-V5<sup>K282A</sup> **(A)** or Atg32-V5 with mutated *RSP5*-binding motif (Atg32-AAAA-V5) **(B)** recombinant proteins were harvested at indicated times. Total protein extracts were prepared, and samples were analyzed by western blots. Anti-V5 antibody was used to visualize Atg32-V5 protein. **(C)** Wild-type or mutant forms of Atg32-V5 protein levels were quantified as the Atg32-V5/Pgk1 ratio. The symbol \* indicates significant difference between Atg32-V5 and Atg32<sup>K282A</sup>-V5 on one side and Atg32-V5 and Atg32-AAAA-V5 on the other side ( $P < 0.05$ ).

**Figure 9: Evaluation of mitophagy in ubiquitination-deficient Atg32 mutants.** (A) *atg32Δ* cells grown in a CMS-L medium and expressing Idp1-GFP fusion protein and Atg32-V5 recombinant protein with mutation K282A or mutated Rsp5-binding motif (AAAA) were harvested at indicated times. Mitophagy was assessed using mitophagy-dependent processing of the Idp1-GFP tool as described in Fig. 1B. (B) Mitophagy induction was quantified as the ratio of GFP/(Idp1-GFP+GFP). The symbols \*\* and \* indicate significant differences between Atg32-V5 and Atg32-AAAA-V5 ( $P < 0.01$ ) or between Atg32-V5 and Atg32-K282A ( $P < 0.05$ ), respectively.

**Table1 : List of peptides found after mass spectrometry analysis of Atg32 protein.**

Annotated sequence	Modifications
[K]. GTLQINFHSDGFIMK.[S]	1xOxidation [M14]
[K]. SLTSSTNSFVMPK.[L]	1xOxidation [M14]
[K]. SMPPDSSSTTIHTCSEAQTGEDK.[G]	1xCarbamidomethyl [C14] ; 1xOxidation [M2]
[R]. IVQYSQGKPVIPICQPGQVIQVK.[N]	1xCarbamidomethyl [C14] ; 1xGG [K8]
[R]. IVQYSQGKPVIPICQPGQVIQVK.[N]	1xCarbamidomethyl [C14]
[K]. SMPPDSSSTTIHTCSEAQTGEDK.[G]	1xCarbamidomethyl [C14]
[K]. SMPPDSSSTTIHTCSEAQTGEDKGLLDPHLSVLELLSK.[T]	1xCarbamidomethyl [C14]
[R]. CSSQTTNGSILSSSDTSEEEQELLQAPAADIINI.K.[Q]	1xCarbamidomethyl [C1]
[K]. MNTFVLHALSKPLK.[F]	
[K]. QGQEGANVVSPSHPFK.[Q]	
[M]. VLEYQQR.[E]	
[K]. YHDSATFPQYTGIVIIIFQELR.[E]	
[K]. SLTSSTNSFVMPK.[L]	
[K]. SSEFSIDESNR.[I]	
[K]. TPFENQDDDGDEDEAFEEDSVITK.[S]	
[R]. TGSSFYQSIPK.[E]	
[K]. EYQSLFELPK.[Y]	
[K]. EKTPFNEQDDDGDEDEAFEEDSVITK.[S]	
[R]. EMVSLNLR.[I]	
[K]. FLENLNK.[S]	
[K]. LLFPPVVVTNK.[R]	
[K]. LLFPPVVVTNKR.[D]	
[R]. LQDLSLEYGEDVNEEDNDDEAIHTK.[S]	
[K]. GLLDPHLSVLELLSK.[T]	
[K].GTLQINFHSDGFIMK.[S]	

## Supplementary information

**S1 Figure: Atg32-V5 recombinant protein localizes into mitochondria and restores mitophagy in *atg32Δ* mutant cells upon nitrogen starvation.** (A) *atg32Δ* mutant cells grown in a CMS-L medium and expressing Atg32-V5 protein were harvested in a mid-exponential phase of growth. Then, cells were lysed and purified mitochondria prepared as described in Vigie et al. [34] were loaded on a 20–60% sucrose gradient. Fractions were collected and analyzed by immunodetection. Anti-V5 antibody was used to visualize Atg32-V5, and anti-Porin antibody was used to detect mitochondria-containing fractions. (B) Mitophagy was assessed using mitophagy-dependent processing of the Idp1-GFP tool in *atg32Δ* mutant and *atg32Δ*-expressing Atg32-V5. Cells were harvested at indicated times. The total protein extracts corresponding to  $5 \times 10^6$  cells/50 ug proteins per line were separated by 12.5% SDS-PAGE and analyzed by immunodetection using anti-GFP antibody.

**S2 Figure: The Atg32 protein is degraded upon nitrogen starvation.** (A) *atg32Δ* mutant cells grown in a CMS-L medium and expressing Atg32-V5 protein were harvested at indicated times. To inhibit the proteasome, 75  $\mu$ M MG-132 was added to the cell culture at the beginning of starvation. Total protein extracts were prepared afterwards, and samples were analyzed by western blots. Anti-V5 antibody was used to visualize Atg32-V5 protein; Pgk1 was used as a

loading control. Anti-ubiquitin (Ub) was used to detect the level of ubiquitinated proteins. **(B)** The Atg32-V5/Pgk1 ratio was quantified for all tested conditions.

**S3 Figure: Degradation of Atg32 protein is not impaired in autophagy-deficient mutants under normal growth condition.** **(A)** *atg5Δ*, *atg8Δ*, and *atg11Δ* mutant cells transformed with a plasmid expressing Atg32-V5 were grown in a CMS-L medium. Cells were harvested at indicated times. **(B)** The Atg32-V5/Pgk1 ratios were quantified at T0 and 48 h time points for all tested strains; \*\*  $p < 0.01$ . **(C)** *atg5Δ* mutant cells expressing Atg32-V5 were treated with MG-132 at time point 8 h. Cells were harvested at indicated time points and total protein extracts were prepared and analyzed by immunodetection. Anti-V5 antibody was used to visualize Atg32-V5 protein.

**S4 Figure: (A) The Atg32 protein is degraded upon rapamycin treatment and stabilized by the proteasome inhibition.** *atg32Δ* mutant cells grown in a CMS-L medium and expressing Atg32-V5 protein were harvested at T0 and treated with 0.2  $\mu\text{g/ml}$  rapamycin in presence or absence of 75  $\mu\text{M}$  MG-132 for 3 h, 6 h, and 24 h. Total protein extracts were prepared afterwards, and samples were analyzed by immunodetection. Anti-V5 antibody was used to visualize Atg32-V5 protein. **(B) The Atg32 protein is degraded in BY4742 strain.** BY4742 cells transformed with a plasmid expressing Atg32-V5 grown in a CMS-L medium were harvested at indicated times. To inhibit proteasome, MG-132 was added to the cell culture at 8 h time point. **(C)** The Atg32-V5/Pgk1 ratios were quantify for all tested conditions— \*\* $P < 0.01$ . **(D) MG-123 stabilizes the Atg32 protein in exponentially growing cells.** *atg32Δ* mutant cells grown in a CMS-L medium and expressing Atg32-V5 protein were harvested at T0 and treated with 75  $\mu\text{M}$  MG-132. Cells were harvested at exponential (T8) and stationary (T24, T48) phase, and total protein extracts were prepared and analyzed by immunodetection. Anti-V5 antibody was used to visualize Atg32-V5 protein.

**S5 Figure: The effect of MG-132 and PMSF treatment on cell growth and Atg32-V5 protein degradation.** **(A)** Addition of proteasome inhibitor MG-132 (75  $\mu\text{M}$  MG-132) and inhibitor of vacuolar proteolysis PMSF (2 mM) do not affect growth and growth yield in *atg32Δ*

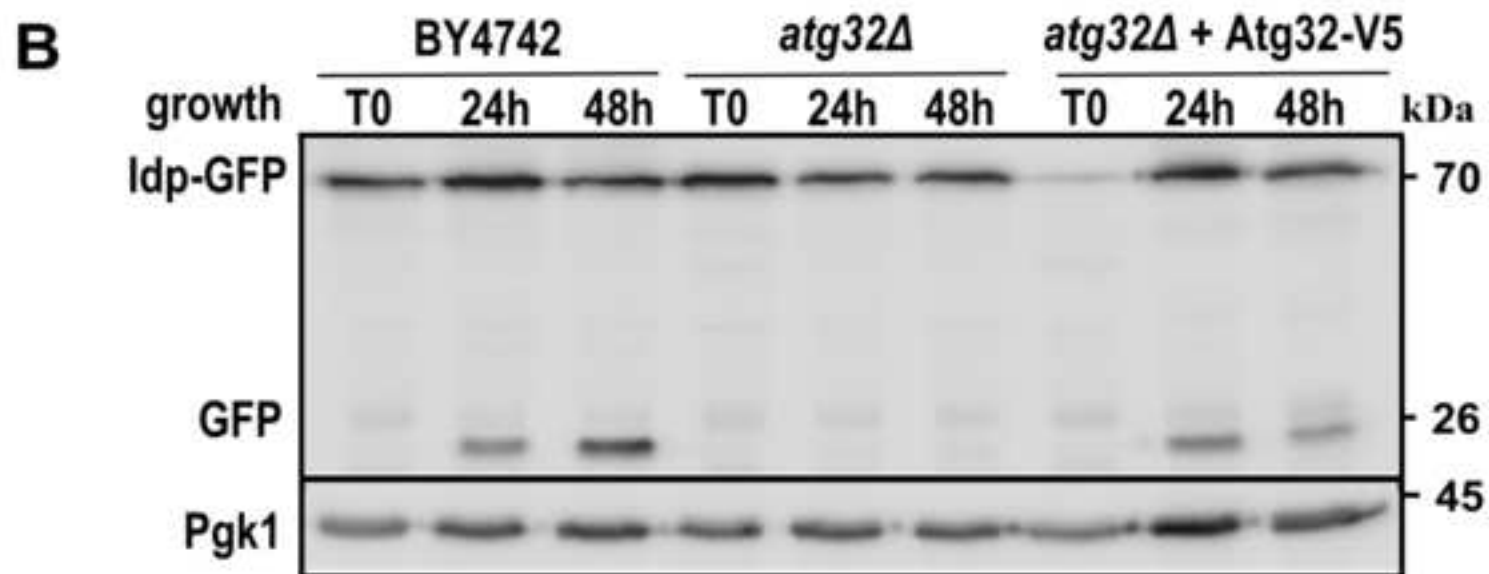
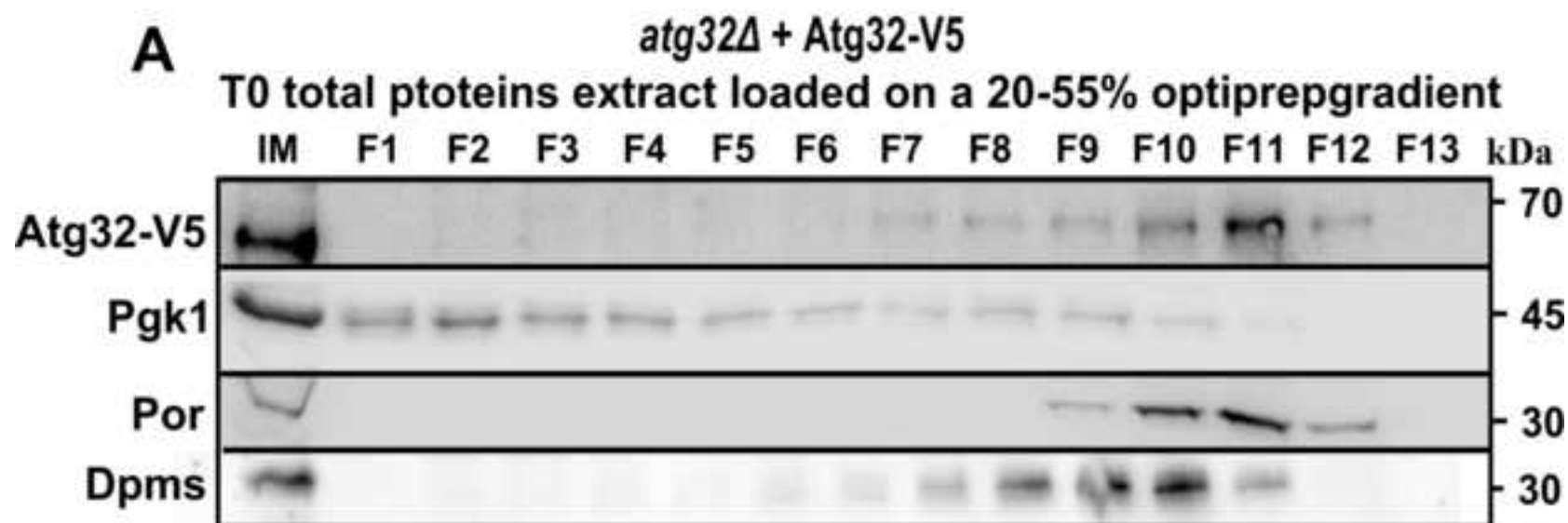
mutant cells expressing Atg32-V5 plasmid and grown in a CMS-L medium. The Y-axis is represented in logarithmic scale (n = 5 for control and MG-132; n = 3 for PMSF). **(B)** *atg32Δ* cells grown in a CMS-L medium and expressing Atg32-V5 protein were harvested at indicated time points. To inhibit proteasome, MG-132 was added to the cell culture at 8 h time point. To inhibit vacuolar proteolysis, 2 mM PMSF was added to the cell culture at T8; this step was repeated twice during the course of cell growth. Total protein extracts were prepared afterwards, and samples were analyzed by western blots. Anti-V5 antibody was used to visualize Atg32-V5 protein. To detect modified Atg32-V5 forms (bands with a higher molecular weight) after MG-132 treatment, two different revelation times of blots are presented.

**S6 Figure : Inhibition of the proteasome with MG-132 does not affect autophagy.** BY4742 **(A)** and *atg32Δ* mutant **(B)** cells expressing GFP-Atg8 protein grown in a CMS-L medium in presence or absence of MG-132 were harvested at indicated times. Total protein extracts from  $2 \times 10^7$  cells were prepared and separated by 12.5% SDS-PAGE gel as described in the Material and Methods section. Proteins were detected using antibodies against GFP or Pgk1.

**S7 Figure: Purification of Atg32-V5-6HIS.** **(A)** Lysate from *atg32Δ* mutant cells expressing *pATG32-V5-6HIS* was prepared as described in the Material and Methods section. Next, lysate was loaded on a Ni-NTA column, the non-retained fraction, as well as the two washes W1 and W2, were recovered. The bounded proteins were then eluted and 500  $\mu$ l fractions were collected. **(B-D)** 250  $\mu$ l of each fraction absorbing at 254 nm (from F12 to F22) were precipitated with TCA. Pellets were resuspended in 20  $\mu$ l of the loading buffer; 10  $\mu$ l were loaded on the gel to be revealed with the colloidal blue **(B)** and 5  $\mu$ l were used for immunodetection with anti-histidine **(C)** or anti-ubiquitin antibodies **(D)**, respectively.

**S8 Figure: Mass spectrometry analysis.** **(A)** SEQUEST spectra, **(B)** MASCOT spectra, and **(C)** Protein coverage.

# Figure 1



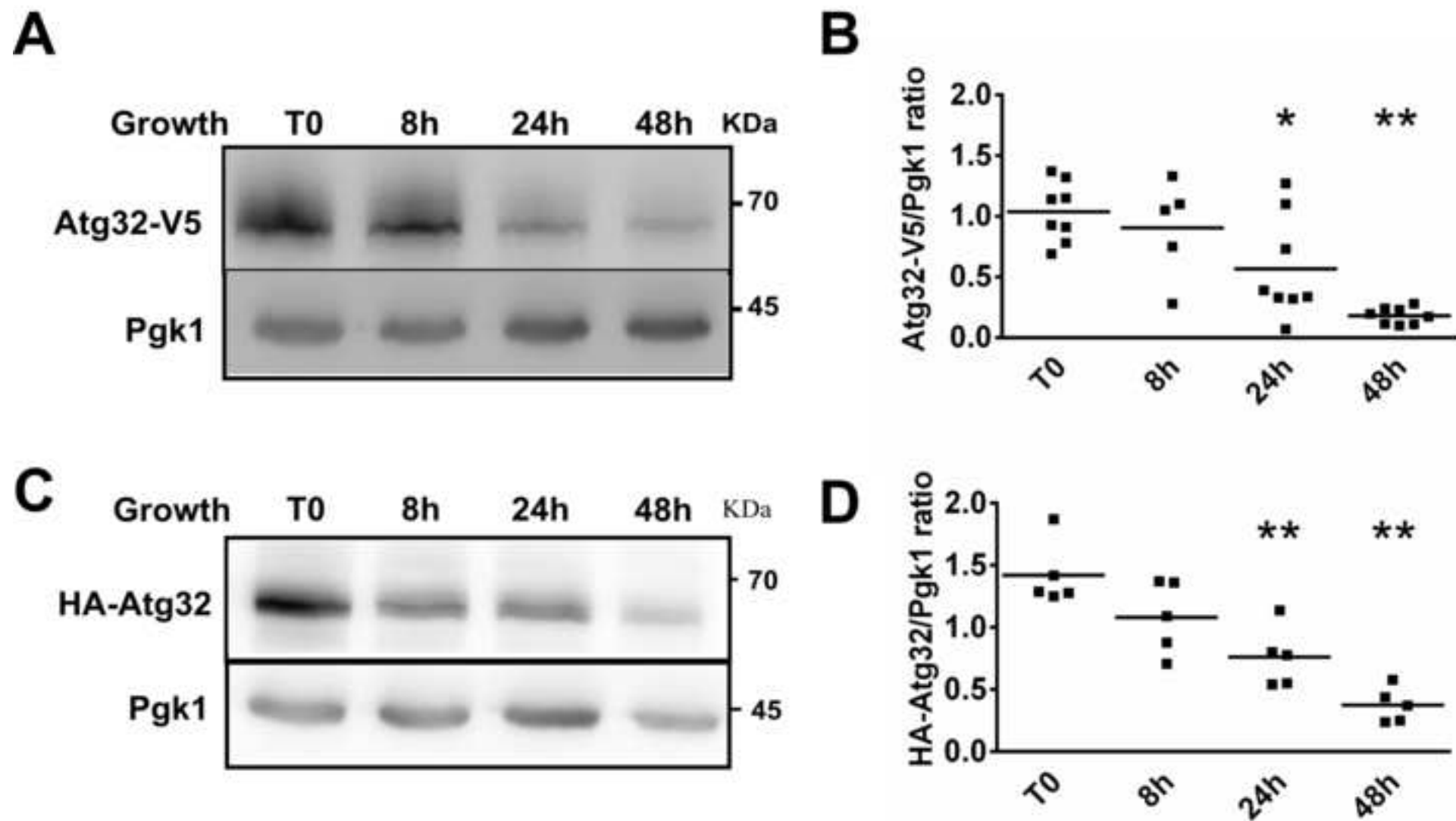
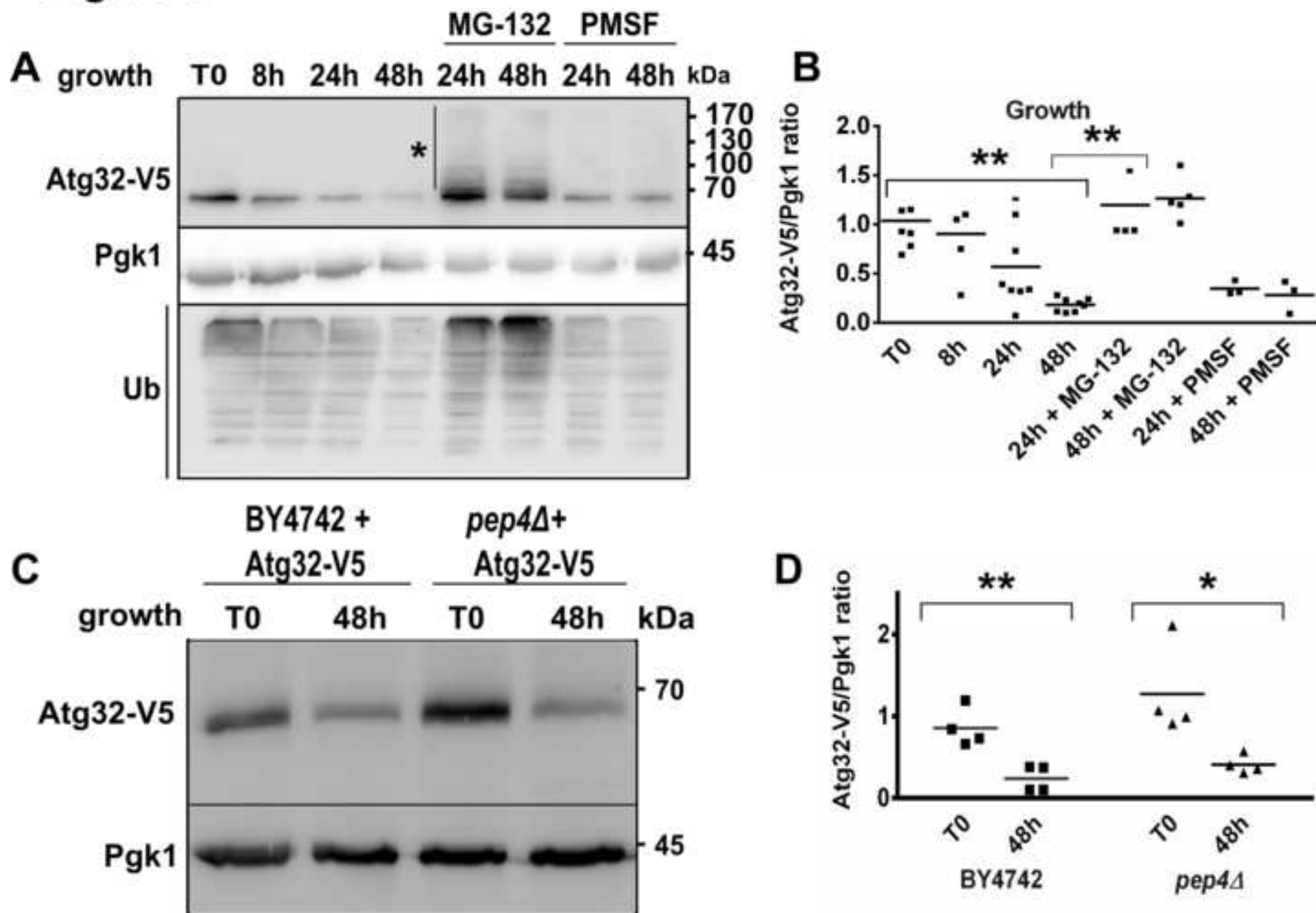
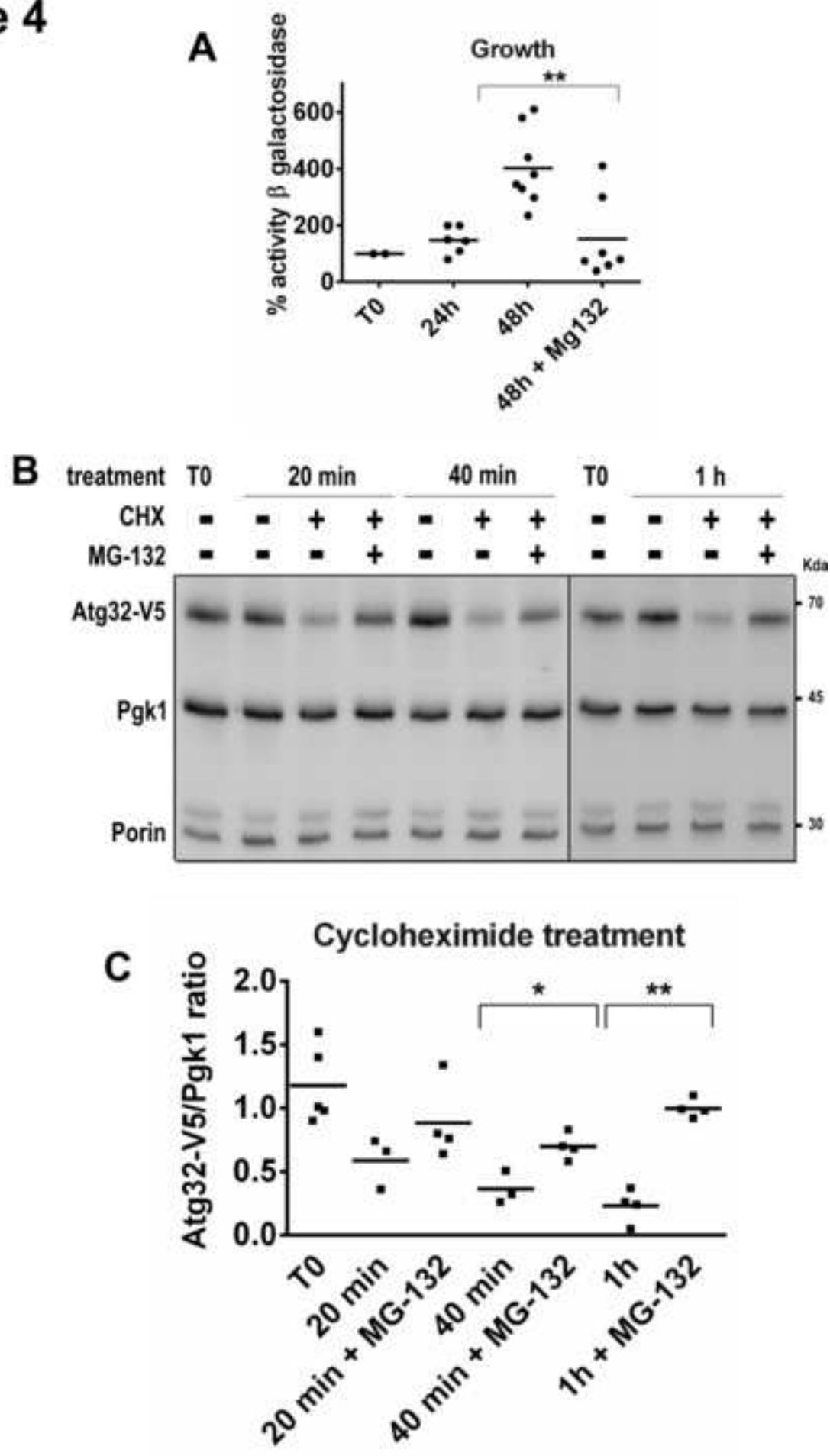
**Figure 2**

Figure 3



## Figure 4



# Figure 5

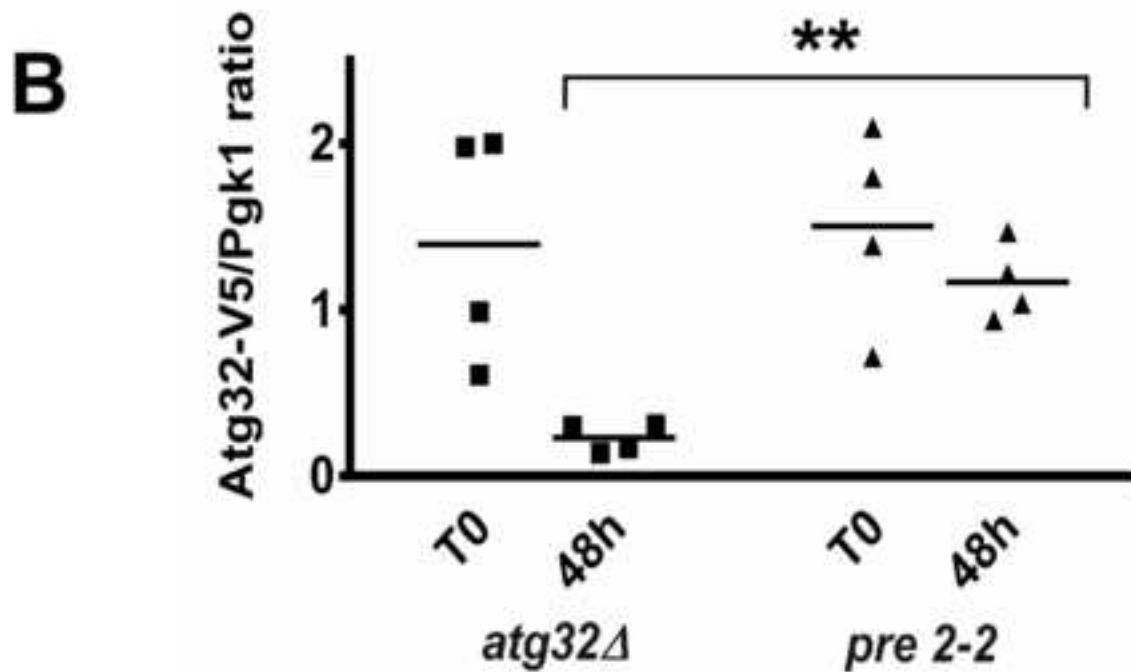
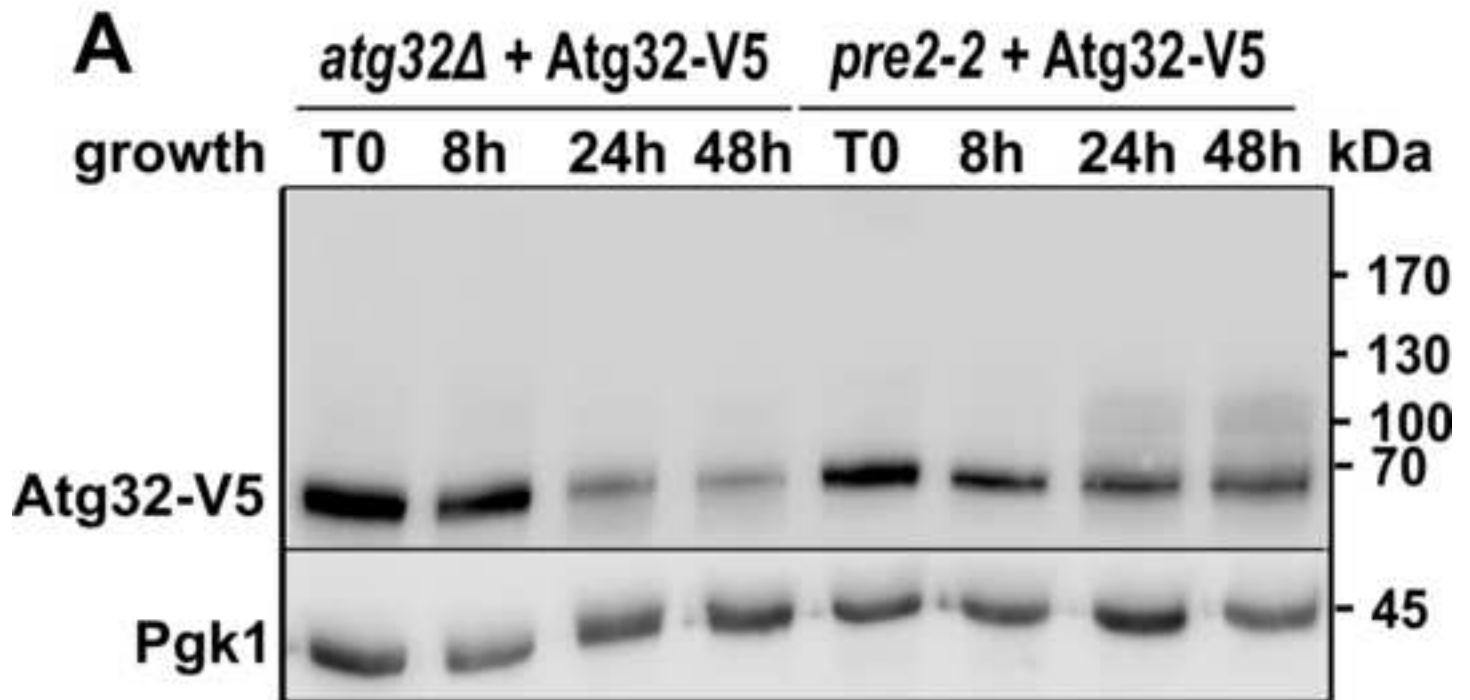


## Figure 6

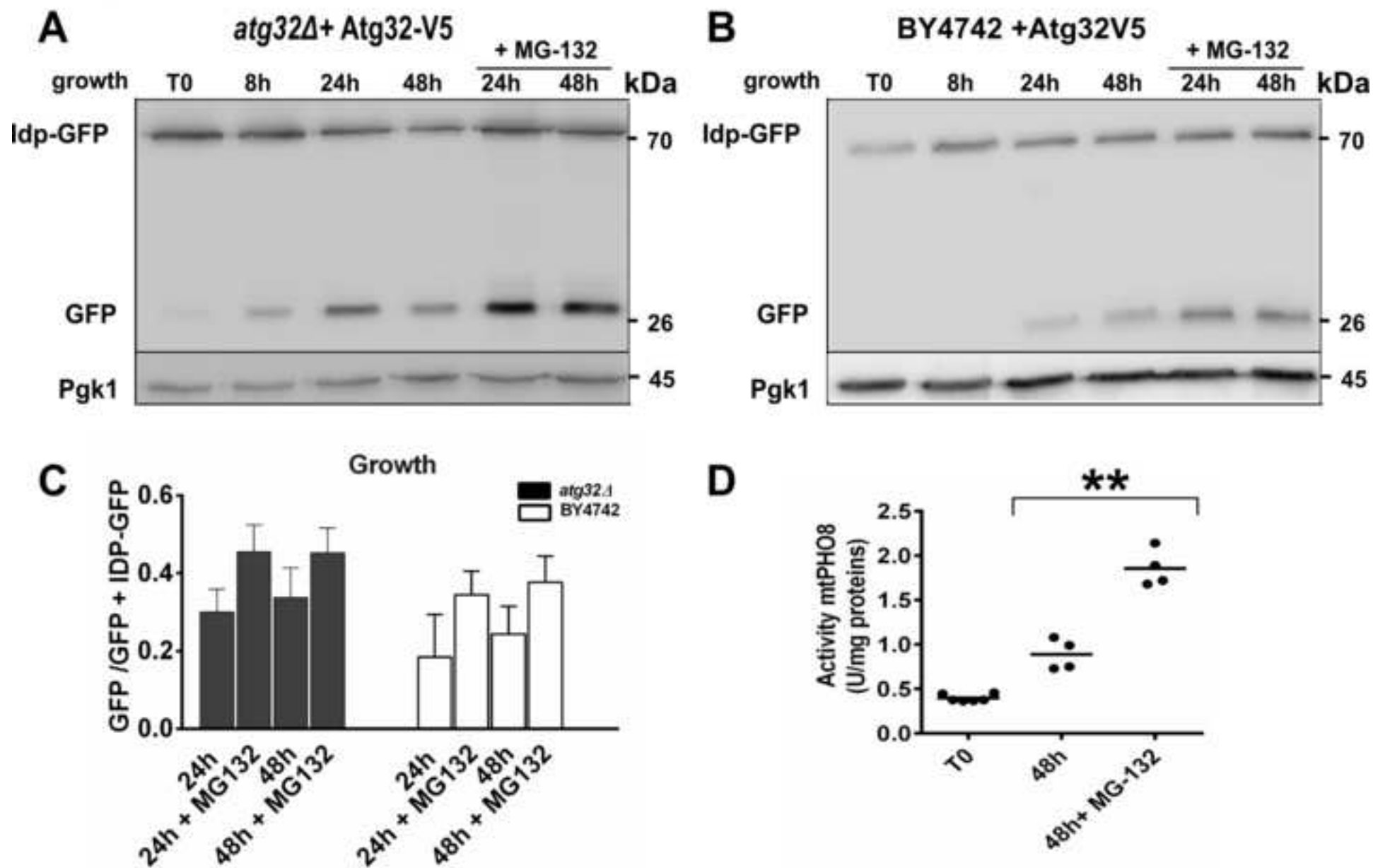


# Figure 7

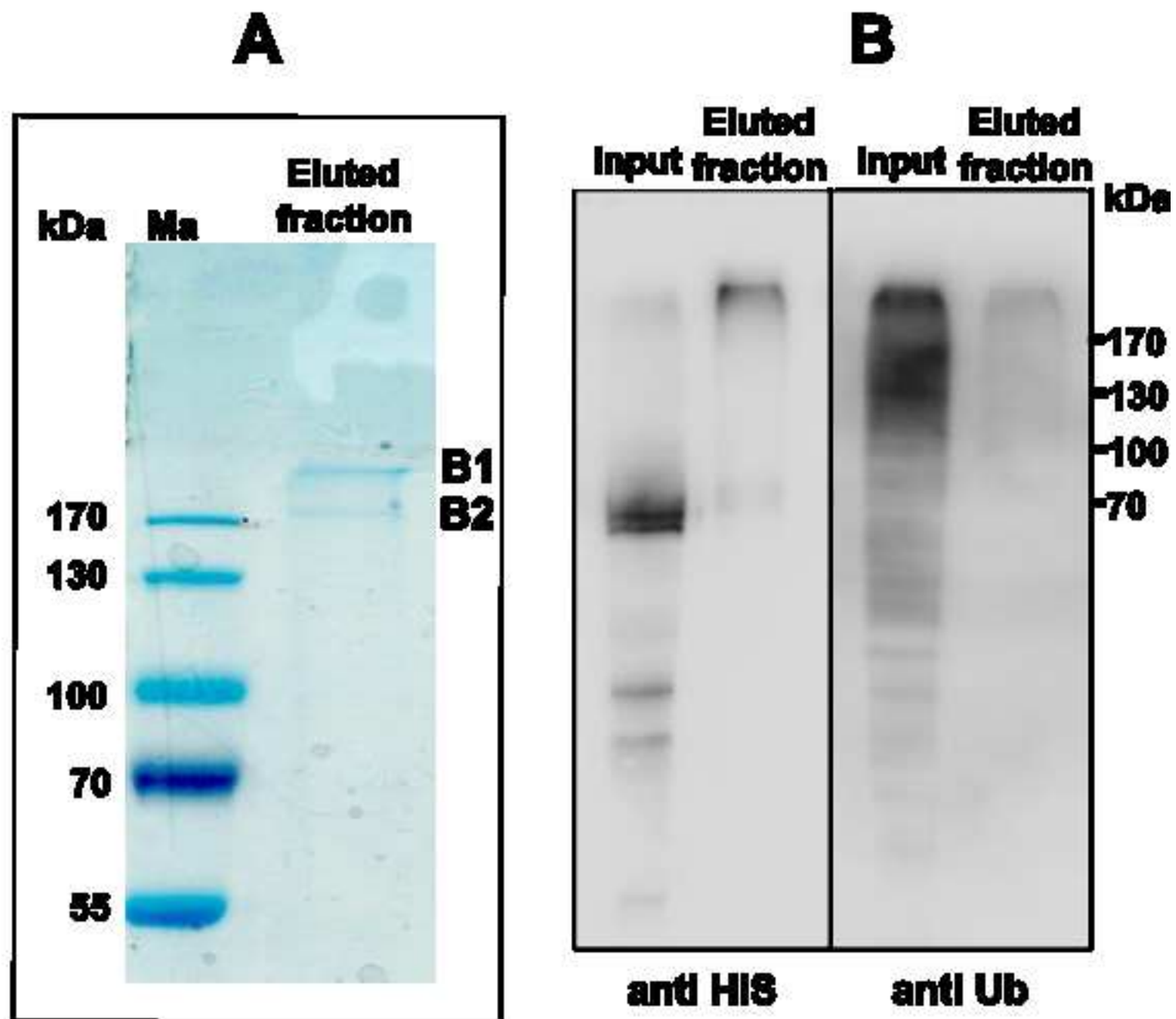


# Figure 8

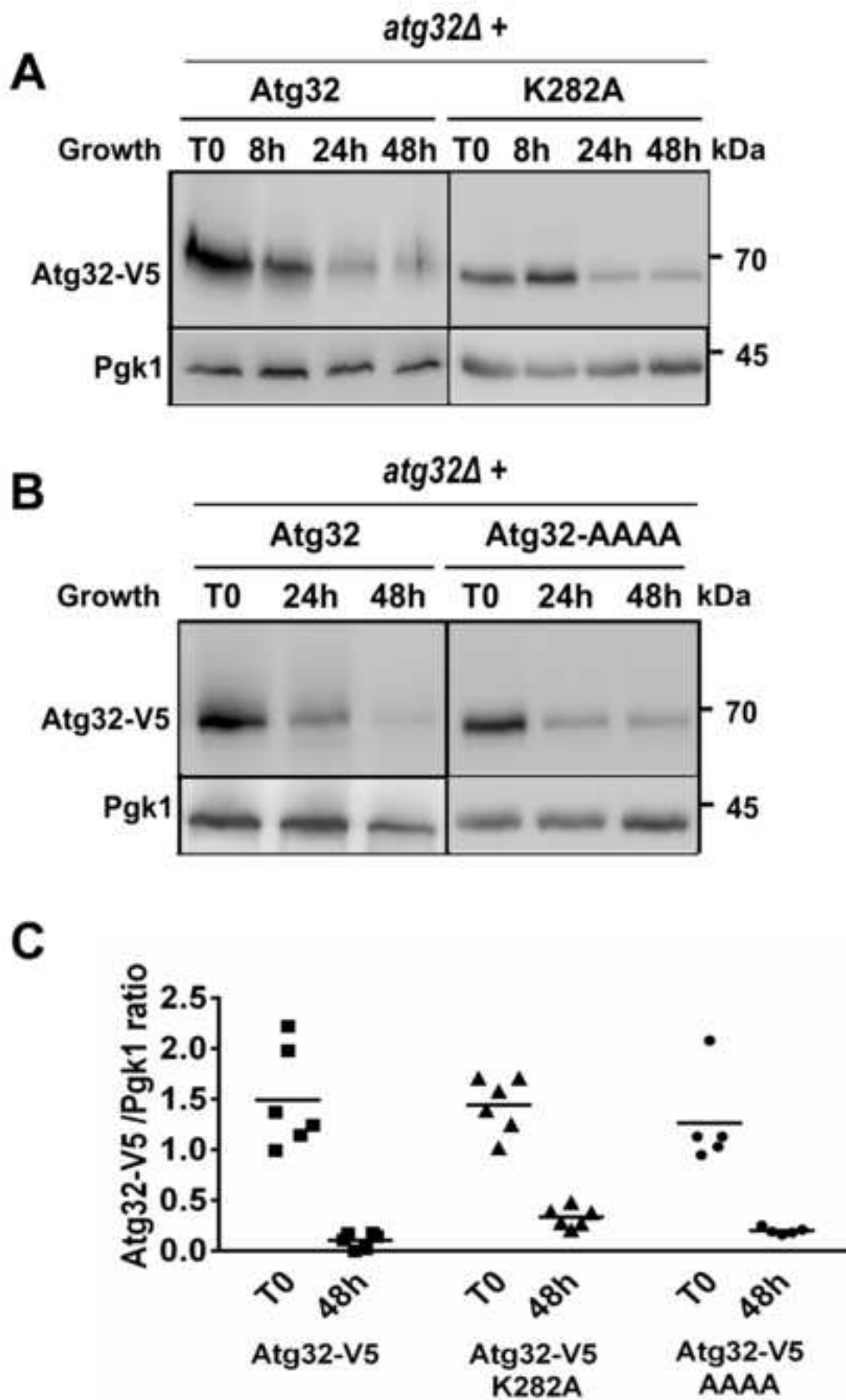
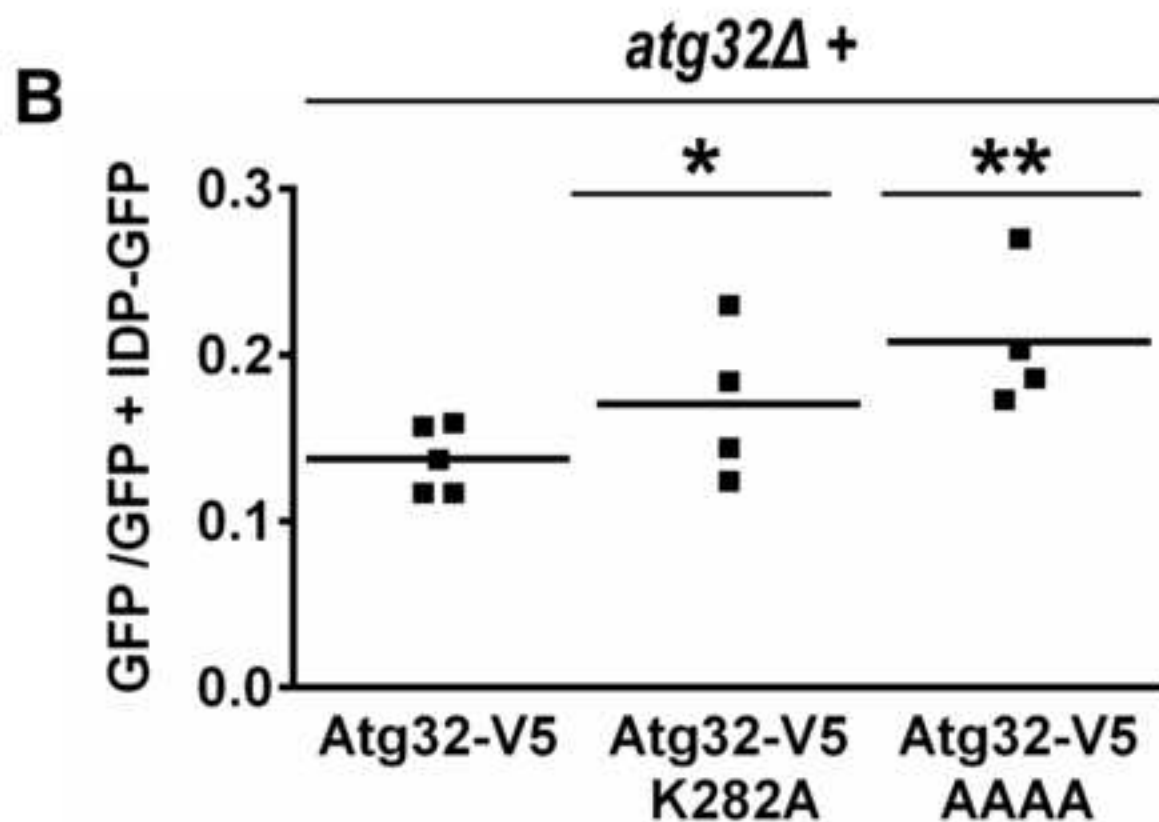
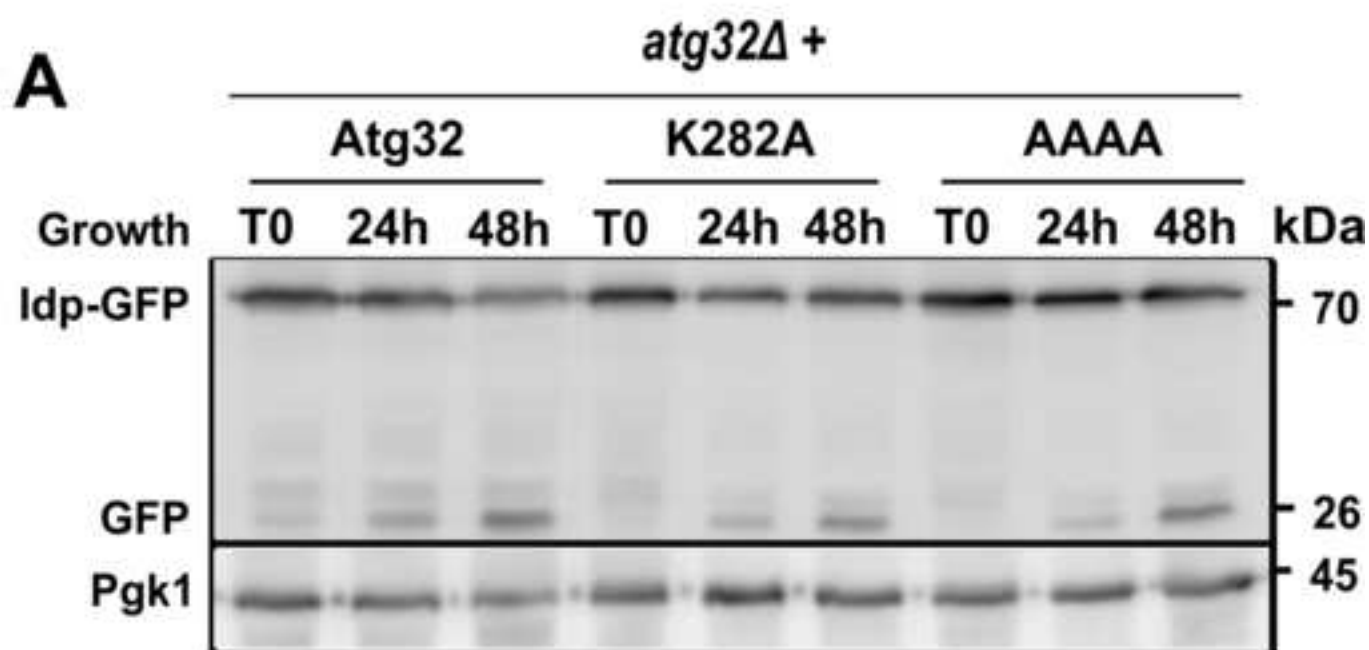


# Figure 9

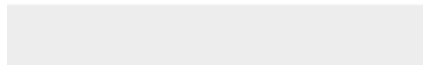




[Click here to access/download](#)

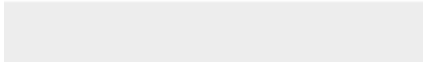
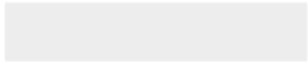
**Supporting Information**

Compil supplementary figures Oct2020.pdf



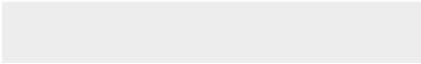


Click here to access/download  
**Supporting Information**  
Compil data on graphs.pdf





Click here to access/download  
**Supporting Information**  
Original blots oct 2020.pdf



## **The yeast mitophagy receptor Atg32 is ubiquitinated and degraded by the proteasome**

Nadine Camougrand<sup>(a,b)</sup>, Pierre Vigie<sup>(a,b)</sup>, Cécile Gonzalez<sup>(a,b,d)</sup>, Stephen Manon<sup>(a,b)</sup> and Ingrid Bhatia-Kiššová<sup>(c)</sup>

<sup>a</sup> CNRS, UMR5095, 1 rue Camille Saint-Saëns, 33077 Bordeaux, France

<sup>b</sup> Université de Bordeaux, UMR5095, 1 rue Camille Saint-Saëns, 33077 Bordeaux, France

<sup>c</sup> Comenius University, Faculty of Natural Sciences, Department of Biochemistry, Ilkovicova 6, 84215 Bratislava, Slovak Republic

<sup>d</sup> Present address: IBCP, UMR5086, Université de Lyon, 7 passage du Vercors, 69367 Lyon cedex 07, France

Correspondence: [n.camougrand@ibgc.cnrs.fr](mailto:n.camougrand@ibgc.cnrs.fr)

**Abstract:** Mitophagy, the process that degrades mitochondria selectively through autophagy, is involved in the quality control of mitochondria in cells grown under respiratory conditions. In yeast, the presence of the Atg32 protein on the outer mitochondrial membrane allows for the recognition and targeting of superfluous or damaged mitochondria for degradation. Post-translational modifications such as phosphorylation are crucial for the execution of mitophagy. In our study we monitor the stability of Atg32 protein in the yeast *S. cerevisiae* and show that Atg32 is degraded under normal growth conditions, upon starvation or rapamycin treatment. The Atg32 turnover can be prevented by inhibition of the proteasome activity, suggesting that Atg32 is also ubiquitinated. Mass spectrometry analysis of purified Atg32 protein revealed that at least lysine residue in position 282 is ubiquitinated. Interestingly, the replacement of lysine 282 with alanine impaired Atg32 degradation only partially in the course of cell growth, suggesting that additional lysine residues on Atg32 might also be ubiquitinated. Our results provide the

foundation to further elucidate the physiological significance of Atg32 turnover and the interplay between mitophagy and the proteasome.

## **Introduction**

Mitochondria are organelles in charge of many crucial functions in cells. In eukaryotes, they are known to be the powerhouse of cells by producing ATP via oxidative phosphorylation; they are also involved in different synthesis pathways such as the synthesis of certain amino acids and lipids and in signaling pathways, such as apoptosis and calcium. Mitochondrial dysfunctions have been associated with aging and with an increasing number of pathologies, including neurodegenerative diseases, cancer, and metabolic perturbation. To maintain cell survival and homeostasis, cells have developed ways to remove superfluous or damaged cell components and organelles such as mitochondria. Mitophagy is one of the processes involved in mitochondrial quality control. Mitophagy is a selective form of autophagy [1,2]. Macroautophagy (hereafter called autophagy) is conserved among eukaryotic species and involves specific lytic compartments: the vacuole in yeast and lysosomes in mammals. It also involves specific autophagy-related (Atg) proteins. To date, more than 40 Atg proteins have been identified, about half are involved in the core autophagy machinery, and the rest are implicated in specific autophagy processes and regulations.

In mammalian cells, mitophagy and recognition of the mitochondria that need to be removed are complex processes. Two main mechanisms of mitophagy signaling have been identified: ubiquitin-mediated mitophagy and receptor-mediated mitophagy. To be degraded by mitophagy, mitochondria must be labeled with a flag that is recognized by autophagic machinery. For these mitophagy-signaling pathways, ubiquitin/proteins, receptors/adaptors containing the

LIR (LC3-interacting region) domain act to recruit LC3 family members for mitochondria and thus induce mitophagy.

In yeast, Atg32 is the only characterized mitophagy receptor, which suggests mitophagy could be a simpler mechanism in yeast than in mammals [3,4]. The Atg32 protein is an outer mitochondrial membrane protein with its C-terminus in the intermembrane space and its N-terminus in the cytosol [3,4]. As mammalian protein receptors, Atg32 possesses the Atg8-interacting motif (AIM, LIR domain). When mitophagy is induced, Atg32 interacts with Atg11, a cytosolic adaptor protein required for selective autophagy. Atg11 is believed to target mitochondria to the pre-autophagosomal structure (PAS), where an autophagosome is generated to enclose the mitochondria. At the PAS, Atg32 interacts with Atg8, a protein anchored in autophagosome membranes, and the Atg32-Atg8 interaction facilitates the formation of autophagosomes surrounding mitochondria [3,4,5,6]. Both interactions are required for the recruitment of mitochondria to the phagophore followed by their sequestration within autophagosomes and their degradation in the vacuole.

The Atg32 expression is regulated by multiple factors. It has been shown that N-acetylcysteine (NAC), which increases the cellular level of reduced glutathione (GSH), inhibits mitophagy [7] through suppression of Atg32 expression [4]. Indeed, the absence of an Opi3 protein, an enzyme required in the conversion of phosphatidylethanolamine to phosphatidylcholine, causes an increase in intracellular reduced glutathione, leading to a decrease in Atg32 protein expression [8]. Moreover, the absence of some components of the NatA N-acetyltransferase complex also results in a decrease in Atg32 protein expression [9]. However, the precise role of NatA concerning Atg32 protein remains unclear. In addition, it has

been shown that Atg32 phosphorylation on serines 114 and 119, is required for mitophagy activation [10,11]. More recently, Levchenko et al. detected another post-translational modification of Atg32 when mitophagy was induced by rapamycin treatment in a *pep4Δ* background, where vacuolar proteolysis is impaired. However, its precise nature remains to be characterized [12].

Because mitophagy induction is highly regulated, we reasoned, as a key mitophagy factor, Atg32 protein may be subject to degradation control. In this study, we monitored the expression and the stability of the Atg32 protein during mitophagy in the yeast *S. cerevisiae*. We showed the existence of an interplay between mitophagy and the proteasome. We demonstrated that a novel post-translational modification of Atg32, ubiquitination at least on lysine 282 residue, modulated Atg32 protein level during the cell growth. Because uncontrolled mitophagy activation can lead to dire consequences, understanding Atg32 regulation would help us understand the control of mitophagy activity and also the cooperation between the proteasome and mitophagy.

## **Material and methods**

### **Yeast strains, plasmids and growth conditions**

All yeast strains used in this study are listed in the supplementary Table I and derived from BY4742 (Euroscarf bank). Yeast cells were grown aerobically at 28°C in complete minimal synthetic medium (CMS; 0.175% yeast nitrogen base without amino acids and ammonium sulfate, 0.5% ammonium sulfate, 0.1% potassium phosphate, 0.2% Drop-Mix, 0.01% of auxotrophic amino acids and nucleotide, pH 5.5), supplemented with 2% lactate as a carbon source (CMS-L). Cell growth was followed by optical density at 600 nm. Atg32 expression was examined in cells harvested in the mid-exponential phase of growth (1.5–2 OD<sub>600</sub>; T0), after 8 h

(8 h; late exponential phase), after 1 day (24 h; early stationary phase), and after 2 days (48 h; late stationary phase) of culture. To inhibit the proteasome, 75  $\mu$ M MG-132 + 0.003% SDS were added to the cell culture at 8 h time point. To inhibit vacuolar proteolysis, 2 mM PMSF was added to the cell culture at 8 h time point; this step was repeated twice during the course of cell growth. For starvation experiments, cells were harvested at the mid-exponential phase of growth (1.5–2 OD<sub>600</sub>; T0), washed three times with water and incubated in a nitrogen starvation medium (-N; 0.175% yeast nitrogen base without amino acids and ammonium sulfate, and 2% lactate, pH 5.5) for 3-, 6- or 24 h (-N3h, -N6h, -N24h). The *pre2-2* mutant strain was unable to grow in the lactate-containing medium; for this reason, the experiments including *pre2-2* mutant strain were performed in a CMS medium supplemented with 2% galactose as a carbon source (CMS-G). The *pre2-2* mutant strain was a gift of Dr. Sagot (UMR5095 CNRS, France).

Mitophagy was studied in cells expressing the mitochondrial matrix Idp1-GFP protein, and subjected to nitrogen starvation or during different phases of growth. The plasmid *pIDP1-GFP* was a gift from Dr. Abeliovich (Hebrew University of Jerusalem, Israel). To study autophagy, cells were transformed with plasmid *pGFP-ATG8* kindly provided by Dr. Dan Klionsky (Michigan University, USA). The plasmid expressing HA-Atg32 from copper promoter was a gift from Dr. Dan Klionsky. The plasmid expressing Atg32-V5-6HIS from *ATG32* promoter was a gift from Axel Athané (UMR5095 CNRS, France). To prepare the *pPROM-ATG32- $\beta$ -galactosidase* plasmid, the promoter of *ATG32* gene was amplified by PCR using forward primer (5'-GTGATGTATCCACAGGGAATTCCGCTC-3') and reverse primer (5'-CTTTTAGATGAGGATCCTTTACCT-3'), and cloned into *Bam*H1-digested YEp357 plasmid kindly provided by Dr. Pinson (UMR5095 CNRS, France). The plasmid *pYES2-ATG32-V5*

expressing mutated Atg32<sup>K282A</sup>-V5 or Atg32-AAAA-V5 proteins were generated using the QuikChange Site-Directed Mutagenesis approach with the following primers: K282A forward (5'-CAATATTCTCAAGGCGCGCCTGTAATA-3'), K282A reverse (5'-GATCGGTATTACAGGCGCGCCTTGAGA-3'); Rsp5-binding motif forward (5'-AAAGAATACCAATCTCTTTTTGAAGCAQGC GGCAGCTCACGATTCCGCAACATTC-3'); Rsp5-binding motif reverse (5'-TTGCGGGAATGTTGCGGAATCGTGAGCTGCCGCTGCTTCAAAAAGAGATTGGTA-3').

### **Preparation of protein extracts and western blots**

For preparation of total protein extracts,  $2 \times 10^7$  cells were harvested by centrifugation, washed with water, and resuspended in 450  $\mu$ l of water and 50  $\mu$ l of lysis buffer (1.85 M NaOH, 3.5%  $\beta$ -mercaptoethanol). After 10 min on ice, 50  $\mu$ l of trichloroacetic acid 3 M was added followed by another incubation of 10 min on ice. Proteins were pelleted by centrifugation, 8 min at 13 000 g, washed with acetone and resuspended in 20  $\mu$ l of 5% SDS and 20  $\mu$ l of loading buffer (2%  $\beta$ -mercaptoethanol, 2% SDS, 0.1 M Tris-HCl, pH 8.8, 20% glycerol, 0.02% bromophenol blue). Samples were boiled for 5 min and 50  $\mu$ g of proteins/total protein extracts corresponding to  $5 \times 10^6$  cells per line were separated by electrophoresis by 12.5% SDS-PAGE and subjected to immunoanalysis with either anti-GFP (Roche), anti-Pgk1 (Invitrogen), anti-porin (Invitrogen), anti-Dpms1 (Invitrogen), anti-HA (Roche), anti-V5 (Invitrogen), anti-HIS (Euromedex) and anti-ubiquitin (Calbiochem) antibodies. Detection was performed with ECL<sup>+</sup> reagent (Luminata Forte, Perkin Elmer). Pgk1, the cytosolic phosphoglycerate kinase, was used as a loading control. The Atg32-V5/Pgk1, HA-Atg32/Pgk1 or GFP/GFP + Idp-GFP ratios were quantified by using ImageJ software (NIH). Results of calculations were expressed as the mean  $\pm$

SEM. To study Atg32-V5 turnover, between 5 and 8 independent experiments were carried out for each tested condition; one representative western blot result is presented for each experimental condition. *P*-values were assessed using paired Student's *t*-tests; \* *P* < 0.05 or \*\* *P* < 0.01 were considered statistically significant.

For preparation of cell lysates,  $5 \times 10^7$  cells were broken with glass beads in a buffer containing 0.6 M sorbitol, 20 mM MES pH 6 plus protease inhibitor cocktail (Roche); lysates were centrifuged 10 min at 800 g. The supernatants, an equivalent of 400  $\mu$ g of proteins, were loaded on 20–55% OptiPrep density gradients in a buffer with 0.6 M sorbitol 20 mM MES pH6, 5 mM EDTA, pH6 plus protease inhibitor cocktail (Roche). Fractions were collected, precipitated with TCA and pellets were resuspended in 20  $\mu$ l of 5% SDS and 20  $\mu$ l of loading buffer (2%  $\beta$ -mercaptoethanol, 2% SDS, 0.1 M Tris-HCl, pH 8.8, 20% glycerol, 0.02% bromophenol blue). Samples were boiled for 5 min and 4  $\mu$ l of samples were separated by 12.5% SDS-PAGE and subjected to immunoanalysis.

### **Monitoring mitophagy by western blot**

BY4742, *atg32 $\Delta$*  mutant cells and *atg32 $\Delta$*  cells expressing Atg32-V5 and the mitochondrial matrix Idp1-GFP were grown in a CMS-L medium in presence or absence of MG-132 or exposed to nitrogen starvation, respectively. At different times (as indicated in each figure), total protein extracts were prepared from  $2 \times 10^7$  cells as described above. Extracts were immunoblotted, 12.5 % SDS-PAGE gels were used. Under basal condition (T0), only the Idp1-GFP form (75 kDa) was detected with a monoclonal mouse anti-GFP antibody. Upon mitophagy induction, Idp1-GFP (75 kDa) and free GFP (27 kDa) were detected with anti-GFP antibodies.

Pgk1 was used as a loading control. Quantification of GFP signals was done using ImageJ software by calculating the ratio of free GFP to total GFP (GFP/GFP + Idp1-GFP). Between 4 and 5 independent experiments were carried out for each experimental condition; one representative western blot result is presented.

### **Monitoring autophagy by western blot**

BY4742 and *atg32Δ* cells expressing Atg32-V5 and GFP-Atg8 were grown in a CMS-L medium in presence or absence of MG-132. At different times (as indicated in each figure), total protein extracts were prepared from  $2 \times 10^7$  cells as described above. Extracts were immunoblotted. Under basal condition (T0), only the GFP-Atg8 form (40.6 kDa) was detected with anti-GFP antibody. Upon autophagy induction, GFP-Atg8 localized in autophagosome membranes is delivered into vacuoles, here the proteolysis of GFP-Atg8 releases an intact GFP moiety (27 kDa) that can be detected with anti-GFP antibodies. Pgk1, was used as a loading control. Three independent experiments were carried out for each examined condition; one representative result is shown.

### **ALP activity**

Alkaline phosphatase activity was measured on *pho8Δ* strain, expressing the mitochondria-targeted truncated version of Pho8, mtPho8Δ60 [13], during the mid-exponential (T0) and the stationary phase (48 h) in absence or presence of MG-132. For each point,  $5 \times 10^7$  cells expressing mitochondria-targeted Pho8Δ60 (mtPho8Δ60) were harvested and lysed with glass beads in lysis buffer

(20 mM PIPES, 0.5% Triton X-100 0.5%, 50 mM KCl, 100 mM potassium acetate, 10 mM MgCl<sub>2</sub>, 10 μM ZnSO<sub>4</sub>, 2 mM PMSF). After centrifugation, 20 μl of supernatant were put with 80 μl of water and 400 μl of activity buffer (250 mM Tris HCl pH 8, 0.4% Triton X-100, 10 mM MgCl<sub>2</sub>, 10 μM ZnSO<sub>4</sub>, 125 mM p-nitrophenyl-phosphate) during 20 minutes at 30°C. The reaction was stopped by the addition of 500 μl of 1 M glycine pH 11. Activity was then measured by optical density at 400 nm. Protein concentration was measured with the Lowry method. ALP activities were expressed as arbitrary fluorescence units/minute/mg proteins (AU/min/mg). 4 independent experiments were carried out for each condition. Results of quantification were expressed as the mean ± SEM. *P*-values were assessed using paired Student's t-tests; \*\* *P* < 0.01 were considered statistically significant.

### **β-galactosidase activity**

BY4742 cells, expressing β-galactosidase protein under control of *ATG32* promoter were grown in a lactate-containing medium and harvested at different time points: mid-exponential phase of growth (T<sub>0</sub>), late exponential phase of growth (8 h), early stationary phase of growth (24 h) and late stationary phase of growth (48 h). For proteasome inhibition, 75 μM MG-132 + 0.003% SDS were added at 8 h time point. To measure β-galactosidase activity, five OD<sub>600</sub> (corresponding to 5.0 × 10<sup>7</sup> cells) were harvested and broken with glass beads in lysis buffer (100 mM Tris-HCL pH 8, 1 mM DTT, 20% glycerol, 2 mM PMSF) during 4 min at 20 hertz using Mixer Mill MM400 (Retsch). Then, 20 μl of cell lysate were used to measure β-galactosidase activity by absorbance at 420 nm in 60 mM Na<sub>2</sub>HPO<sub>4</sub>, 40 mM NaH<sub>2</sub>PO<sub>4</sub>, 10 mM KCl, 1 mM MgSO<sub>4</sub>, 50 mM β-mercaptoethanol, pH 7 and with 0.8 mg/ml of ortho-Nitrophenyl-β-galactoside (ONPG). Protein concentrations were measured using Lowry's method and

activities were normalized to T0. Between 5 and 8 independent experiments were carried out for each experimental condition. Results of quantification were expressed as the mean  $\pm$  SEM. *P*-values were assessed using paired Student's *t*-tests; \*\* *P* < 0.01 were considered statistically significant.

### **Atg32 purification**

To purify Atg32 protein,  $20 \times 10^7$  cells expressing Atg32-V5-6xHIS and grown until late stationary phase (48 h) in the presence of 75  $\mu$ M MG-132 were collected, and lysates were prepared as described in Becuwe et al. [14]. Cells were precipitated with TCA to a final concentration of 10% overnight at 4°C, and lysed with glass beads for 20 min at 4°C. After centrifugation, the lysate was collected and centrifuged at 16,000 *g* for 10 min. The pellet was resuspended with 30  $\mu$ l of 1 M non buffered Tris and 200  $\mu$ l of guanidinium buffer (6 M GuHCl, 20 mM Tris-HCl, pH 8, 100 mM K<sub>2</sub>HPO<sub>4</sub>, 10 mM imidazole, 100 mM NaCl, and 0.1% Triton X-100) and incubated for 1 h at room temperature on a rotating platform. After centrifugation (16,000 *g* for 10 min at room temperature), the lysate was loaded on a HisTrap FF Crude column (GE Healthcare Life Sciences). The column was then washed with a speed of 1 ml/min with guanidinium buffer, then with wash buffer 1 (20 mM Tris-HCl, pH 8.0, 100 mM K<sub>2</sub>HPO<sub>4</sub>, 20 mM imidazole, 100 mM NaCl, and 0.1% Triton X-100) and then with wash buffer 2 (20 mM Tris-HCl, pH 8.0, 100 mM K<sub>2</sub>HPO<sub>4</sub>, 10 mM imidazole, 1 M NaCl, and 0.1% Triton X-100). His6-tagged proteins were finally eluted with an elution buffer (50 mM Tris-HCl, pH 8.0, and 250 mM imidazole). Fractions absorbing at 254 nm were pooled, analyzed by 11% SDS-PAGE and submitted to blue colloidal staining and immuno-analysis.

### **Sample preparation and protein digestion for MS analysis**

After colloidal blue staining, both obtained bands (B1, B2) were cut out from the SDS-PAGE gel and subsequently cut in 1 mm x 1 mm gel pieces. Gel pieces were destained in 25 mM ammonium bicarbonate, 50% acetonitrile (ACN), rinsed twice in ultrapure water and shrunk in ACN for 10 min. After ACN removal, gel pieces were dried at room temperature, covered with the trypsin solution (10 ng/ $\mu$ l in 50 mM  $\text{NH}_4\text{HCO}_3$ ), rehydrated at 4 °C for 10 min, and finally incubated overnight at 37 °C. Spots were then incubated for 15 min in 50 mM  $\text{NH}_4\text{HCO}_3$  at room temperature with rotary shaking. The supernatant was collected, and an  $\text{H}_2\text{O}/\text{ACN}/\text{HCOOH}$  (47.5:47.5:5) extraction solution was added onto gel slices for 15 min. The extraction step was repeated twice. Supernatants were pooled and concentrated in a vacuum centrifuge to a final volume of 100  $\mu$ l. Digests were finally acidified by the addition of 2.4  $\mu$ l formic acid (5%, v/v) and stored at -20 °C.

### **nLC-MS/MS analysis**

Peptide mixture was analyzed on the Ultimate 3000 nanoLC system (Dionex, Amsterdam, The Netherlands) coupled to the Electrospray Orbitrap Fusion™ Lumos™ Tribrid™ Mass Spectrometer (Thermo Fisher Scientific, San Jose, CA). Ten microliters of peptide digests were loaded onto a 300- $\mu$ m-inner diameter x 5-mm  $\text{C}_{18}$  PepMap™ trap column (LC Packings) at a flow rate of 10  $\mu$ L/min. The peptides were eluted from the trap column onto an analytical 75-mm id x 50-cm  $\text{C}_{18}$  Pep-Map column (LC Packings) with a 4–40% linear gradient of solvent B in 45 min (solvent A was 0.1% formic acid and solvent B was 0.1% formic acid in 80% ACN). The separation flow rate was set at 300 nL/min. The mass spectrometer operated in positive ion mode at a 1.8-kV needle voltage. Data were acquired using Xcalibur 4.1 software in a data dependent

mode. MS scans ( $m/z$  375-1500) were recorded at a resolution of  $R = 120\,000$  (at  $m/z$  200) and an AGC target of  $4 \times 10^5$  ions collected within 50 ms. Dynamic exclusion was set to 60 s and top speed fragmentation in HCD mode was performed over a 3 s cycle. MS/MS scans with a target value of  $3 \times 10^3$  ions were collected in the ion trap with a maximum fill time of 300 ms. Additionally, only +2 to +7 charged ions were selected for fragmentation. Other settings were as follows: no sheath nor auxiliary gas flow, heated capillary temperature, 275 °C; normalized HCD collision energy of 30% and an isolation width of 1.6  $m/z$ . Monoisotopic precursor selection (MIPS) was set to Peptide and an intensity threshold was set to  $5 \times 10^3$ .

## Results

### Amount of the mitophagy receptor Atg32 decreases during the stationary phase

Mitophagy in yeast is induced during nitrogen starvation, during the stationary phase of growth, or through rapamycin treatment, where cells are grown in a strictly respiratory carbon source medium. To study Atg32 expression in cells grown in a lactate-containing medium (CMS-L), we C-terminally tagged the Atg32 protein with a V5-6HIS epitope (hereafter referred to as Atg32-V5), and the tagged protein was expressed under the control of its promoter. First, we ensured the fusion protein Atg32-V5 was localized to mitochondria by analyzing total cellular extracts from cells harvested in the mid-exponential growth phase on a 20–55% OptiPrep gradient (Fig. 1A) or isolated mitochondria on a 20–60% sucrose gradient (Fig. S1A). In both cases, Atg32-V5 is colocalized with porin, an outer mitochondrial membrane protein. Moreover, by using mitophagy-dependent processing of the Idp1-GFP technique [15] we showed that Atg32-V5 protein was able to reverse the mitophagy defect of the *atg32 $\Delta$*  mutant strain in

both the stationary phase of cell growth (Fig. 1B) as well as during starvation (Fig. S1B). These observations align with the data of Levchenko *et al.* (2016), who showed that the C-terminal tagging of Atg32 by a ZZ tag did not interfere with mitophagy induced by nitrogen starvation or rapamycin treatment [12].

We then determined Atg32 expression from cells harvested in the mid-exponential phase of growth (1.5-2 OD<sub>600</sub>; T0), after 8 hours (late exponential phase; 8 h), after 1 day (early stationary phase; 24 h), and after 2 days (late stationary phase; 48 h) of culture. We found that under respiratory conditions, the Atg32-V5 protein level decreased during cell growth and almost completely disappeared in the stationary phase (Fig. 2A, B). Similarly, we observed that when the Atg32 protein was N-terminally tagged with an HA epitope, its amount also decreased gradually during cell growth into the stationary phase (Fig. 2C, D). It is evident that mitophagy alone cannot be responsible for the decreasing amount of Atg32 protein, as cells in the stationary phase still contain mitochondria, and mitochondrial functions are essential for their viability.

At the same time, during the first 3 hours of nitrogen starvation, Atg32-V5 levels dropped by 40% on average, changing only minimally and steadying at about 50% of the original amount after 24 hours (Fig. S2A,B). Moreover, Atg32-V5 degradation was not compromised under normal growth conditions in cells lacking Atg5 or Atg8, two essential autophagy effectors, or Atg11, a protein required for selective autophagy degradation (Fig. S3A, B). Okamoto *et al.* (2009) described a similar disappearance of the Atg32 protein in *atg7Δ* mutant strains [4]. Assuming Atg32 is essential for only mitophagy, this finding was surprising. The reason for this finding is uncertain; however, a small quantity of Atg32 might be sufficient to mediate the selective elimination of mitochondria. Alternatively, a yet to be identified posttranslational

modification of Atg32 might function in mitophagy. Also, we cannot exclude the possibility that during respiratory growth, Atg32 might be involved in unknown pathways related to mitochondrial function.

### **Atg32 turnover can be prevented by inhibition of the proteasome**

To understand why the Atg32 protein level decreases when mitophagy is induced, we examined both possibilities that could lead to its reduction: increased degradation and a reduced synthesis of the Atg32 protein. As first, we evaluated the effect of inhibitors of the two main cellular proteolytic pathways (vacuolar-autophagy systems and the ubiquitin-proteasome) on the Atg32 protein level. We observed that the addition of PMSF, an inhibitor of serine proteases that blocks several yeast vacuolar proteases (e.g., proteinase B and carboxypeptidase Y) but does not affect proteasome function, only slightly affected Atg32 protein levels, in an increment probably corresponding to the part of a protein that is degraded by mitophagy (Fig. 3A, B; 24 h and 48 h). Accordingly, the degradation of Atg32-V5 was not compromised in cells lacking Pep4, a vacuolar protease (Fig. 3C, D), confirming that degradation of Atg32 in the vacuole does not play a significant role in degradation control of the Atg32 protein.

Meanwhile, the addition of MG-132, a proteasome inhibitor that reduces the degradation of ubiquitin-conjugated proteins in mammalian cells and effectively blocks the proteolytic activity of the 26S proteasome in yeast, counteracted the Atg32 protein loss observed during the stationary growth phase (Fig. 3A, upper panel) and rapamycin treatment (Fig. S4A). We observed the same Atg32 protein level dynamic in the BY4742 strain expressing Atg32-V5 (Fig. S4B, C). **Further, inhibition of proteasomal activity stabilized the Atg32 protein in exponentially growing cells, in which there is no detectable mitophagy yet (T8; Fig. S4D).** However, MG-132

had only a limited effect on Atg32-V5 levels during nitrogen starvation (Fig. S2A,B). In Figures 3A and S2A (lower panels), the accumulation of ubiquitin-conjugated complexes (Ub) becomes easily detectable because these complexes are not degraded in the presence of MG-132; this serves as evidence that MG-132 is a potent proteasome inhibitor in yeast. Also, the Atg32-V5 level was restored with MG-132 treatment in *atg5Δ* mutant cells in the stationary phase (Fig. S3C).

The addition of MG-132 or PMSF did not significantly affect cell growth or growth yield (Fig. S5A). Furthermore, the simultaneous addition of MG-132 and PMSF had no significant cumulative effect on the reduction of Atg32 protein levels (Fig. S5B). Consistent with these observations, Atg32 may be degraded in both an autophagy-dependent and autophagy-independent manner.

To answer the question of whether the reduction of the Atg32 protein level during the stationary phase in respiratory conditions is due to a decrease in Atg32 synthesis or an increase in Atg32 degradation, we examined *ATG32* promoter activity. We used a construct pPROM-*ATG32-lac Z* in which the reporter gene *lacZ* was expressed from the *ATG32* promoter. Interestingly, we found that *ATG32* promoter activity increased through the course of cell growth (Fig. 4A). In the late stationary phase, *ATG32* promoter activity increased threefold to fourfold compared to *ATG32* promoter activity in cells in the early exponential phase of growth (T0). MG-132 treatment prevented this rise in *ATG32* promoter activity (Fig. 4A).

To evaluate further whether the Atg32 protein is subject to degradation control, we monitored the Atg32 protein turnover. To assess the alteration of Atg32 protein levels, *atg32Δ* mutant cells expressing ATG32-V5 were grown in a minimal lactate medium, and in the mid-

exponential growth treated with cycloheximide (250 µg/ml CHX) to turn off protein expression. After the first 20 minutes of CHX treatment, the Atg32-V5 protein level had already decreased dramatically compared to the levels of the cytosolic protein Pgk1 or of mitochondrial protein porin, indicating that Atg32 turnover is rapid (Fig 4B, C). Additionally, Atg32-V5 was significantly stabilized upon treatment by the proteasome inhibitor MG-132; hourly inhibition of the proteasomal turnover in combination with the cycloheximide resulted in a more-than-fourfold increase in the amount of the Atg32 protein (from 15 percent to approximately 68 percent;  $P = 0.015$ ) (Fig. 4B, C). These results suggest that the half-life of the Atg32 protein is very short and is degraded by the proteasome.

Consistent with the requirement of the chymotryptic activity of the proteasome in proteasome-mediated proteolysis, Atg32-V5 turnover was impaired in yeast mutant cells that contain a mutation in the protein Pre2 (Fig. 5). Pre2 is the  $\beta 5$  subunit of the 20S proteasome, which is required for efficient assembly of the 20S proteasome catabolic core particle essential for degrading the protein into fragments [16]. The expression of the fusion protein Atg32-V5 decreased significantly in the stationary phase in the medium with galactose in the control strain (*atg32 $\Delta$*  + Atg32-V5), just as it would in a lactate-containing medium, whereas we observe a less pronounced change for the *pre2-2* mutant strain (Fig. 5). This supports the hypothesis of the involvement of the proteasome in the disappearance of the Atg32-V5 protein in the stationary phase of cell growth.

Our data showed that under respiratory conditions, the Atg32 protein had a high turnover rate. Its level decreased during mitophagy, whereas *ATG32* promoter activity increased suggesting the decrease of the Atg32 protein level during the stationary phase is due to an

increase of Atg32 degradation. Our observations support the hypothesis that Atg32 might regulate its own protein level and activity.

The fact that treatment with MG-132 prevented the disappearance of Atg32 indicates that Atg32 protein degradation seems to be directly or indirectly dependent on proteasome activity. These results imply that Atg32 is ubiquitinated and targeted for proteasomal degradation. Accordingly, several bands exhibiting a molecular weight shift of Atg32-V5 (Figs. 3A upper panel, asterisk mark; 5A; S3C; S4A, B; S5B) ranging between 70 and 190 kDa were identified in protein extracts prepared from cells following MG-132 treatment or in *pre2-2* mutant cells. They may correspond to ubiquitinated Atg32 protein forms that were stabilized within cells due to dysfunctional proteasome.

### **Inhibition of the proteasome with MG-132 stimulates mitophagy**

It has been shown that cells lacking the Atg32 protein are deficient in mitophagy induction and that Atg32 overexpression is responsible for an increase in mitophagy [3, 4]. We showed Atg32-V5 is degraded under normal cell growth conditions (Figs. 2, 3, 5, S4B), but the protein did not disappear in the stationary phase when cells were treated with MG-132 (Figs. 2, 3, S4B) or in the *pre2-2* mutant (Fig. 5). To check whether the higher Atg32 protein level in the stationary phase after MG-132 treatment correlated with an increase of mitophagy, we assessed mitophagy induction in cells treated or untreated with MG-132. We first studied mitophagy in BY4742 + Atg32-V5 or *atg32Δ* + Atg32-V5 cells growing in respiratory conditions and expressing the mitochondrial Idp1-GFP fusion protein. Under basal conditions, Idp1-GFP is exclusively located in the mitochondrial matrix, and only the Idp1-GFP band (Fig. 6A, B; T0, 75 kDa) can be visualized by immunoanalysis. When mitophagy is induced, mitochondria are

trapped within autophagosomes and delivered into the vacuole to be degraded. GFP moiety is much more resistant to hydrolase degradation than Idp1 moiety, and thus residual GFP (27 kDa) will remain in the vacuolar lumen and serves as evidence of mitophagy induction. In untreated control cells, the GFP band first appeared in the mid-exponential phase (8 h), indicating mitophagy was activated (Fig. 6A, B). MG-132 stimulated both Idp1-GFP cleavage (Fig. 6A–C) and ATG32-V5 level (Fig. 3), consistent with the published data [3, 4] demonstrating a direct correlation between Atg32 content and mitophagy activity. To confirm these results, we measured alkaline phosphatase (ALP) activity in BY4742 cells expressing the mitochondria-targeted Pho8 $\Delta$ 60 (mtPho8 $\Delta$ 60) protein [15]. In control cells, we observed a twofold increase in ALP activity in the late stationary phase (48 h) compared to the mid-exponential phase (T0; Fig. 6D). Furthermore, at the 48 h point, MG-132 treatment induced a fourfold increase in ALP activity compared with that of T0, confirming proteasome inhibition by MG-132 causes an increase in mitophagy in the stationary phase compared to mitophagy of untreated cells. Notably, MG-132 had no stimulating effect on macroautophagy (Fig. S6).

### **Identification of ubiquitination site in Atg32 protein by LC-MS/MS analysis**

To confirm our hypothesis that the level and the activity of the Atg32 protein is regulated by ubiquitination, we purified Atg32 protein from *atg32 $\Delta$*  mutant cells expressing Atg32-V5-6xHIS harvested in the late stationary growth phase (48 h) in the presence of MG-132. The cell lysate was loaded on an affinity Ni-NTA column, as described in the Material and Methods section. After elution, individual fractions were examined by western blot (Fig. S7) first. The presence of Atg32-V5 was confirmed by immunodetection with antibodies directed against histidine and ubiquitin (Fig. S7C,D). Subsequently, fractions absorbing at 254 nm (Fig. S7A)

were pooled together, separated on 11% SDS-PAGE, and submitted to blue colloidal staining (Fig. 7A) or immunoanalysis using antibodies directed against histidine and ubiquitin (Fig. 7B), respectively.

Two bands (B1 and B2) were detected by colloidal blue staining (Fig. 7A). Nevertheless, Atg32-V5 did not migrate at its expected mass of 58.9 kD. Although we detected a small amount of protein of theoretical size in eluted fractions (Fig. S7C), most of the signal was discovered in oligomer form with a high mass (larger than 170 kD) despite the presence of SDS. The shift in mobility of Atg32 after purification is a surprising finding but not impossible to understand. Atg32 is a protein inserted into the outer membrane of the mitochondria. It has already been observed that a mitochondrial membrane protein such as the ATP synthase subunit 9 is mainly found in the form oligomers in SDS-PAGE gel despite the presence of detergents in the gel [17, 18].

To ascertain Atg32 ubiquitination, the B1 and B2 bands were submitted to a standard proteomics workflow as described in the Material and Methods section, including an on-gel proteolysis step and an analysis by LC-MS/MS of peptides. Specifically, trypsin digestion of ubiquitinated proteins cleaves off all but the two C-terminal glycine residues of ubiquitin from the modified protein. These two C-terminal glycine (GG) residues remain linked to the epsilon amino group of the modified lysine residue in the tryptic peptide derived from the digestion of the substrate protein. The presence of the GG on the side chain of that Lys prevents cleavage by trypsin at that site, resulting in an internal modified Lys residue in a formerly ubiquitinated peptide.

Atg32 was unambiguously identified in a sample obtained from the B1 band based on 21

unique peptides leading to 55.6% sequence coverage (Table 1 and Fig. S8). One of these peptides was unambiguously shown to bear the typical GG tag (+144 Da) remaining after tryptic proteolysis of ubiquitination of Lysines using two distinct search engines (SEQUEST and MASCOT) and manual validation (visual inspection of the related MS/MS spectrum). The simultaneous detection into the MS/MS spectrum of 20 b fragments and 22 y fragments (over 22 possible fragments of each) ascertains the presence of a typical GG tag on the lysine 282 and confirms at least one ubiquitination site into Atg32 (Table 1 and Fig. S8). However, the Atg32 protein contains 43 lysines, and only 17 were covered by MS analysis. Thus, 26 lysines remain to be tested. In a sample obtained from the band B2, MS analysis identified a histidine-rich protein which was also found ubiquitinated.

### **Investigation of Atg32 expression in ubiquitination-deficient Atg32 mutants**

To understand the specific role of proteasome-mediated Atg32 turnover, the identification of the specific pathway that selects Atg32 for degradation is required.

Because our principal aim was to determine the involvement of lysine 282 residue in Atg32 turnover, we replaced lysine 282 with alanine (mutant K282A). We found that the Atg32<sup>K282A</sup>-V5 mutant form is also degraded during growth. When compared to wild-type Atg32 protein, there is about 10–15% ( $P < 0.05$ ) more mutant protein in the late stationary phase cells (Fig. 8A, C; 48 h). The fact that Atg32 expression was not fully restored in the K282A mutant could indicate that additional lysine residues on Atg32 might also be ubiquitinated and thus involved in degradation control and regulation of mitophagy activity of Atg32.

When the Atg32 protein sequence was analyzed, we noticed the presence of an Rsp5-

binding motif (Leu-Pro-Lys-Tyr, LPKY) at the position 243-246. The *RSP5* gene encodes an essential ubiquitin ligase. Proteasomal substrates are usually first recognized by a ubiquitin ligase (E3), which works with a ubiquitin-activating enzyme (E1) and a ubiquitin-conjugating enzyme (E2) to decorate the substrates with the ubiquitin molecule. Ubiquitin-modified substrates are then delivered to the proteasome for degradation [19]. Because the ubiquitin ligase E3 is the rate-limiting and substrate-recognition component of the proteasome system, we examined the involvement of Rsp5 in Atg32 turnover. We replaced the LPKY motif in the *ATG32* sequence with AAAA (Ala-Ala-Ala-Ala), and we evaluated the expression of this mutant protein during cell growth. The turnover rate of the Atg32-AAAA-V5 protein was significantly ( $P<0.05$ ) impaired compared to the wild-type protein (Fig. 8B, C). This result thus indicates that the ubiquitination of Atg32 is not a straightforward process and could be (i) executed at various other lysine residues besides lysine 282 and (ii) governed by several E3 ligases (from more than 60 identified) involved in ubiquitin-mediated degradation in the yeast *S. cerevisiae*.

Next, we assessed mitophagy induction in the stationary phase in the different mutant cells potentially involved in Atg32 ubiquitination, such as Atg32<sup>K282A</sup> and Atg32-AAAA. We observed that the mitophagy activity in these two mutants is very similar to that of the control strain, with only a slight but significant increase in strains expressing K282A ( $P<0.05$ ) or Atg32-AAAA ( $P<0.01$ ) (Fig. 9 A, B).

These data suggest the link between Atg32 expression, its turnover, and that mitophagy may be more complex than we expected.

## Discussion

### Regulation of mitophagy by ubiquitination

Atg32 executes a key role as a receptor for multiple mitophagy inducing pathways and governs the final turnover of mitochondria. Therefore, a thorough regulation of its activity is expected. Besides regulation of its gene expression, post-translational modifications seem to control Atg32-mediated mitophagy. However, the pathways perceiving mitochondrial damage/impairment and Atg32 activation are not fully understood.

In this work, we were interested in (i) the expression and the stability of the Atg32 protein during mitophagy and (ii) the relationship between mitophagy, Atg32, and the proteasome. We observed that the Atg32-V5 protein was expressed in the mid-exponential phase of growth, disappeared progressively with growth, and was almost entirely missing in the stationary phase of growth as well as during longer durations of nitrogen starvation or upon rapamycin treatment. Several groups have already shown that Atg32 protein was expressed during growth in respiratory conditions and disappeared in the stationary phase of growth [4,20]. Wang *et al.* (2013) demonstrated that Atg32 is processed by Yme1 protease, resulting in Atg32 C-terminus cleavage, and this processed form is required for mitophagy [20]. We tagged Atg32 protein with a V5 tag in the C-terminus, and this recombinant protein may be subjected to Yme1 dependent processing, resulting in the loss of the V5 tag upon mitophagy induction. However, in Wang *et al.*'s study, Atg32 processing by Yme1 was weak and slow in cells grown in the presence of lactate as a carbon source, only about 5% of Atg32 was cleaved by Yme1 in both nitrogen starvation and in the stationary phase of growth [20]. Moreover, in the same article, the authors showed the disappearance of Atg32 tagged in N-terminus with a TAP tag in the

stationary phase of growth, and we also observed Atg32 turnover with the use of HA-Atg32 fusion protein. Therefore, our results concerning the disappearance of Atg32-V5 in the stationary phase of growth are in line with the published data, and Yme1 probably only plays a minor role in the disappearance of Atg32-V5 recombinant protein in this phase.

Considering the important role of the proteasome in the regulation of numerous proteins of the outer mitochondrial membrane [21,22], we assessed whether the proteasome is also involved in Atg32 degradation. Indeed, blocking the proteolytic activity of proteasome by MG-132 allowed us to prevent a decline in the Atg32 levels through the course of growth and in the stationary phase and to stabilize the modified form of Atg32. Moreover, in the proteasome *pre2-2* mutant strain, the Atg32 levels decreased to a much lesser extent than did control cells. Furthermore, the limited effect of treatment with PMSF, an inhibitor of vacuolar serine proteases, or of the deletion of the vacuolar protease Pep4 indicated that only a small part of Atg32 is degraded by mitophagy. We showed that the half-life of the Atg32 protein is short and that Atg32 protein levels are regulated by proteasome activity. Moreover, our results suggest that this regulatory mechanism is already active in exponentially growing cells, hence, before mitophagy induction. To some extent, our results differ from the observations that Levchenko et al. (2016) published. Besides differences in strains, the only explanation we can offer is that a difference in growing conditions and/or mitophagy induction leads to the involvement of various pathways regulating expression/stability of Atg32; one pathway can be more dependent on vacuolar degradation while another can undergo proteasomal degradation control.

Previous studies have shown that overexpression of Atg32 stimulates mitophagy, while it has long been known that the absence of Atg32 protein causes mitophagy impairment in yeast

[3,4]. These published data suggest that mitophagy is dependent on the amount of Atg32 protein present. Our results are in line with this observation. We showed that upon proteasome inhibition with MG-132, there is an increase in the amount of Atg32 protein, which correlates with the stimulation of mitophagy in the stationary phase of growth when compared to control (untreated) cells. It is expected that during this stimulation/induction of mitophagy, the amount of Atg32 protein is crucial, and our findings suggest that the proteasome may regulate the Atg32 protein amount so that yeast cells can control mitophagy activity.

Recently, it was found that two other Atg proteins are regulated by ubiquitination: Atg14 is degraded by the ubiquitin-proteasome system as a means to modulate autophagy activity [23], and Atg9 is degraded by the proteasome under normal conditions but stabilized upon starvation and rapamycin treatment [24].

Altogether, our data indicate that, as in mammalian cells, an interplay exists between mitochondria degradation by autophagy and the proteasome. It has been shown that outer mitochondrial membrane ubiquitin ligases, such as mammalian MULAN, MARCHV/MITOL, and yeast Mdm30, can ubiquitinate proteins involved in mitochondrial fusion and fission, targeting them for proteasome degradation and thus affecting mitochondrial dynamics [25,26,27]. These ligases ensure outer mitochondrial membrane quality control. Moreover, the Rsp5 E3 ligase has been shown to ubiquitinate Mdm34 and Mdm12, two components of ERMES, and this event is required for efficient mitophagy in yeast [28].

In mammals, mitophagy is governed by two different pathways. Numerous data show that the UPS plays a major role in Parkin-dependent mitophagy. Chan et al. (2011) observed robust recruitment of the 26S proteasome onto mitochondria, leading to widespread degradation

of mitochondrial outer membrane proteins via the UPS [29]. Strikingly, activation of the UPS not only precedes mitophagy but is also required for mitophagy. Inhibition of the UPS causes complete abrogation of mitophagy [27]. *Tanaka et al.* showed that ubiquitination of the mitofusins Mfn1 and Mfn2, two large GTPases that mediate mitochondrial fusion, is induced by Parkin upon membrane depolarization and leads to their degradation in a proteasome- and p97-dependent manner [30]. More recently, *Wei et al.* showed that proteasome-dependent mitochondrial membrane rupture is necessary for Parkin-mediated mitophagy in mammalian cells, in part via the cytoplasmic exposure to an IMM mitophagy receptor [31]. Concerning the pathway involving receptors, ubiquitination could play a different role. In mammalian cells, such a situation was observed in the case of the FUNDC1 receptor, which is primarily involved in mitophagy during hypoxia. This receptor is regulated by both phosphorylation and ubiquitination [32,33,34,35]. The mitochondrial PGAM5 phosphatase interacts with and dephosphorylates FUNDC1 serine 13 (Ser-13) residue upon hypoxia or carbonyl cyanide p-trifluoromethoxyphenylhydrazone treatment. Dephosphorylation of FUNDC1 catalyzed by PGAM5 enhances its interaction with LC3. CK2 phosphorylates FUNDC1 to reverse the effect of PGAM5 in mitophagy activation. Indeed, the mitochondrial E3 ligase MARCH5 plays a role in regulating hypoxia-induced mitophagy by ubiquitinating and degrading FUNDC1 to limit excessive mitochondria degradation [34]. Our study shows that, in yeast, in addition to phosphorylation regulation, Atg32-V5 turnover seems to be dependent on proteasome activity, and lysine 282 and Rsp5-binding motif are identified as one of the targets of ubiquitination. The fact that the mutation of the Rsp5-binding motif, Rsp5 being an E3 ligase, slightly but significantly perturbs Atg32 expression and mitophagy could indicate that this E3 ligase is

involved in the regulation of Atg32. However, we can not exclude the participation of other E3 ligases. Indeed, the effect of these mutations on mitophagy is rather subtle compared to the data obtained with inhibition of the proteasome by MG-132. This could be due to the presence of various different ubiquitination sites present in *ATG32* sequence.

Further study aimed at revealing other potential ubiquitination sites in Atg32 protein as well as examining strains with mutated both ubiquitination and phosphorylation sites could shed more light on this process.

Ubiquitination of mitochondrial proteins can play two different roles: (i) ubiquitination of proteins allows their turnover by proteasomal degradation and, consequently, their abundance and quality control; and (ii) ubiquitination of proteins localized on the outer mitochondrial membrane is a signal to trigger mitophagy. In the case of Atg32 or FUNDC1 mitophagy receptors, different post-translational modifications take place to modulate its activity and regulate mitophagy level. We can hypothesize that ubiquitination will be useful for regulating Atg32's own expression and controlling the mitophagy level. This would prevent excessive mitochondria degradation and ensure a fine-tuned mitochondria turnover.

### **Why is Atg32 regulated by multiple posttranslational modifications?**

During mitophagy induction, Atg32 is activated by a post-translational modification. This, however, does not answer the question of why the Atg32 protein is subjected to several different post-translational modifications, such as phosphorylations, ubiquitination, or other unknown modifications, and what the roles of these modifications are. Are these modifications dependent on mitophagy induction conditions (e.g., nutrient starvation, stationary phase of growth, or rapamycin treatment)? Previously, we showed that depending on the condition of induction,

mitophagy may exploit various signaling pathways [36]. The need of cells to employ various pathways could reflect different purposes of self-eating mitochondria in cell physiology at certain moments, the bioenergetic state/deficit of cells, a cell's capacity to carry a burden of damaged components, and so on. Upon starvation and in the stationary phase, mitophagy requires the same key proteins, Atg32, Atg11, and Atg8; however, in this study we demonstrated that Atg32 turnover rates differ under both conditions, which supports the idea that Atg32 can be regulated through more than one mechanism. In mammalian cells, mitophagy also has several distinct variants based on the biological distinctions of cells: Type 1 mitophagy, which occurs during nutrient deprivation; Type 2 mitophagy, which is stimulated by mitochondrial damage; and micromitophagy [37].

From the published data, phosphorylation of Atg32 at serine 114 and serine 119 by a serine/threonine protein kinase Ck2 seems to be required for the interaction with the adaptor protein Atg11 and targeting mitochondria for a degradation into the vacuole [38]. Thus, vacuolar degradation is responsible for Atg32 stability bearing this kind of modification. What is the fate of Atg32 on mitochondria that have not been selected for mitophagy? We assumed that Atg32 could be eliminated by a separate pathway of degradation in its unmodified form or after acquiring another type of modification. In fact, our results suggest that Atg32 could also be ubiquitylated, and mitophagy can be regulated by ubiquitination/deubiquitination events.

Additional experiments are needed to further investigate how cells control the level and activity of Atg32 to be able to understand the mechanisms by which cells control selective degradation of mitochondria, and the physiological significance of mitophagy. In addition, an interesting question is whether Atg32 is also involved in other cellular processes. Future studies

of yeast will address these important questions.

### **Acknowledgments and fundings**

The work in the laboratories of the authors was supported by grants from the Slovak APVV agency (SK-FR-2015-0005) (to IBK), the CNRS, the University of Bordeaux and the Doctoral International Program from IDEX of Bordeaux supported by Agence Nationale pour la Recherche (ANR-10-IDEX-03-02) (to NC and PV). France/Slovakia collaboration was supported by Campus France (Stefanik n° 35809VC) (to NC and IBK). We thank Drs Sagot, Klionsky, Pinson and Abeliovich, and Mr Athané for the gift of strains and material and Drs Chaignepain and Claverol (CGFB, Bordeaux) for helpful discussions.

### **Bibliography**

- [1] Lemasters JJ; Selective mitochondrial autophagy, or mitophagy, as a targeted defense against oxidative stress, mitochondrial dysfunction, and aging. *Rejuvenation Res.* 2005; 8: 3-5
- [2] Kissová I, Salin B, Schaeffer J, Bhatia S, Manon S, Camougrand N. Selective and non-selective autophagic degradation of mitochondria in yeast. *Autophagy.* 2007; 3: 329-336.
- [3] Kanki T, Wang K, Cao Y, Baba M, Klionsky DJ. Atg32 is a mitochondrial protein that confers selectivity during mitophagy. *Dev Cell.* 2009; 17: 98-109
- [4] Okamoto K, Kondo-Okamoto N, Ohsumi Y. Mitochondria-anchored receptor Atg32 mediates degradation of mitochondria via selective autophagy. *Dev Cell.* 2009; 17: 87-97.
- [5] Kondo-Okamoto N, Noda NN, Suzuki SW, Nakatogawa H, Takahashi I, Matsunami

- M, Hashimoto A, Inagaki F, Ohsumi Y, Okamoto K. Autophagy-related protein 32 acts as autophagic degron and directly initiates mitophagy. *J Biol Chem.* 2012; 287: 10631-10638.
- [6] Mao K, Wang K, Liu X, Klionsky DJ. The scaffold protein Atg11 recruits fission machinery to drive selective mitochondria degradation by autophagy. *Dev Cell.* 2013; 26: 9-18.
- [7] Deffieu M, Bhatia-Kissová I, Salin B, *et al.* Glutathione participates in the regulation of mitophagy in yeast. *Journal of Biological Chemistry.* 2009; 284:14828-14837.
- [8] Sakakibara K, Eiyama A, Suzuki SW, Sakoh-Nakatogawa M, Okumura N, Tani M, Hashimoto A, Nagumo S, Kondo-Okamoto N, Kondo-Kakuta C, Asai E, Kirisako H, Nakatogawa H, Kuge O, Takao T, Ohsumi Y, Okamoto K. Phospholipid methylation controls Atg32-mediated mitophagy and Atg8 recycling. *EMBO J.* 2015, 34:2703- 2719.
- [9] Eiyama A, Okamoto K. Protein N-terminal Acetylation by the NatA Complex Is Critical for Selective Mitochondrial Degradation. *J Biol Chem.* 2015; 290: 25034-25044.
- [10] Mao K, Wang K, Zhao M, Xu T, Klionsky DJ. Two MAPK-signaling pathways are required for mitophagy in *Saccharomyces cerevisiae*. *J Cell Biol.* 2011;193: 755-767.
- [11] Aoki Y, Kanki T, Hirota Y, Kurihara Y, Saigusa T, Uchiumi T, Kang D. Phosphorylation of Serine 114 on Atg32 mediates mitophagy. *Mol Biol Cell.* 2011; 22: 3206-3217.
- [12] Levchenko M, Lorenzi I, Dudek J. The Degradation Pathway of the Mitophagy Receptor Atg32 Is Re-Routed by a Posttranslational Modification. *Plos One.* 2016;11: e0168518.

- [13] Kanki T, Wang K, Baba M, Bartholomew CR, Lynch-Day MA, Du Z, Geng J, Mao K, Yang Z, Yen WL, Klionsky DJ. A Genomic Screen for Yeast Mutants Defective in Selective Mitochondria Autophagy. *Mol Biol Cell* 2009,20:4730-4738.
- [14] Becuwe M, Vieira N, Lara D, Gomes-Rezende J, Soares-Cunha C, Casal M, Haguenaer-Tsapis R, Vincent O, Paiva S, Léon S. A molecular switch on an arrestin-like protein relays glucose signaling to transporter endocytosis. *J Cell Biol.* 2012,196:247-259.
- [15] Klionsky D et al. Guidelines for the Use and Interpretation of Assays for Monitoring Autophagy. 2012, *Autophagy*, 8: 445-454.
- [16] Arendt CS and Hochstrasser M. Eukaryotic 20S proteasome catalytic subunit propeptides prevent active site inactivation by N-terminal acetylation and promote particle assembly. *EMBO J.* 1999; 18:3575-3585
- [17] Arselin G, Vaillier J, Graves PV, Velours J. ATP Synthase of Yeast Mitochondria. Isolation of the Subunit H and Disruption of the ATP14 Gene. *J Biol Chem.* 1996, 271: 20284-20290.
- [18] Velours J, Paumard P, Soubannier V, Spannagel C, Vaillier J, Arselin G, Graves PV. Organization of the yeast ATP synthase FO: a study based on cysteine mutants, thiol modification and cross-linking reagents *Biochimica and Biophysica Acta* 2000, 1458: 443-456.
- [19] Finley D, Ulrich HD, Sommer T, Kaiser P. The ubiquitin-proteasome system of *Saccharomyces cerevisiae*. *Genetics.* 2012; 192:319-360.
- [20] Wang K, Jin M, Liu X, Klionsky DJ. Proteolytic processing of Atg32 by the mitochondrial i-AAA protease Yme1 regulates mitophagy. *Autophagy.* 2013; 9: 1828-1836.
- [21] Karbowski M, Youle RJ. Regulating mitochondrial outer membrane proteins by ubiquitination and proteasomal degradation. *Curr Opin Cell Biol.* 2011; 23: 476-482.
- [22] Braun RJ and Westermann B. With the Help of MOM: Mitochondrial Contributions to Cellular Quality Control. *Trends Cell Biol.* 2017; 27: 441-452.
- [23] Liu CC, Lin YC, Chen YH, Chen CM, Pang LY, Chen HA, Wu PR, Lin MY., Jiang ST,

- Tsai TF, Chen RH. Cul3-KLHL20 ubiquitin ligase governs the turnover of ULK1 and VPS34 complexes to control autophagy termination *Mol. Cell*, 61 (2016), pp. 84-97
- [24] Hu G, Rios L, Yan Z, Jasper AM, Luera D, Luo S, Rao H. Autophagy regulator Atg9 is degraded by the proteasome. *Biochem Biophys Res Commun*. 2020; 522:254-258.
- [25] Yonashiro R, Ishido S, Kyo S et al. A novel mitochondrial ubiquitin ligase plays a critical role in mitochondrial dynamics. *EMBO Journal* 2006; 25: 3618-3626.
- [26] Zhang B, Huang J, Li HL, Liu T, Wang YY, Waterman P, Mao AP, L.G. Xu LG, Zhai Z, Liu D, Marrack P, Shu HB. GIDE is a mitochondrial E3 ubiquitin ligase that induces apoptosis and slows growth. *Cell Res*. 2008; 18: 900-910.
- [27] Cohen MM, Leboucher GP, Livnat-Levanon N, Glickman MH, Weissman AM. Ubiquitin-proteasome-dependent degradation of a mitofusin, a critical regulator of mitochondrial fusion *Mol Biol Cell*. 2008; 19: 2457-2464.
- [28] Belgareh-Touzé N, Cavellini L, Cohen MM. Ubiquitination of ERMES components by the E3 ligase Rsp5 is involved in mitophagy. *Autophagy* 2017; 13: 114-132.
- [29] Chan NC, Salazar AM, Pham AH, Sweredoski MJ, Kolawa NJ, Graham RL, et al. Broad activation of the ubiquitin-proteasome system by Parkin is critical for mitophagy. *Hum Mol Genet*. 2011;20:1726–1737.
- [30] Tanaka A, Cleland MM, Xu S, Narendra DP, Suen DF, Karbowski M, Youle RJ. Proteasome and p97 mediate mitophagy and degradation of mitofusins induced by Parkin. *J Cell Biol*. 2010;191:1367–1380.
- [31] Wei Y, Chiang WC, Sumpter Jr. R, Prashant Mishra P and Beth Levine B. Prohibitin 2 Is an Inner Mitochondrial Membrane Mitophagy Receptor. *Cell*. 2017; 168: 224–238.
- [32] Liu L, Feng D, Chen G, Chen M, Zheng Q, Song P, Ma Q, Zhu C, Wang R, Qi W, Huang L, Xue P, Li B, Wang X, Jin H, Wang J, Yang F, Liu P, Zhu Y, Sui S, Chen Q. Mitochondrial outer-membrane protein FUNDC1 mediates hypoxia-induced mitophagy in mammalian cells. *Nat Cell Biol*. 2012; 14: 177-185.

- [33] Wu W, Tian W, Hu Z, Chen G, Huang L, Li W, Zhang X, Xue P, Zhou C, Liu L, Zhu Y, Zhang X, Li L, Zhang L, Sui S, Zhao B, Feng D. ULK1 translocates to mitochondria and phosphorylates FUNDC1 to regulate mitophagy. *EMBO Rep.* 2014; 15: 566-575.
- [34] Chen Z, Liu L, Cheng Q, Li Y, Wu H, Zhang W, Wang Y, Sehgal SA, Siraj S, Wang X, Wang J, Zhu Y, Chen Q. Mitochondrial E3 ligase MARCH5 regulates FUNDC1 to fine-tune hypoxic mitophagy. *EMBO Rep.* 2017;18: 495-509.
- [35] Chen G, Han Z, Feng D, Chen Y, Chen L, Wu H, Huang L, Zhou C, Cai X, Fu C, Duan L, Wang X, Liu L, Liu X, Shen Y, Zhu Y, Chen Q. A regulatory signaling loop comprising the PGAM5 phosphatase and CK2 controls receptor-mediated mitophagy. *Mol Cell.* 2014; 54: 362-377.
- [36] Vigié P, Cougouilles E, Bhatia-Kiššová I, Salin B, Blancard C, Camougrand N. The mitochondrial phosphatidylserine decarboxylase Psd1 is involved in nitrogen starvation-induced mitophagy in yeast. *J Cell Sci.* 2019 Jan 2;132(1). pii: jcs221655. doi: 10.1242/jcs.221655.
- [37] Lemasters JJ. Variants of mitochondrial autophagy: Types 1 and 2 mitophagy and micromitophagy (Type 3). *Redox Biol.* 2014;2:749-754.
- [38] Kanki T, Kurihara Y, Jin X; Goda T, Ono Y, Aihara M, Hirota Y, Saigusa T, Aoki Y, Uchiumi T, Kang D. Casein kinase 2 is essential for mitophagy. *EMBO Rep.* 2013;14: 788-794.

## Legends to figures

**Figure 1: Atg32-V5 protein localizes to mitochondria and restores mitophagy in *atg32Δ* mutant strain.** (A) *atg32Δ* mutant cells grown in a CMS-L medium and expressing Atg32-V5 fusion protein were harvested in a mid-exponential phase of growth (T<sub>0</sub>). Then cells were lysed and lysates were separated in a 20–55% OptiPrep density gradient. Fractions were collected after centrifugation and analyzed by western blots. Anti-V5 antibody was used to visualize Atg32-V5, and anti-Porin antibody was used to detect mitochondria-containing fractions. P<sub>gk1</sub>, the cytosolic phosphoglycerate kinase, was used as a cytosolic marker; and D<sub>pms</sub>, dolichyl phosphate mannose synthase, was used as an endoplasmic reticulum marker. (B) Mitophagy was

assessed using mitophagy-dependent processing of the Idp1-GFP tool in wild-type (BY4742), *atg32Δ* mutant, or *atg32Δ*-expressing Atg32-V5. Cells were harvested in a mid-exponential phase of growth (T0), an early stationary phase (24 h), or a late stationary phase (48 h). The total protein extracts corresponding to  $5 \times 10^6$  cells/50 ug proteins per line were separated by 12.5% SDS-PAGE and analyzed by immunodetection using anti-GFP antibody.

**Figure 2: The Atg32 protein is degraded during cell growth.** *atg32Δ* mutant cells grown in a CMS-L medium and expressing recombinant proteins were harvested in a mid-exponential phase of growth (T0) and after 8-, 24-, and 48 h from T0. (A,C) Total protein extracts were prepared at indicated times, and samples were analyzed as described in Fig. 1B. Anti-V5 and anti-HA antibodies were used to visualize Atg32-V5 or HA-Atg32 recombinant proteins. (B,D) The Atg32-V5/Pgk1 or HA-Atg32/Pgk1 ratios were quantified by using ImageJ software; \* $P < 0.05$ , \*\* $P < 0.01$ .

**Figure 3: Degradation of the Atg32 protein is prevented by inhibition of the proteasome.** (A) *atg32Δ* mutant cells grown in a CMS-L medium and expressing Atg32-V5 recombinant protein were harvested at indicated time points. To inhibit the proteasome, 75  $\mu$ M MG-132 was added to the cell culture at the 8 h time point. To inhibit vacuolar proteolysis, 2 mM PMSF was added to the cell culture at the 8 h time point; this step was repeated several times during the whole course of cell growth. Total protein extracts were prepared, and protein samples were analyzed as described in Fig. 1B. Anti-V5 antibody was used to visualize Atg32-V5 protein. Anti-ubiquitin (Ub) was used to detect the level of ubiquitinated proteins. (B) Atg32-V5 expression was quantified as the Atg32-V5/Pgk1 ratio; \*\*  $P < 0.01$ . (C) BY4742 and *pep4Δ* mutant cells expressing Atg32-V5 were grown in a CMS-L medium. Cells were harvested in a mid-exponential (T0) and a late stationary phase (48 h) of growth. Total protein extracts were prepared and analyzed by western blots. Anti-V5 antibody was used to visualize Atg32-V5 protein. (D) The Atg32-V5/Pgk1 ratio was quantified at T0 and 48 h time points for all tested strains— \* $P < 0.05$  and \*\* $P < 0.01$ .

**Figure 4: Evaluation of *ATG32* promoter activity and Atg32 protein stability.** (A) BY4742 cells grown in a CMS-L medium and expressing  $\beta$ -galactosidase under the *ATG32* promoter were harvested in a mid-exponential phase of growth (T0) and after 24 h and 48 h from T0 in the absence or presence of MG-132. After cell lysis, the  $\beta$ -galactosidase activity was measured. Results were obtained from 6 independent experiments and are expressed as the % of T0. The symbol \*\* indicates significant difference between 48 h in the absence of and 48 h in the presence of MG-132 ( $P < 0.01$ ). (B) *atg32 $\Delta$*  mutant cells grown in a CMS-L medium and expressing Atg32-V5 protein were harvested in a mid-exponential phase (T0) and then treated with 250  $\mu$ g/ml of cycloheximide (CHX) in the presence or absence of 75  $\mu$ M MG-132 for 20 min, 40 min, and 1 h. Total protein extracts were analyzed by western blots. Anti-V5 antibody was used to visualize Atg32-V5 protein. Pgk1 was used as a loading control; Porin was used as a mitochondrial protein marker. At least 3 independent experiments were carried out for each condition. (C) Atg32-V5 expression was quantified as the Atg32-V5/Pgk1 ratio; \*  $P < 0.05$  and \*\* $P < 0.01$ .

**Figure 5: Degradation of Atg32 protein is impaired in *pre2-2* mutant cells.** (A) *atg32 $\Delta$*  and *pre2-2* mutant cells transformed with a plasmid expressing Atg32-V5 were grown in a CMS-G medium. Cells were harvested in a mid-exponential phase of growth (T0) and after 8, 24, and 48 h of cell growth. (B) The Atg32-V5/Pgk1 ratio was quantified at T0 and 48 h time points for all tested strains— \*\*  $P < 0.01$ .

**Figure 6: Stabilization of Atg32 protein by proteasome inhibition stimulates mitophagy.** (A,B) *atg32 $\Delta$*  mutant (A) and BY4742 (B) cells expressing Atg32-V5 and Idp1-GFP proteins grown in a CMS-L medium were harvested at indicated times of growth. To inhibit the proteasome, 75  $\mu$ M MG-132 was added to the cell culture at the 8 h time point. Total protein extracts were prepared and analyzed as described in Fig. 1B. Proteins were detected using antibodies against GFP or Pgk1. (C) GFP/GFP+Idp1-GFP ratios were quantified at the 24 h and

48 h time points for all tested conditions. Error bars represent standard error of the mean. **(D)** BY4742 cells expressing mtPHO8 $\Delta$ 60 protein grown in a CMS-L medium were harvested at the mid-exponential (T0) and late stationary (48 h) phases. MG-132 was added as described in (A). ALP activity was measured as described in the Material and Methods section. The symbol \*\* indicates significant difference between the 48-h time point with and without MG-132 ( $P < 0.01$ ).

**Figure 7: Atg32 purification and mass spectrometry analysis.** **(A)** *atg32 $\Delta$*  mutant cells expressing Atg32-V5-6HIS were grown in a CMS-L medium until a late stationary phase (48 h) in presence of MG-132. Cells were lysed and loaded on a Ni-NTA column as described in the Material and Methods section. After the last elution, collected fractions absorbing at 254 nm (from 14 to 17) were pooled together, precipitated with TCA. Pellet was resuspended in 60  $\mu$ l of the loading buffer, 50  $\mu$ l (eluted fraction) were loaded on a 11% SDS-PAGE. After migration, the gel was colored with colloidal blue. The bands B1 and B2 were excised and analyzed by mass spectrometry. **(B)** 5  $\mu$ L of pooled fraction from A (Eluted fraction) were separated in a 11% SDS-PAGE gel. Proteins were analyzed by western blots using antibodies against histidine (anti HIS) or ubiquitin (anti Ub), respectively. Input: 50  $\mu$ L of cell lysate prepared in (A) was precipitated with TCA, pellet was resuspended in 50  $\mu$ L of the loading buffer, and 4  $\mu$ L were loaded on the gel.

**Figure 8: Evaluation of Atg32 degradation in ubiquitination-deficient Atg32 mutants.** *atg32 $\Delta$*  cells grown in a CMS-L medium and expressing wild-type Atg32-V5 or Atg32-V5<sup>K282A</sup> **(A)** or Atg32-V5 with mutated *RSP5*-binding motif (Atg32-AAAA-V5) **(B)** recombinant proteins were harvested at indicated times. Total protein extracts were prepared, and samples were analyzed by western blots. Anti-V5 antibody was used to visualize Atg32-V5 protein. **(C)** Wild-type or mutant forms of Atg32-V5 protein levels were quantified as the Atg32-V5/Pgk1 ratio. The symbol \* indicates significant difference between Atg32-V5 and Atg32<sup>K282A</sup>-V5 on one side and Atg32-V5 and Atg32-AAAA-V5 on the other side ( $P < 0.05$ ).

**Figure 9: Evaluation of mitophagy in ubiquitination-deficient Atg32 mutants.** (A) *atg32Δ* cells grown in a CMS-L medium and expressing Idp1-GFP fusion protein and Atg32-V5 recombinant protein with mutation K282A or mutated Rsp5-binding motif (AAAA) were harvested at indicated times. Mitophagy was assessed using mitophagy-dependent processing of the Idp1-GFP tool as described in Fig. 1B. (B) Mitophagy induction was quantified as the ratio of GFP/(Idp1-GFP+GFP). The symbols \*\* and \* indicate significant differences between Atg32-V5 and Atg32-AAAA-V5 ( $P < 0.01$ ) or between Atg32-V5 and Atg32-K282A ( $P < 0.05$ ), respectively.

**Table1 : List of peptides found after mass spectrometry analysis of Atg32 protein.**

Annotated sequence	Modifications
[K]. GTLQINFHSDGFIMK.[S]	1xOxidation [M14]
[K]. SLTSSTNSFVMPK.[L]	1xOxidation [M14]
[K]. SMPPDSSSTTIHTCSEAQTGEDK.[G]	1xCarbamidomethyl [C14] ; 1xOxidation [M2]
[R]. IVQYSQGKPVIPICQPGQVIQVK.[N]	1xCarbamidomethyl [C14] ; 1xGG [K8]
[R]. IVQYSQGKPVIPICQPGQVIQVK.[N]	1xCarbamidomethyl [C14]
[K]. SMPPDSSSTTIHTCSEAQTGEDK.[G]	1xCarbamidomethyl [C14]
[K]. SMPPDSSSTTIHTCSEAQTGEDKGLLDPHLSVLELLSK.[T]	1xCarbamidomethyl [C14]
[R]. CSSQTTNGSILSSSDTSEEEQELLQAPAADIINI.K.[Q]	1xCarbamidomethyl [C1]
[K]. MNTFVLHALSKPLK.[F]	
[K]. QGQEGANVVSPSHPFK.[Q]	
[M]. VLEYQQR.[E]	
[K]. YHDSATFPQYTGIVIIIFQELR.[E]	
[K]. SLTSSTNSFVMPK.[L]	
[K]. SSEFSIDESNR.[I]	
[K]. TPFENQDDDGDEDEAFEEDSVITK.[S]	
[R]. TGSSFYQSIPK.[E]	
[K]. EYQSLFELPK.[Y]	
[K]. EKTPFNEQDDDGDEDEAFEEDSVITK.[S]	
[R]. EMVSLNLR.[I]	
[K]. FLENLNK.[S]	
[K]. LLFPPVVVTNK.[R]	
[K]. LLFPPVVVTNKR.[D]	
[R]. LQDLSLEYGEDVNEEDNDDEAIHTK.[S]	
[K]. GLLDPHLSVLELLSK.[T]	
[K].GTLQINFHSDGFIMK.[S]	

## Supplementary information

**S1 Figure: Atg32-V5 recombinant protein localizes into mitochondria and restores mitophagy in *atg32Δ* mutant cells upon nitrogen starvation.** (A) *atg32Δ* mutant cells grown in a CMS-L medium and expressing Atg32-V5 protein were harvested in a mid-exponential phase of growth. Then, cells were lysed and purified mitochondria prepared as described in Vigie et al. [34] were loaded on a 20–60% sucrose gradient. Fractions were collected and analyzed by immunodetection. Anti-V5 antibody was used to visualize Atg32-V5, and anti-Porin antibody was used to detect mitochondria-containing fractions. (B) Mitophagy was assessed using mitophagy-dependent processing of the Idp1-GFP tool in *atg32Δ* mutant and *atg32Δ*-expressing Atg32-V5. Cells were harvested at indicated times. The total protein extracts corresponding to  $5 \times 10^6$  cells/50 ug proteins per line were separated by 12.5% SDS-PAGE and analyzed by immunodetection using anti-GFP antibody.

**S2 Figure: The Atg32 protein is degraded upon nitrogen starvation.** (A) *atg32Δ* mutant cells grown in a CMS-L medium and expressing Atg32-V5 protein were harvested at indicated times. To inhibit the proteasome, 75  $\mu$ M MG-132 was added to the cell culture at the beginning of starvation. Total protein extracts were prepared afterwards, and samples were analyzed by western blots. Anti-V5 antibody was used to visualize Atg32-V5 protein; Pgk1 was used as a

loading control. Anti-ubiquitin (Ub) was used to detect the level of ubiquitinated proteins. **(B)** The Atg32-V5/Pgk1 ratio was quantified for all tested conditions.

**S3 Figure: Degradation of Atg32 protein is not impaired in autophagy-deficient mutants under normal growth condition.** **(A)** *atg5Δ*, *atg8Δ*, and *atg11Δ* mutant cells transformed with a plasmid expressing Atg32-V5 were grown in a CMS-L medium. Cells were harvested at indicated times. **(B)** The Atg32-V5/Pgk1 ratios were quantified at T0 and 48 h time points for all tested strains; \*\*  $p < 0.01$ . **(C)** *atg5Δ* mutant cells expressing Atg32-V5 were treated with MG-132 at time point 8 h. Cells were harvested at indicated time points and total protein extracts were prepared and analyzed by immunodetection. Anti-V5 antibody was used to visualize Atg32-V5 protein.

**S4 Figure: (A) The Atg32 protein is degraded upon rapamycin treatment and stabilized by the proteasome inhibition.** *atg32Δ* mutant cells grown in a CMS-L medium and expressing Atg32-V5 protein were harvested at T0 and treated with 0.2  $\mu\text{g/ml}$  rapamycin in presence or absence of 75  $\mu\text{M}$  MG-132 for 3 h, 6 h, and 24 h. Total protein extracts were prepared afterwards, and samples were analyzed by immunodetection. Anti-V5 antibody was used to visualize Atg32-V5 protein. **(B) The Atg32 protein is degraded in BY4742 strain.** BY4742 cells transformed with a plasmid expressing Atg32-V5 grown in a CMS-L medium were harvested at indicated times. To inhibit proteasome, MG-132 was added to the cell culture at 8 h time point. **(C)** The Atg32-V5/Pgk1 ratios were quantified for all tested conditions— \*\* $P < 0.01$ . **(D) MG-123 stabilizes the Atg32 protein in exponentially growing cells.** *atg32Δ* mutant cells grown in a CMS-L medium and expressing Atg32-V5 protein were harvested at T0 and treated with 75  $\mu\text{M}$  MG-132. Cells were harvested at exponential (T8) and stationary (T24, T48) phase, and total protein extracts were prepared and analyzed by immunodetection. Anti-V5 antibody was used to visualize Atg32-V5 protein.

**S5 Figure: The effect of MG-132 and PMSF treatment on cell growth and Atg32-V5 protein degradation.** **(A)** Addition of proteasome inhibitor MG-132 (75  $\mu\text{M}$  MG-132) and inhibitor of vacuolar proteolysis PMSF (2 mM) do not affect growth and growth yield in *atg32Δ*

mutant cells expressing Atg32-V5 plasmid and grown in a CMS-L medium. The Y-axis is represented in logarithmic scale (n = 5 for control and MG-132; n = 3 for PMSF). **(B)** *atg32Δ* cells grown in a CMS-L medium and expressing Atg32-V5 protein were harvested at indicated time points. To inhibit proteasome, MG-132 was added to the cell culture at 8 h time point. To inhibit vacuolar proteolysis, 2 mM PMSF was added to the cell culture at T8; this step was repeated twice during the course of cell growth. Total protein extracts were prepared afterwards, and samples were analyzed by western blots. Anti-V5 antibody was used to visualize Atg32-V5 protein. To detect modified Atg32-V5 forms (bands with a higher molecular weight) after MG-132 treatment, two different revelation times of blots are presented.

**S6 Figure : Inhibition of the proteasome with MG-132 does not affect autophagy.** BY4742 **(A)** and *atg32Δ* mutant **(B)** cells expressing GFP-Atg8 protein grown in a CMS-L medium in presence or absence of MG-132 were harvested at indicated times. Total protein extracts from  $2 \times 10^7$  cells were prepared and separated by 12.5% SDS-PAGE gel as described in the Material and Methods section. Proteins were detected using antibodies against GFP or Pgk1.

**S7 Figure: Purification of Atg32-V5-6HIS.** **(A)** Lysate from *atg32Δ* mutant cells expressing *pATG32-V5-6HIS* was prepared as described in the Material and Methods section. Next, lysate was loaded on a Ni-NTA column, the non-retained fraction, as well as the two washes W1 and W2, were recovered. The bounded proteins were then eluted and 500  $\mu$ l fractions were collected. **(B-D)** 250  $\mu$ l of each fraction absorbing at 254 nm (from F12 to F22) were precipitated with TCA. Pellets were resuspended in 20  $\mu$ l of the loading buffer; 10  $\mu$ l were loaded on the gel to be revealed with the colloidal blue **(B)** and 5  $\mu$ l were used for immunodetection with anti-histidine **(C)** or anti-ubiquitin antibodies **(D)**, respectively.

**S8 Figure: Mass spectrometry analysis.** **(A)** SEQUEST spectra, **(B)** MASCOT spectra, and **(C)** Protein coverage.

## Answers to reviewer 1

*Reviewer #1: In the revised manuscript by Camougrand et al, the authors made modest changes to address concerns raised in their original submission. While I have my doubts that their purification strategy is effectively working (ie, a concern is that the oligomerized band is non-specifically cross-reacting with the anti-his antibody), the authors have now provided the requested data.*

*However, it is somewhat glaring that the authors have now removed data from Figure 8 related to the ubiquitinated band they identified via proteomic analysis. They had previously generated two clonal lines of a K282A mutant, one of which showed no change in Atg32 turnover and the other which mildly stabilized Atg32 at the 8h timepoint. In the revised manuscript, the “negative” data is removed while “significantly ( $P<0.05$ ) impaired” is added to the text. The authors should return “clone 1” to the manuscript for transparency purposes and graphically display the values that led to this conclusion.*

We would like to thank you for all your effort and comments. We believe they helped us to make our manuscript better.

We apologize if the noninclusion in our revised manuscript of the immunoblot result with clone 1 in Figure 4A gave the impression that we are trying to intentionally select the results that fit into our story. By no means was this our intent. We only tried to simplify the presentation of the results and eliminate unnecessary duplication. Let us provide you with a more detailed explanation.

In the original version, we presented in Figure 8A an image of blots for two different clones (1 and 2). In Figure 8C, there is only one column for the mutant K282A (it does not specify if it is clone 1 or clone 2). We apologize for not explaining this better in the text—the column (48h) contains results from 6 independent experiments from 3 different clones that we tested (clone 1 and clone 2 from Figure 8A plus a third clone that was not mentioned in the manuscript). Also, it has to be noted that in the original version, the y-axis of the graph in Figure 8C shows the amount of Atg32-V5 normalized to T0 value of Atg32-V5, which, based on the reviewer's request, was normalized in the revised version to the amount of Pgk1 at each time.

Again, Figure 8 in the revised version of our manuscript does include the results of 6 independent experiments from 3 individual clones. Because quantification normalized to Pgk1 did not show significant changes between individual clones (1-2-3), we decided to keep only one of the clones in part A. When compared to wild-type Atg32 protein, there is about 15% ( $P<0.05$ ) more mutant protein in the late stationary phase cells (Fig. 8A, C; 48 h).

For the reviewer, we attach here the immunoblot results obtained from 3 individual clones with individual quantification for each of them for comparison.

**Figure for reviewer only**

*atg32Δ* +

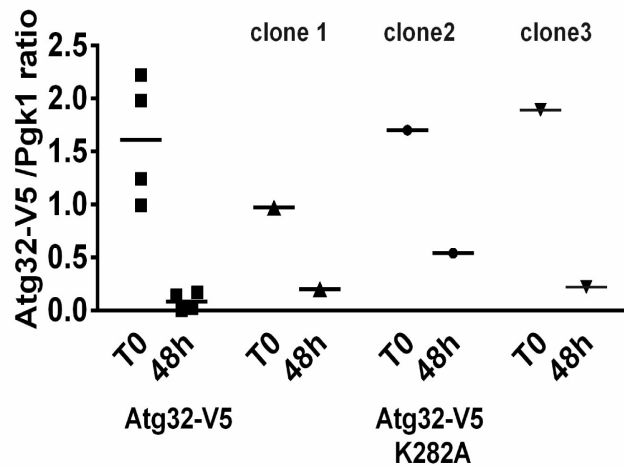
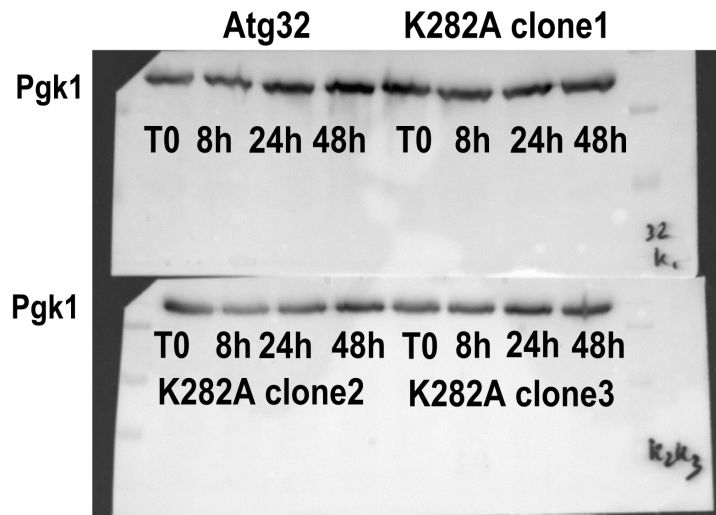
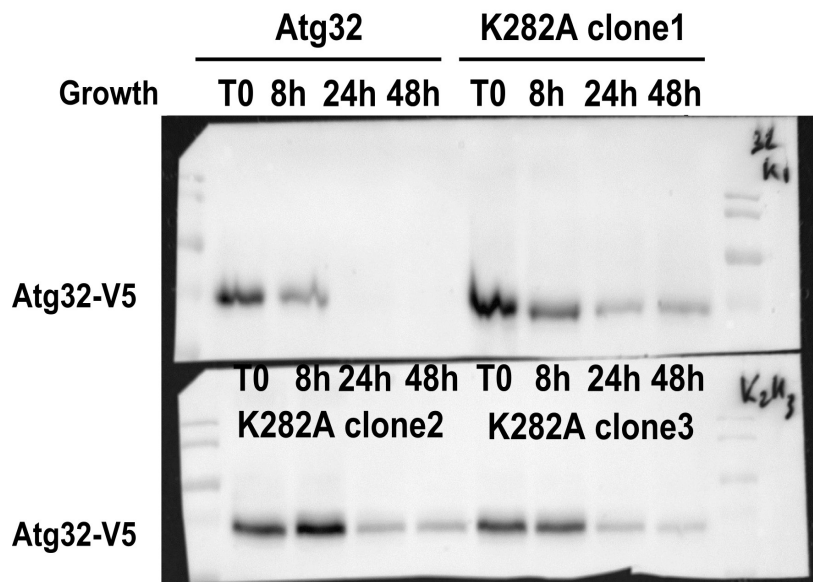


## Figure 8

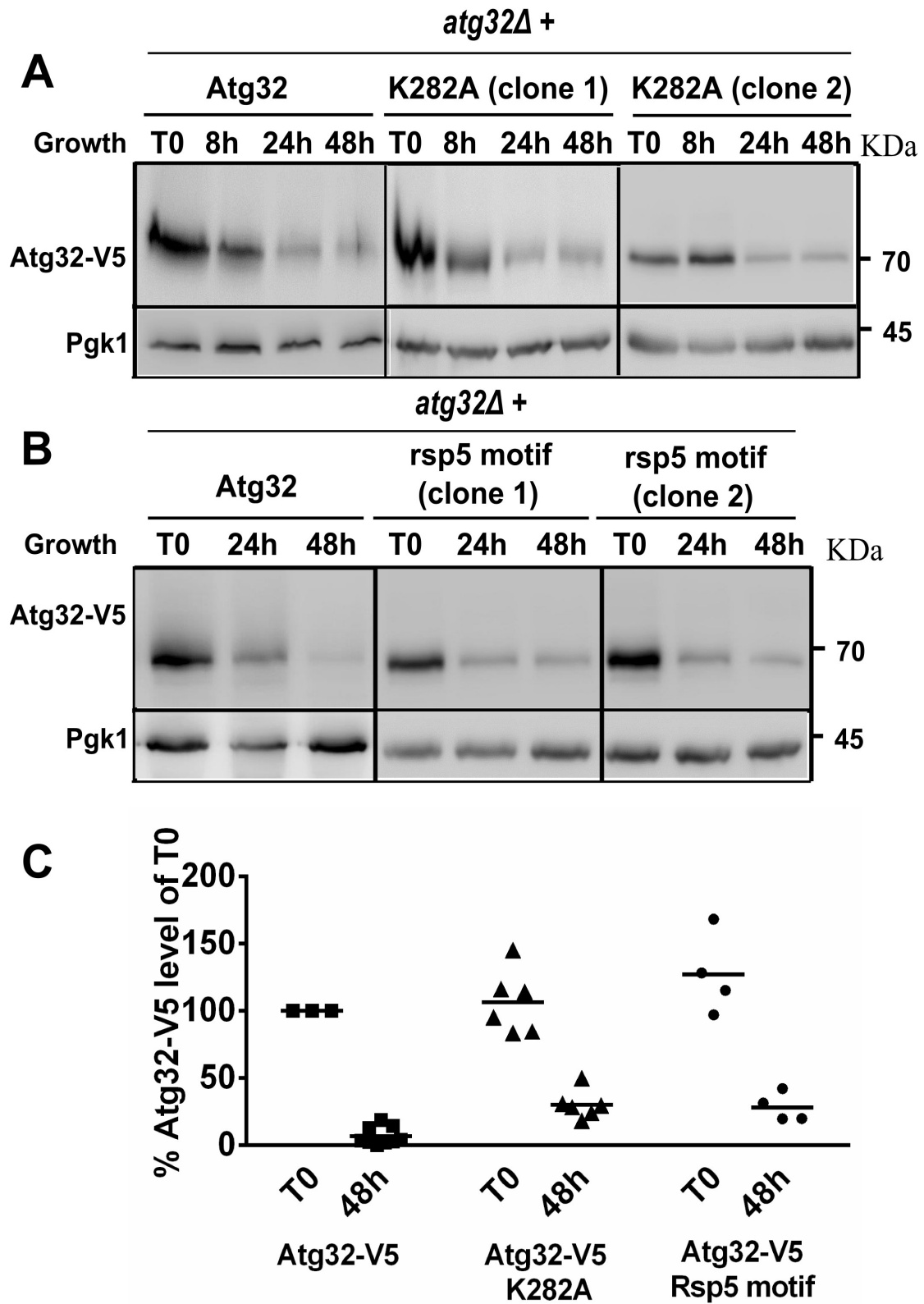
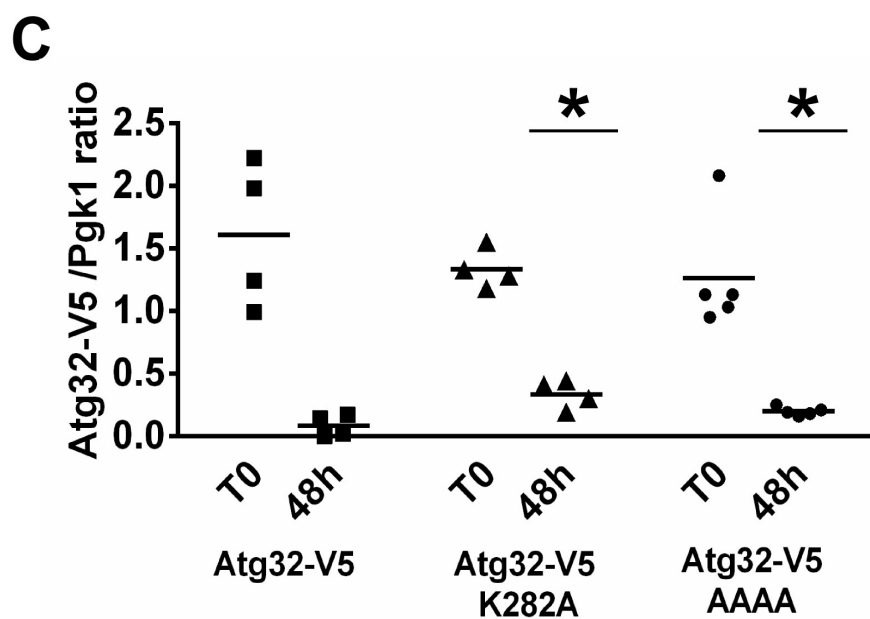
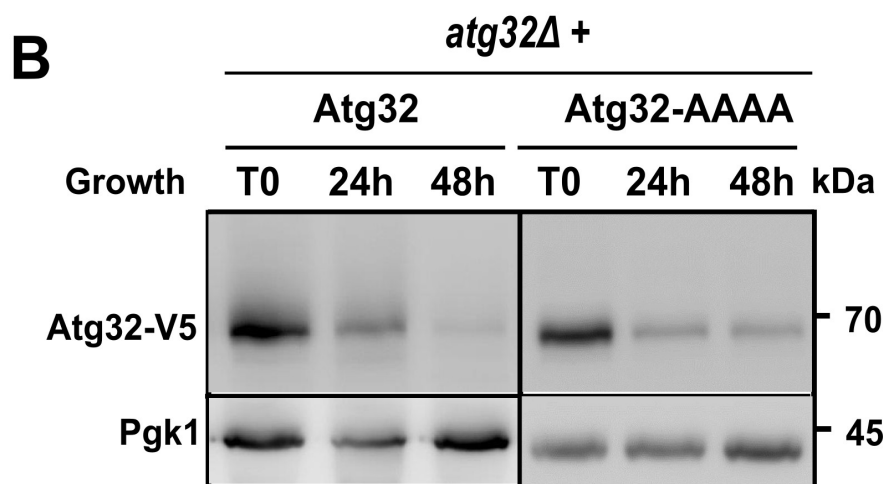
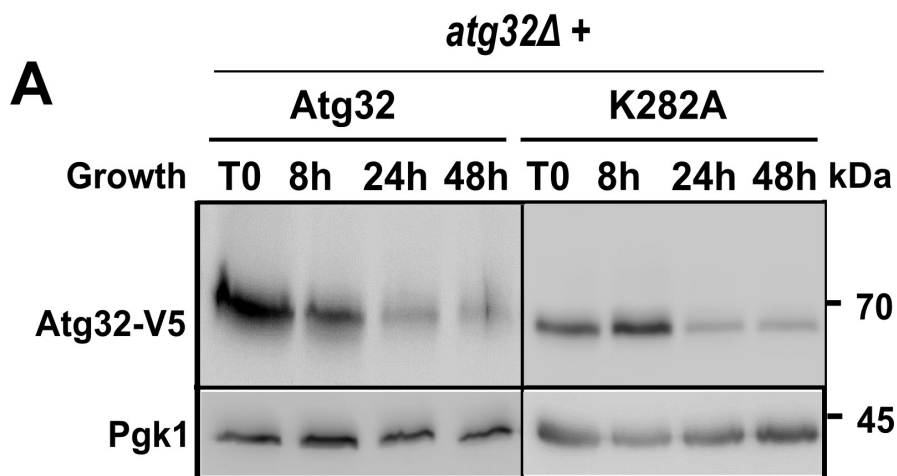


# Figure 8



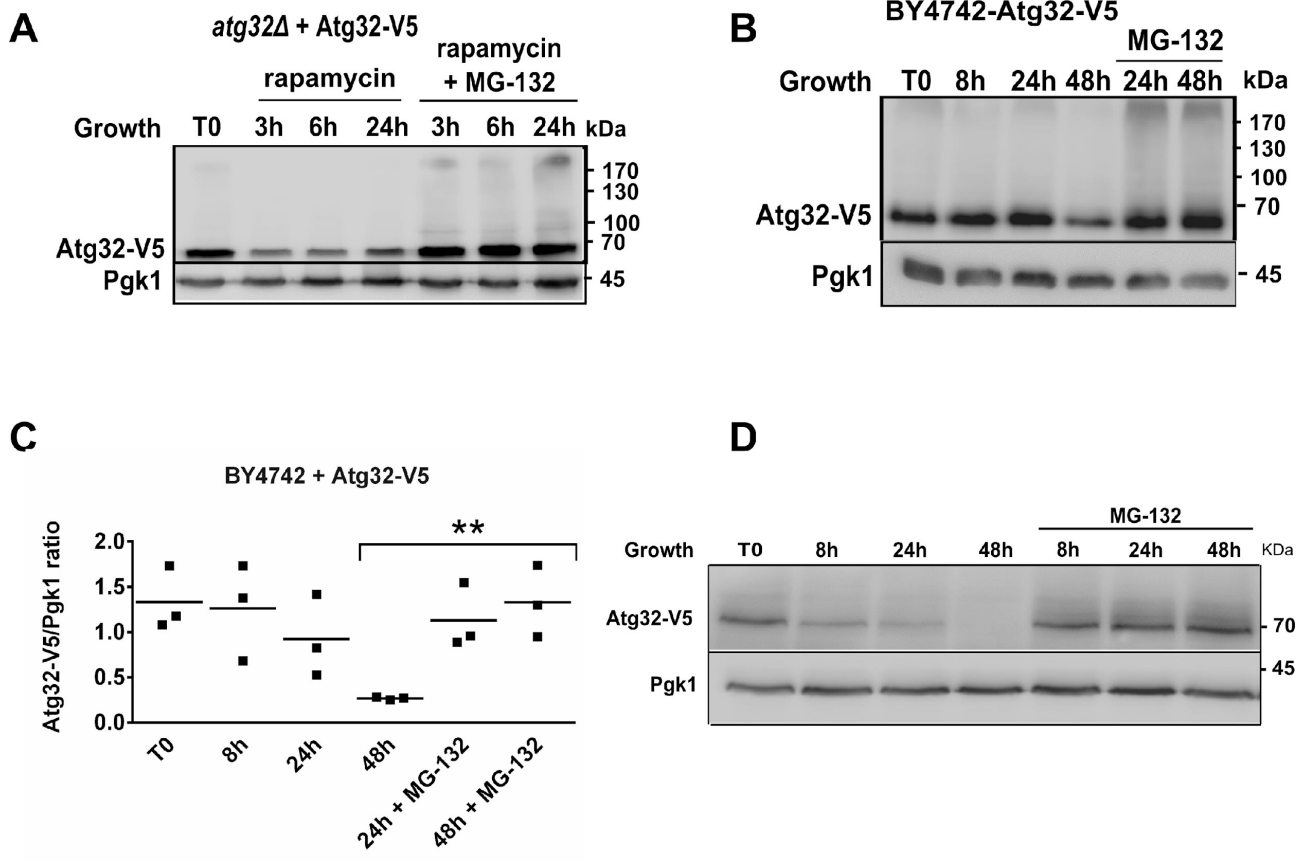
*My other primary concern regarding lengthy treatment with MG-132 was not addressed. In their response, the authors write that “we did not present results from shorter than 24 hours in the presence of inhibitors, so we are not sure what led the reviewer to raise a concern that stabilization of Atg32 occurs only after long incubation times and may be an indirect effect.” This is exactly the point – because the authors do not examine other time points (for example, 1h, 2h, 4h) after MG-132 addition at 8h, they can only state that 16h of treatment leads to stabilization of Atg32 during stationary growth. While the authors now demonstrate that such treatment does not inhibit cell growth, they also cannot state whether the protein is acutely stabilized or stabilized as part of an adaptive cellular response to prolonged proteasomal inhibition.*

In our previous answer we tried to explain to the reviewer that we did not examine the shorter times (fewer than 16 hours; T24) of treatment with MG-132 because our aim was to study levels of Atg32 protein at the beginning of and during the stationary phase—the time of cell growth when mitophagy is induced. We believe that our results provide clear evidence that inhibition of proteasome activity with MG-132 leads to stabilization of Atg32 during the stationary phase and that this correlates with an increase in mitophagy activity.

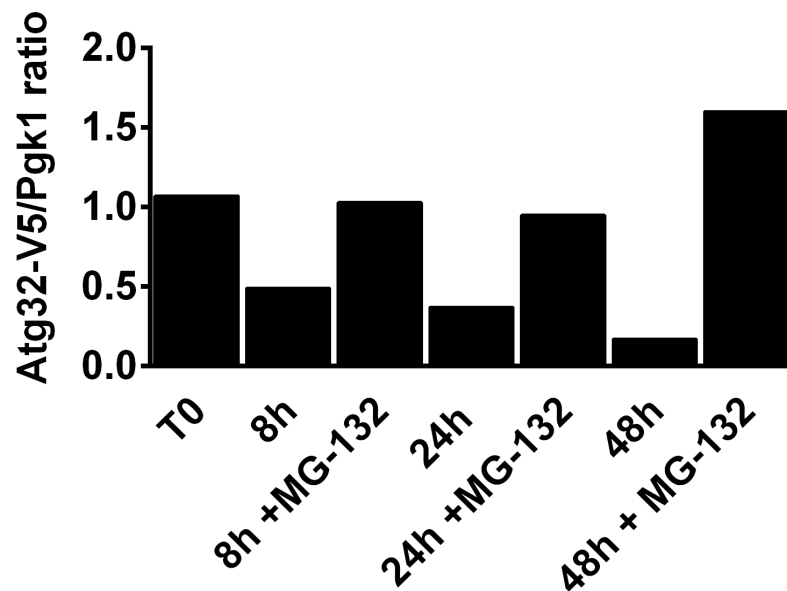
However, to address the reviewer’s comment, we performed an experiment in which MG-132 was added to the culture at T0 (instead of at T8 as we used during our study) and examined the levels of Atg32 after 8 hours (exponential phase, no appreciable mitophagy), 24 hours (early stationary phase, beginning of mitophagy induction), and 48 hours (late stationary phase). The obtained results were included in the manuscript as supplementary Fig. 4D (for your convenience the results are attached to this letter as well). As you can see, the level of Atg32p at T8 is about half compared to the level at T0, and it further decreases to where there is almost no detectable Atg32 when measured at T48. On the contrary, the presence of MG-132 drastically recovers Atg32 levels in both short (8h) and long (24h and 48h) incubation times. We provide the quantification of the immunoblot results here as well. We strongly believe these results support the view that the Atg32 protein is acutely stabilized instead of being stabilized as a part of an adaptive cellular response to prolonged proteasomal inhibition.

New supplementary Figure S4 (with new results in part D - included into manuscript):

### Figure S4



Quantification figure S4D- an average from 2 independent experiment (for reviewer only):



*In exponentially growing cells, where there is no appreciable mitophagy, the authors use short-term MG132 treatment in combination with cycloheximide and observe a very modest inhibition of proteasomal turnover. So while the authors can conclude that Atg32 can be targeted to the proteasome during exponential growth, it is not clear that this is an acute cellular response to regulate mitophagy when cells reach stationary phase. If the authors are unwilling to perform new experiments, they must substantially improve the clarity of the manuscript and acknowledge the potential caveats and alternative explanations of their results.*

Beside our aforementioned explanation, our experiments with cycloheximide (Figs. 4B and 4C) showed that the turnover of the Atg32 protein is extremely rapid compared to other proteins (porin, Pgk1) and that this turnover involves the activity of the proteasome. This also explains why the activity of the promoter increases during growth (Fig. 4A). After one hour with the cycloheximide, the effect of MG-132 is striking and significant ( $P=0.0146$ ; we included data for “1h+cycloheximide+MG-132” in Fig. 4C that were missing in the previous version). Respectfully, we cannot agree with the reviewer’s statement that this change is “very modest.”

Our results support the conclusion that Atg32 can be targeted to the proteasome during exponential growth as well as favoring an acute cellular response to regulate levels of Atg32 protein (as an essential mitophagy regulator) when cells reach the stationary phase.

We slightly modified some parts of the Results and Discussion sections to make the text clearer.

The manuscript was proofread by a native English-speaking person.